Evaluation of thermal and moisture response of highly insulated wood-frame wall assemblies, phase 1: Part II: numerical modelling
Saber, Hamed H.; Ganapathy, G.

National Research Council Canada   Conseil national de recherches Canada

Canada

Evaluation of Thermal and Moisture Response of Highly Insulated Wood-Frame Wall Assemblies — Phase 1

Part II: Numerical Modelling

Report A1-000444.4

Hamed H. Saber and G. Ganapathy

8 January, 2016

Table of Contents

NRC·CNRC

List of Figures

NRC·CNRC

List of Figures of Appendix – A

NRC·CNRC

List of Tables

NRC·CNRC

Acknowledgements

NRC·CNRC

Executive Summary

The National Research Council of Canada (NRC) has undertaken field monitoring and computer modelling to investigate the risk of condensation in wall assemblies having different combinations of increased thermal resistance (R-value) of cavity insulation and of selected exterior insulation products. The field monitoring of residential 38 mm x 140 mm (2 x 6 in) wood-frame wall systems that had been constructed using different types of exterior insulation products were undertaken at the Field Exposure of Walls Facility (FEWF) of NRC-Construction, located in Ottawa; the primary intent was to investigate the risk of condensation and mould growth in three mid-scale (1219 mm x 1829 mm / 4 ft. x 6 ft.) wall specimens installed in the FEWF. The first specimen was constructed by installing 25 mm (1 in) thick EPS insulation panels; the second specimen was constructed with 51 mm (2 in) thick XPS insulation panels, whereas; the third specimen was constructed by installing 76 mm (3 in) thick mineral fibre batt insulation; all insulation products were installed outboard of the sheathing membrane. The three wall specimens were installed side-by-side in the FEWF and subjected to local climate conditions of Ottawa over a period of one year (August 11, 2013 – October 1, 2014).

The first stage of the work program included the experimental design, installation of test specimens, commissioning of instrumentation, operation of the test facility, collection and monitoring of data, and data analyses. The second stage of the work program included conducting: material characterization of the exterior insulation products (EPS, XPS and mineral fibre insulation), model benchmarking, and parametric model simulation study.

In this report, the hygrothermal model, hygIRC-C, was benchmarked against the measured data. Results showed that the model predictions were in good agreement with the experimental data obtained from the different wall specimens. Thereafter, the hygrothermal model was used to conduct parametric analyses to predict the risk of condensation and mould growth in full-scale wall assemblies that incorporated exterior insulation products when these walls were subjected to different Canadian climates.

Similar to a previous NRC project [69], the simulation parameters that were used in this project (indoor conditions, outdoor conditions, air leakage rate, and other simulation parameters) were the same as that recommended by the Task Group (TG) on Properties and Position of Materials in the Building Envelope[*]. The hygrothermal performance of walls with exterior insulations was compared to the National Building Code of Canada's prescribed reference wall. The reference wall consists of interior drywall ((12.7 mm / 0.5 in) thick), polyethylene membrane air and vapour barrier (6 mil thick), 38 mm x 140 mm (2 x 6 in) wood-frame with friction-fit glassfibre batt insulation of R-24, and oriented strand board (OSB) (11 mm / 7/16 in thick).

The performance was expressed using the mould index criteria, which allowed sufficient resolution to assess the risk of moisture condensation and related risk of mould growth in the wall assemblies. The development of the mould index has been on-going for several years with the most recent work, as was used in this project, having being provided by Ojanen et al. [68]. The mould index levels range in value from 0 to 6, with 0 being equivalent to no growth and 6 indicating 100% coverage of either heavy or tight mould growth. The visual identification of mould growth on surfaces is given an index level value of 3.

---

[*] TG acting on behalf of the NBCC Standing Committee on Housing and Small Buildings (SCHSB).

The R-values of the outboard insulation were R-3.9 (RSI-0.69), R-10 (RSI-1.76) and R-12.5 (RSI-2.20), and the Water Vapour Permeance (WVP) for these insulation products had, respectively, values of 27, 114, and 2130 ng/(Pa•s•m²) (0.5, 2.0 and 37.2 US perm). All wall assemblies were subjected to different climatic conditions of Canada as represented by selecting a set of cities that included: Vancouver (BC), St John's (NL), Ottawa (ON), Edmonton (AB) and Yellowknife (NT).

For each climatic location, the weather data was analyzed to identify the orientation of the wall assembly with the highest exfiltration rate. Note that a higher exfiltration rate would result in a greater risk to the formation of condensation and mould growth within the wall. As such, for each climatic condition, all numerical simulations were conducted for the wall assemblies that faced the predominant direction that would provide the highest exfiltration rate. Furthermore, it was determined that walls of the third storey were subjected to higher exfiltration rates as compared to walls in lower stories. Thus, all wall assemblies investigated in this study were walls of the third storey of low-rise buildings; this was assumed to represent the worst case scenario. Also, a sensitivity analysis was conducted to investigate the effect of different air leakage rates on the hygrothermal performance of the wall assembly and to determine the locations within the wall that were most at risk due to air leakage.

After conducting the numerical simulations for all wall assemblies, and based on the air leakage paths considered in this study, the different wall locations at risk for the formation of condensation and mould growth were identified and for which the corresponding value for mould index was calculated. It is important to point out that the wall locations at risk of mould growth would change by considering different air leakage paths within the wall assembly.

The simulation results were summarized in a simple form using the following two parameters:

- Overall average mould index, and
- Overall maximum mould index.

The two above parameters were determined for a two year simulation period (i.e. average year followed by a wet year, selected from long-term meteorological data for each location).

The results showed that no risk of condensation occurred in the wall assemblies when it was assumed that no air leakage occurred. Whereas, for the instance when100% of a nominal air leakage rate of 0.1 L/(s•m²) (at 75 Pa) was assumed, a higher risk of condensation and mould growth was obtained as compared to that for a 50% air leakage rate (i.e. 0.05 L/(s•m²) at 75 Pa). Also, the results showed that the values for the overall average and maximum mould index in walls with different types of exterior insulations were lower than that of the reference, NBC-compliant wall. In regard to insulation in the stud-cavity, the values for the overall average and maximum mould index in walls having R-24 (RSI-4.23) stud-cavity insulation were higher than that of walls with R-19 (RSI-3.35) insulation. Regarding the effect of the climatic locations on the performance of the reference wall, EPS wall and XPS wall, St John's appeared to have the most severe climate in comparison to the other four locations investigated (Vancouver, Ottawa, Edmonton, and Yellowknife); the greatest values of the overall average mould index of the wall configurations amongst the five locations occurred at this location. For the wall having mineral fibre insulation, however, the values of overall average mould index were approximately the same for St John's and Vancouver.

Evaluation of Thermal and Moisture Response of Highly Insulated Wood-Frame Wall Assemblies — Phase 1 Part II: Numerical Modelling

Authored by:

Hamed H. Saber and Gnanamurugan Ganapathy

A Report for the

Canada Mortgage and Housing Corporation (CMHC) and Natural Resources Canada (NRCan)

National Research Council Canada
Ottawa ON K1A 0R6 Canada

8 January, 2016

NRC·CNRC

Evaluation of Thermal and Moisture Response of Highly Insulated Wood-Frame Wall Assemblies — Phase 1 Part II: Numerical Modelling

Hamed H. Saber and Gnanamurugan Ganapathy

1. Introduction

A brief review of literature is provided on the moisture performance of the building envelope of housing and small buildings in cold climates [1-12]. Ojanen and Kumaran [1] studied the effect of over- pressurization of residential houses on the moisture performance of the building envelope for both uniform and non-uniform airflow through wall assemblies. A related question was whether a 10 Pa over-pressurization limit was acceptable for homes located across Canada. The results showed that the amount of moisture accumulation depends on the rate of exfiltration of the climatic conditions. As well, the results showed that the uniform airflow condition through the walls produced an earlier onset of wetting and faster drying than the non-uniform airflow condition (i.e. entry at interior and top of wall, exit at base of wall). The non-uniform airflow condition, however, presented more risk of moisture related damage to wall components than the uniform airflow condition.

The modelling study that was carried out by Karagiozis and Kumaran [2] focused on moisture content of components and total moisture accumulation in walls of six different vapour retarders incorporated in a typical Canadian residential wall within three Canadian cities. No airflow was considered in that study. It was concluded that vapour control of the building envelope was important for buildings located in cold climates and in general, moisture accumulates in the wall during the heating season but dries out in the summer.

The study by Ojanen and Kumaran [3] looked at the effect of adding exterior insulation to the sheathing or using sheathing with an increased thermal resistance. In that study, the moisture accumulation due to different air leakage paths was examined as well as the effect of varying indoor relative humidity (RH) on the hygrothermal performance. The results of the simulation showed that increasing the temperature of the interior surface of the of exterior insulated sheathing significantly reduced the amount of moisture accumulation and this in turn lead to higher tolerances for indoor RH and air leakage within the wall assembly.

The study reported by Kumaran and Haysom [4] provided the basis for placement of low permeance materials within building envelopes in cold climates. The key assumption in that study was that diffuse air leakage occurred across the assembly up to the allowable code limit

NRC·CNRC

of 0.1 L/(s•m^2). Another study by the same authors [5] showed that by adding 25 mm of mineral fiberboard sheathing on the outside of the studs, the stud-cavity was warm enough to prevent condensation on the interior face and water accumulation was reduced.

Chown and Mukhopadhyaya [6] provided a brief history of the development of air and vapour barrier provisions in the National Building Code of Canada (NBCC) since the first NBCC was published in 1941 to the most recent changes made in 2005 [13-15]. The key change in 1990 NBCC [13] was to separate the functions of air barrier and vapour retarder thus allowing for the possibility of placing low permeance materials exterior to the main thermal resistance of the wall. This change raised the possibility that someone using a low-permeance material as an air-barrier might choose to place it close to the outer surface of the wall where condensation could form on its interior face. To reduce the probability of incorrect placement, the 1990 NBCC [13] included a restriction on the location of low-permeance air barriers. These air barriers had to be placed so that the inner surface remained above the dew point of the interior air when the outside temperature was 10°C above the January design temperature. Also, that study [6] further refined the basis for placement of low-permeance materials for mild and humid climates where the expectation is that indoor Relative Humidity (RH) would likely exceed 34%.

Straube [7] investigated the role of vapor barriers on hygrothermal performance with the aid of simple and transparent diffusion calculations supported by measurements from full-scale natural exposure monitoring. That study explored the phenomenon of summertime condensation, the drying of roofs and walls, and multiple vapor barrier layers as well as the importance of assessing both the interior and exterior climate. The results showed that the addition of insulated sheathing increased the temperature of the back of the sheathing and this reduced the frequency and severity of condensation due to air leakage. It was recommended that the preconceptions of many building codes, standards, and designers need to be modified to acknowledge the facts of low-permeance vapor barriers [7].

A design protocol for the application of insulating sheathing in low-rise buildings with high interior relative humidity (maximum 60%) for different locations across Canada was developed in a study by Brown et al. [8]. That study consisted of conducting parametric study using a HAM model to determine the hygrothermal performance of walls with a range of thermal insulation, air tightness and vapour permeance. For the air leakage investigated in that study, the results showed that moisture that accumulated during the heating season dried out in the non-heating season. The authors suggested that further investigations are required in order to set a threshold air leakage so as to minimize the risk of condensation. In another study, the same authors [9] have undertaken modelling exercise to simulate uncontrolled indoor humidity of residential buildings. A moisture balance method was developed to estimate the indoor humidity in buildings which is an important input to the hygrothermal models.

Maref et al. [10-12] conducted a research field study at the NRC's Field Exposure of Walls Facility (FEWF) that focused on the hygrothermal and energy performance of retrofitted wall systems by adding exterior insulations of different air and vapour permeance. For the purpose of comparison, a reference wall with no exterior insulation (i.e. non-retrofitted wall system) was tested. The objective was to assess the winter and summer condensation (i.e. inward moisture) within these wall systems. Results showed that the addition of an exterior insulating sheathing

raised the temperatures of the stud-cavity materials and maintained them above the dew point temperature of the interior air, thus reducing the likelihood and duration of interstitial condensation, within limits, but condensation can still take place during the coldest period of winter. Also, the wall systems with exterior insulation were less prone to interstitial condensation than similar wall without such exterior thermal insulation.

The objective of this study was first to benchmark the hygIRC-C model against the test data, and then use it to investigate the risk of condensation and mould growth in 2 x 6 wood-frame wall assemblies with and without exterior insulation when these walls are subjected to different climatic conditions of Canada.

2. Project Overview

NRC has undertaken field monitoring and numerical modelling to investigate the risk of condensation in wall assemblies having different combinations of increased thermal resistance (R-value) of cavity insulation and of selected insulation products. The field monitoring of different wall assemblies was undertaken in the NRC's Field Exposure of Walls Facility (FEWF). Three wall assemblies were tested in Phase 1 and another three wall assemblies were tested in Phase 2. Table 1 provides a description of the wall assemblies of Phase 1 and Phase 2. This report focuses on the three wall assemblies of Phase 1. In this phase, three mid-scale 1219 mm x 1829 mm (4 ft. x 6 ft.) having 38 mm x 140 mm (2 x 6-in.) wood-frame walls that were constructed using different types of exterior insulation products that included: 25 mm (1 in) EPS; 51 mm (2 in) XPS, and, 76 mm (3 in) mineral fibre insulation. The three specimens were installed side-by-side in the FEWF and exposed to local climate conditions of Ottawa over a one year period; the test period started on August 11, 2013 and ended on October 1, 2014. The scope of work included the experimental design, installation of test specimens, commissioning of instrumentation, operation of the test facility, collection and monitoring of data, data analyses, material characterization of the exterior insulations (EPS, XPS and mineral fibre insulation) and numerical modelling.

This report focuses on the numerical modelling where the NRC's hygrothermal model, hygIRC-C, was benchmarked against the FEWF test data of different wall specimens. Thereafter, the model was used to conduct parametric analyses in order to investigate the risk of condensation and mould growth in different wall assemblies, subjected to different climatic conditions of a select set of locations in Canada. The hygIRC model description and record of benchmarking are available in Appendix – A1.

3. Model Benchmarking

Having previously benchmarked the present model to several tests undertaken in controlled laboratory conditions as described previously, a subsequent and important step was to benchmark the present model against the field measurements for three wall systems described below. This report provides a brief description of the constructed wall specimens (full details are available in [72]. Thereafter, information is provided regarding assumptions, and initial and boundary conditions that were used in conducting model benchmarking.

NRC·CNRC

3.1 Wall Specimens

Three mid-scale (1219 mm x 1829 mm / 4 ft. x 6-ft.) residential 38 mm x 140 mm (2 x 6-in.) wood-frame wall test specimens were installed side-by-side in the Field Exposure of Walls Facility (FEWF). The different material layers and the dimensions of the wall specimens are described in Table 1 and shown in Figure 1 to Figure 4. The backup wall for all three design

Table 1. Descriptions of walls for Phase-1 and Phase-2 (Yr 2013-2015)*

Phase	Wall-1 4 ft. x 6 ft.	Wall-2 4 ft. x 6 ft.	Wall-3 4 ft. x 6 ft.
Phase-1: **2 x 6-in. wood framing with exterior insulation**	• Vinyl siding • 1.5 in wide x 7/16" thick furring strip installed vertically • 1 in EPS rigid foam insulation **(exterior insulation)** • Sheathing membrane • 11 mm OSB wood-sheathing • 2x6 nominal stud cavity with R24 glass fiber insulation batts • 6 mil poly air/vapour barrier • ½ in painted drywall	• Vinyl siding • 1.5 in wide x 7/16" thick furring strip installed vertically • 2 in XPS rigid foam insulation **(exterior insulation)** • Sheathing membrane • 11 mm OSB wood-sheathing • 2x6 nominal stud cavity with R24 glass fiber insulation batts • 6 mil poly air/vapour barrier • ½ in painted drywall	• Vinyl siding • 1.5 in wide x 7/16" thick furring strip installed vertically • 3in semi-rigid mineral fibre insulation **(exterior insulation)** • Sheathing membrane • 11 mm OSB wood-sheathing • 2x6 nominal stud cavity with R24 glass fiber insulation batts • 6 mil poly air/vapour barrier • ½ in painted drywall
	Wall-4 **4 ft. x 6 ft.**	**Wall-5** **4 ft. x 6 ft.**	**Wall-6** **4 ft. x 6 ft.**
Phase-2: **Different wood framing with interior insulation**	• Vinyl siding • Sheathing membrane • 11 mm OSB wood-sheathing • 2x6 nominal stud cavity with R24 glass fiber insulation batts • 2 in (2 layers of 1 in thick) XPS rigid foam insulation (interior insulation) • 6 mil poly air/vapour barrier • ½ in painted drywall	• Vinyl siding • Sheathing membrane • 11 mm OSB wood-sheathing • 2x10 nominal stud cavity (2x6 and 2x4 studs together) with 2 in spray foam insulation on interior side of the OSB + glass fiber filling the rest of the cavity • 6 mil poly air/vapour barrier • ½ in painted drywall	• Vinyl siding • Sheathing membrane • 11 mm OSB wood-sheathing • 2x12 nominal stud cavity (2x4 stud + 2x4 gap + 2x4 stud) with cellulose insulation filling in entire cavity • 6 mil poly air/vapour barrier • ½ in painted drywall

* layers listed from exterior to interior

strategies consisted of interior drywall ((12.7 mm / 0.5 in) thick), polyethylene membrane air and vapour barrier (6 mil thick), 38 mm x 140 mm (2 x 6-in.) wood-frame with friction-fit glass fibre batt insulation of R-24, and oriented strand board (OSB) (11 mm / 7/16 in. thick). In this project, the backup wall was constructed by adding different types of exterior insulation products of different thicknesses. As shown in Figure 2, the first wall (Wall 1) was constructed by adding an expanded polystyrene (EPS) layer of 25 mm (1 in) thick on the OSB sheathing. The second wall (Wall 2) was constructed with a 51 mm (2 in) thick extruded polystyrene (XPS) panel (Figure 3). The final wall (Wall 3) was constructed with 76 mm (3 in) thick mineral fibre insulation (Figure 4).

As a part of the test protocol, fully described in [72], all Heat Flux Transducers (HFTs) used in the three test specimens were calibrated according to ASTM C-1130 "Standard Practice for Calibrating Thin Heat Flux Transducers" [69]. The uncertainty of heat flux measurements was ± 5%. The locations of the HFTs are shown in Figure 2 to Figure 4. Also, the uncertainty of the thermocouple measurements was ± 0.1°C.

3.2 Transient Numerical Simulations

This section presents the assumptions, and initial and boundary conditions that were used in conducting the numerical simulations for different wall specimens that were constructed using EPS, XPS and mineral fibre insulations. As indicated earlier, the hygrothermal properties of these insulations were measured in this project.

3.2.1 Assumptions

It was assumed that all material layers were in direct contact with one another (i.e. the interfacial thermal resistances between all material layers were neglected). The emissivity of all surfaces that bounded the airspaces (i.e. airspaces between exterior insulations, furring strips and vinyl siding) was taken equal to 0.9 [54]. The effects of heat transfer by conduction, convection and radiation within these airspaces on the thermal performance of wall assemblies were determined.

3.2.2 Initial and Boundary Conditions

The initial temperature in all material layers of the respective wall specimens (Wall 1, 2 and 3) was assumed uniform and equal to 10.0°C. Since this initial temperature was not the same as in the test, it was anticipated that the predicted dynamic response of the different wall specimens in the first period of the test (e.g. the first 24 – 48 hr) would be different from that obtained in the test itself. The boundary conditions on the top and bottom surfaces of the wall systems were assumed to be adiabatic (i.e. no edge heat losses). The outdoor surface of the vinyl siding for all wall systems was subjected to a temperature boundary condition. Similarly, the indoor surface of the gypsum board for all wall systems was subjected to a temperature boundary condition. The temperatures on the outdoor and indoor surfaces of different wall specimens, and that changed over time, were taken equal to that measured on these surfaces.
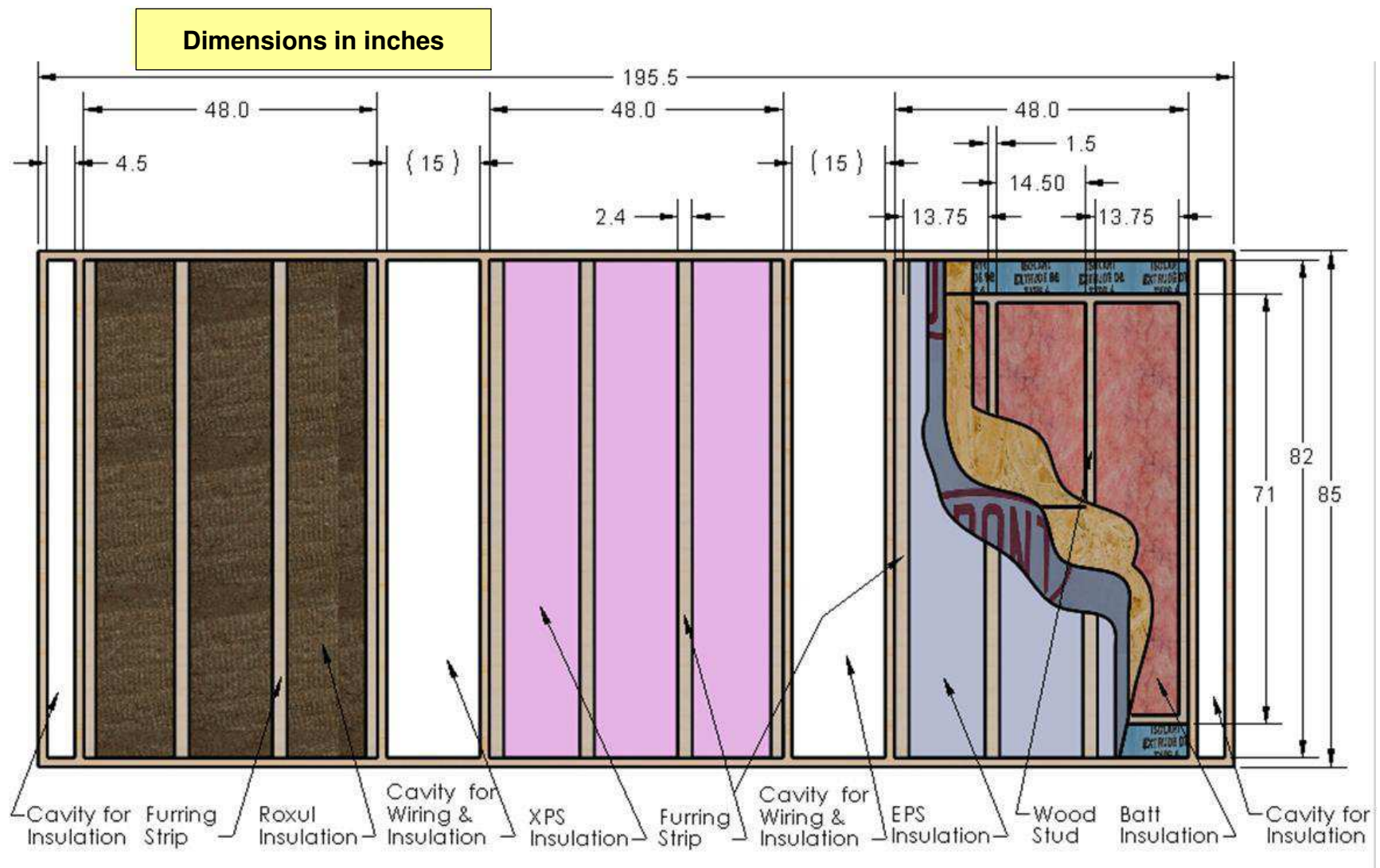
Figure 1. Schematic of three residential 38 mm x 140 mm (2 x 6 in.) wood-frame wall test specimens installed side-by-side in the FEWF

EPS Wall Assembly
(Wall 1)

EPS Wall Assembly:
Vinyl siding
Furring Strip
1" EPS insulation
Sheathing membrane
OSB
Batt insulation
Poly air/vapour barrier
Drywall

HFT1
HFT2
HFT3
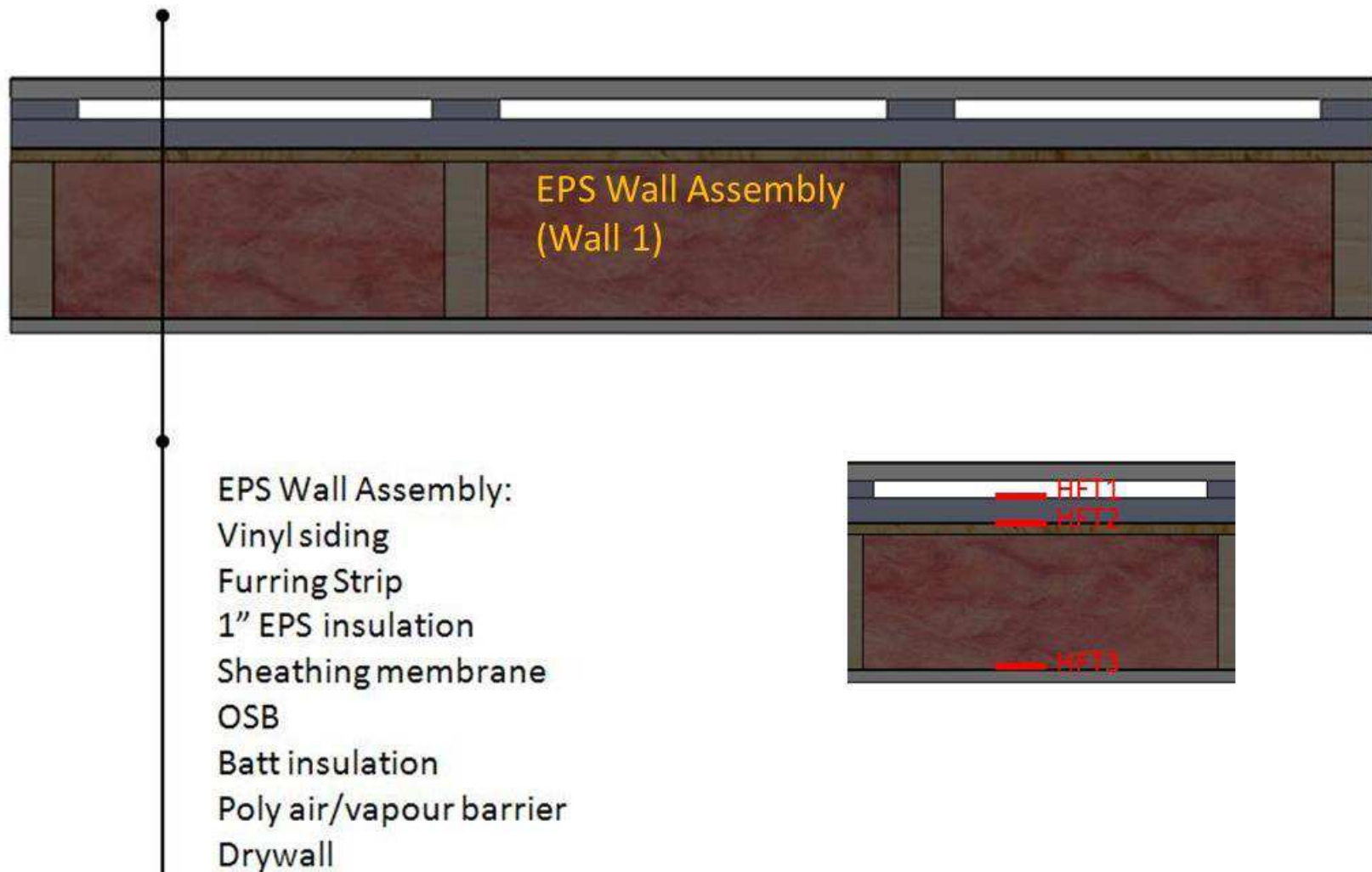
Figure 2. Horizontal cross-section through EPS wall assembly showing locations of Heat Flux Transducers, HFTs (Wall 1)

XPS Wall Assembly
(Wall 2)

XPS Wall Assembly:
Vinyl siding
Furring Strip
2" XPS insulation
Sheathing membrane
OSB
Batt insulation
Poly air/vapour barrier
Drywall

HFT1
HFT2
HFT3
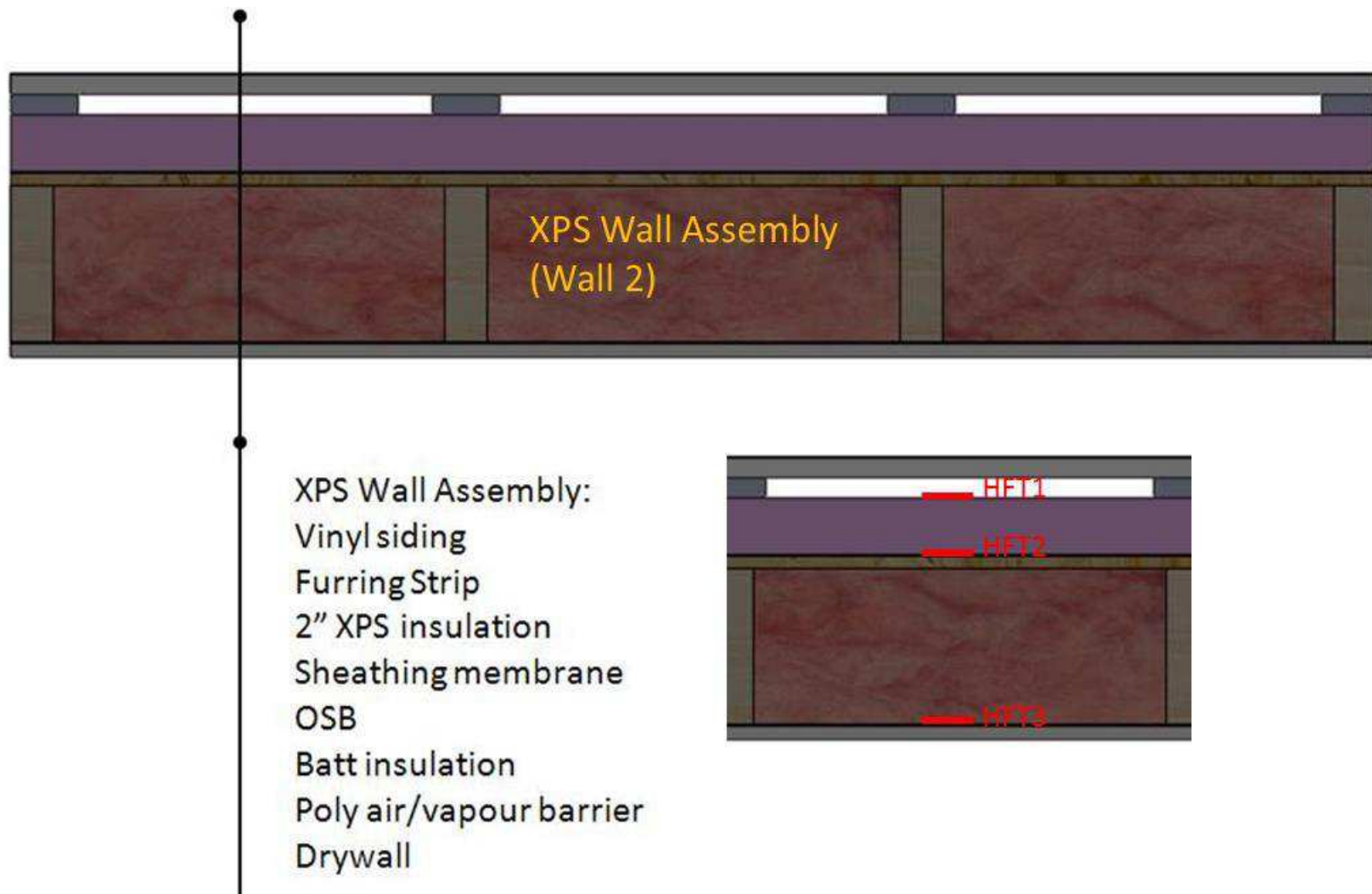
Figure 3. Horizontal cross-section through XPS wall assembly showing locations of Heat Flux Transducers, HFTs (Wall 2)

Mineral Fiber Wall Assembly (Wall 3)

Mineral Fiber Wall Assembly:

Vinyl siding
Furring Strip
3" Mineral fiber
Sheathing membrane
OSB
Batt insulation
Poly air/vapour barrier
Drywall

HFT1
HFT2
HFT3
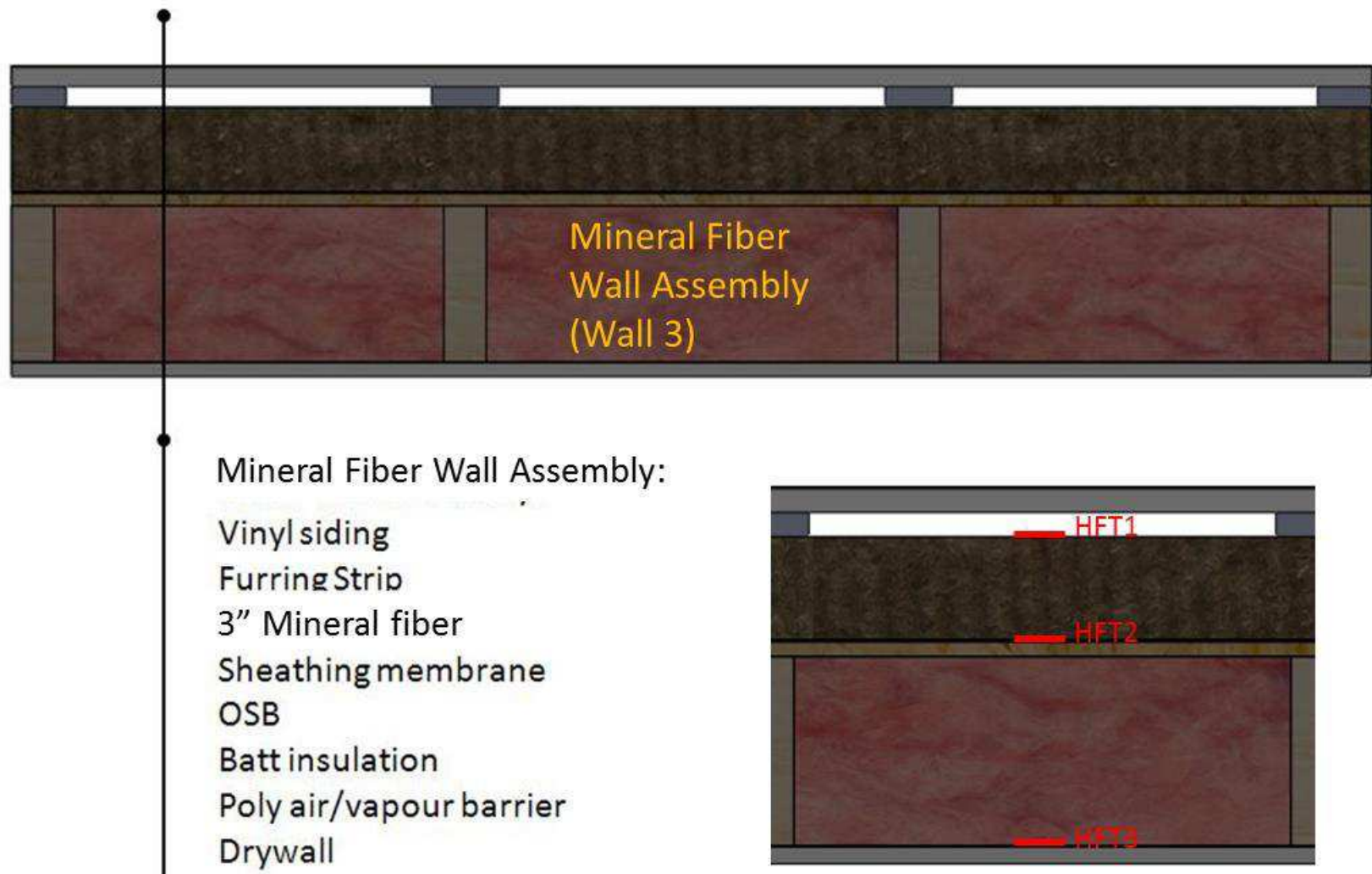
Figure 4. Horizontal cross-section through mineral fibre wall assembly showing locations of Heat Flux Transducers, HFTs (Wall 3)

3.5 Comparison between Model Predictions and Measurements

To benchmark the present model, transient numerical simulations were conducted for the three wall specimens (Figure 1). The full description of all instrumentation (i.e. thermocouples, Heat Flux Transducers (HFTs), Pressure (P) sensors, and Relative Humidity (RH) sensors) and experimental data are available in [72]. In each wall system, three Heat Flux Transducers (HFTs) were used to measure the heat flux at the middle (mid-height and mid-width, see the inserts in Figure 2, Figure 3 and Figure 4) of each wall at three interfaces, namely:

  (a) HFT1 at interface between airspace and exterior insulation;

  (b) HFT2 at interface between exterior insulation and OSB, and;

  (c) HFT3 at interface between polyethylene air barrier membrane and gypsum interface.

For the EPS wall specimen (Wall 1),

Figure 5. EPS wall (Wall 1) ─ Comparison between predicted and measured heat fluxes at interface: (i) airspace – EPS; (ii) EPS – OSB; (iii) poly – gypsum

-i,

-ii and

-iii show comparisons between the measured and the predicted values of heat flux during the test period. In these figures, time = 0 at which experimental data was collected corresponded to August 11, 2013 at 12:36:54 AM. Unlike the other wall specimens, the HFT1 located at the interface between the airspace and exterior insulation in Wall 1 was not functioning properly during the entire test period (

-i). However, as shown in

Figure 5. EPS wall (Wall 1) ─ Comparison between predicted and measured heat fluxes at interface: (i) airspace – EPS; (ii) EPS – OSB; (iii) poly – gypsum

-ii, the predicted heat flux at the EPS – OSB interface is in good agreement with the measurements from the HFT2. Similarly,

-iii shows that the predicted heat flux at the poly – gypsum interface is in good agreement with measurements from the HFT3.

Figure 6-i, Figure 6-ii and Figure 6-iii show comparisons between the measured and predicted values of heat flux during the test period at different locations for the XPS wall specimen (Wall 2). As shown in these figures, the predicted values of heat flux were in good agreement with the measured values at each of the respective interfaces, specifically at the: airspace – XPS interface (Figure 6-i), XPS – OSB interface (Figure 6-ii), and the poly – gypsum interface (Figure 6-iii).

Finally, for the wall specimen having mineral fibre insulation (Wall 3), comparisons are provided in Figure 7-i, Figure 7-ii and Figure 7-iii and in which are shown the predicted values of heat flux that were in good agreement with the measured values at each of the respective interfaces, specifically at the: airspace – mineral fibre interface (Figure 7-i), the mineral fibre – OSB interface (Figure 7-ii), and the poly – gypsum interface (Figure 7-iii).

In summary, the results presented in this section show that the predicted values of heat flux at different locations in the wall assembly are in good agreement with the measured values of heat flux for the three wall systems, namely the : EPS wall specimen (

), XPS wall specimen (Figure 6), and mineral fibre wall specimen (Figure 7).

It is not possible to complete the benchmarking of the model in respect to moisture transport on the basis of the field trials undertaken in the FEWF. This requires conducting experiments in a controlled environment after first conditioning the test specimens to known levels of moisture content. In fact the model has previously been benchmarked in controlled conditions as is described in some detail in Appendix A1.1.
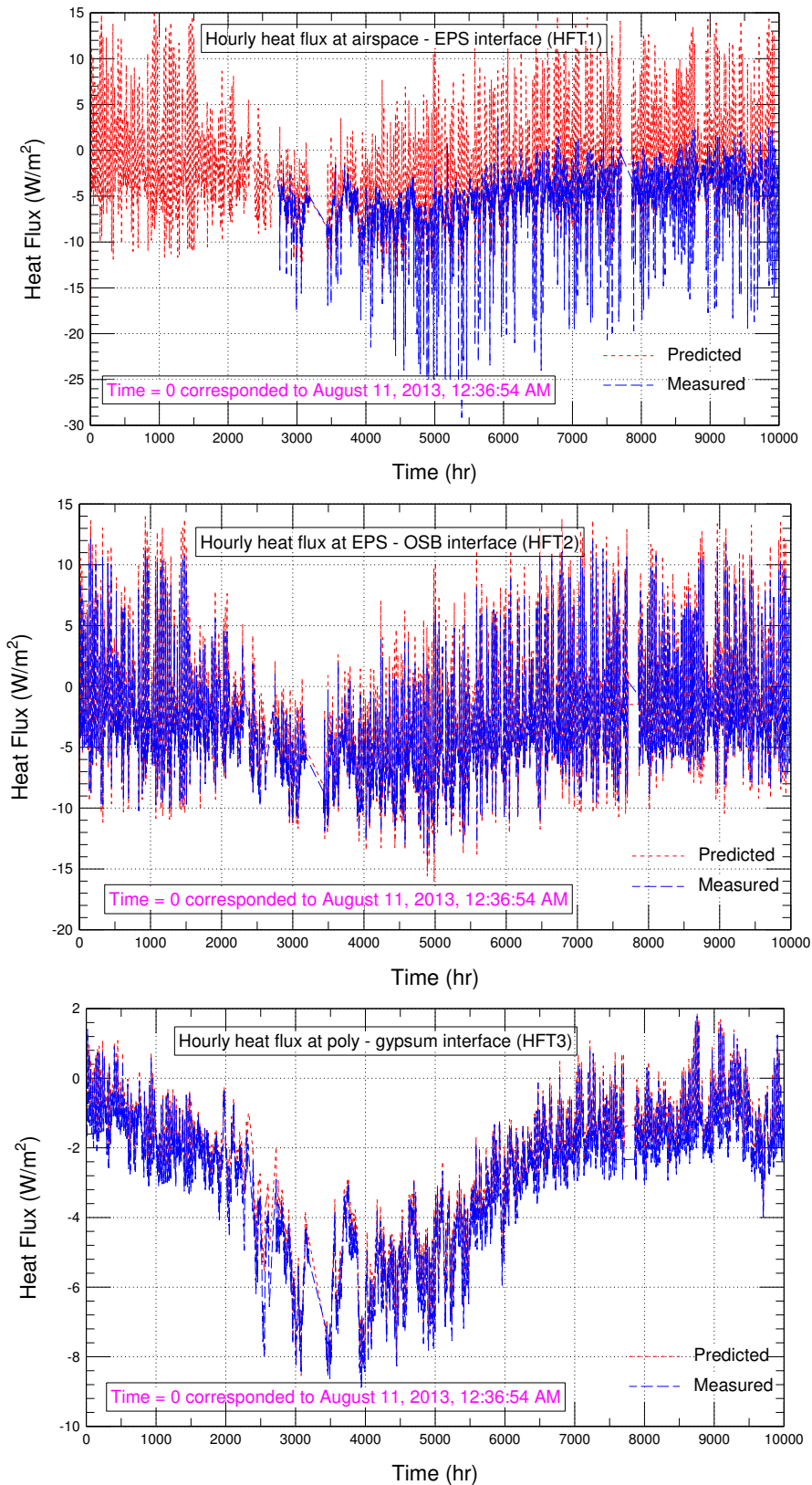
Figure 5. EPS wall (Wall 1) ─ Comparison between predicted and measured heat fluxes at interface: (i) airspace – EPS; (ii) EPS – OSB; (iii) poly – gypsum
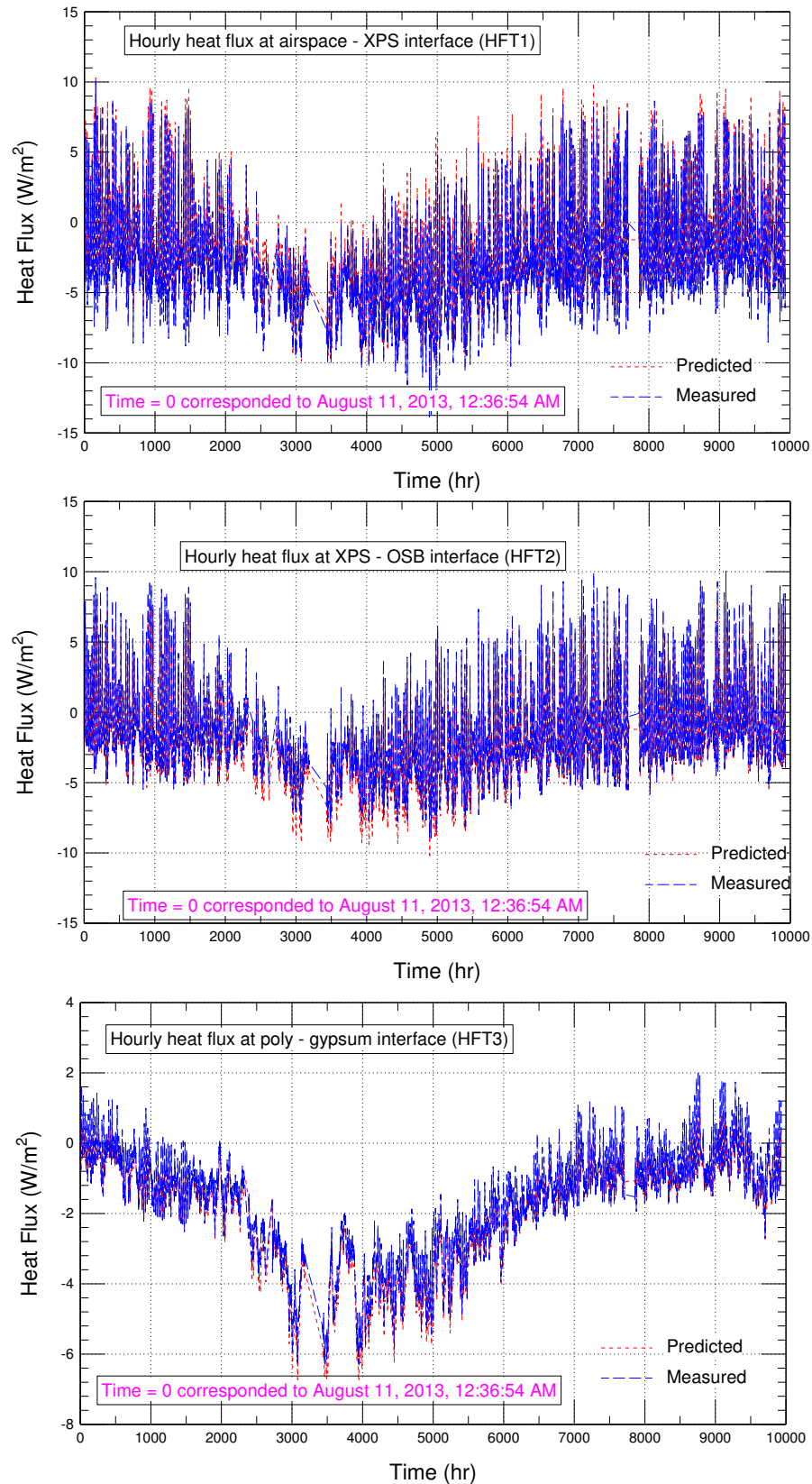
Figure 6. XPS wall (Wall 2) ─ Comparison between predicted and measured heat fluxes at interface: (i) airspace – XPS; (ii) XPS-OSB; (iii) poly-gypsum
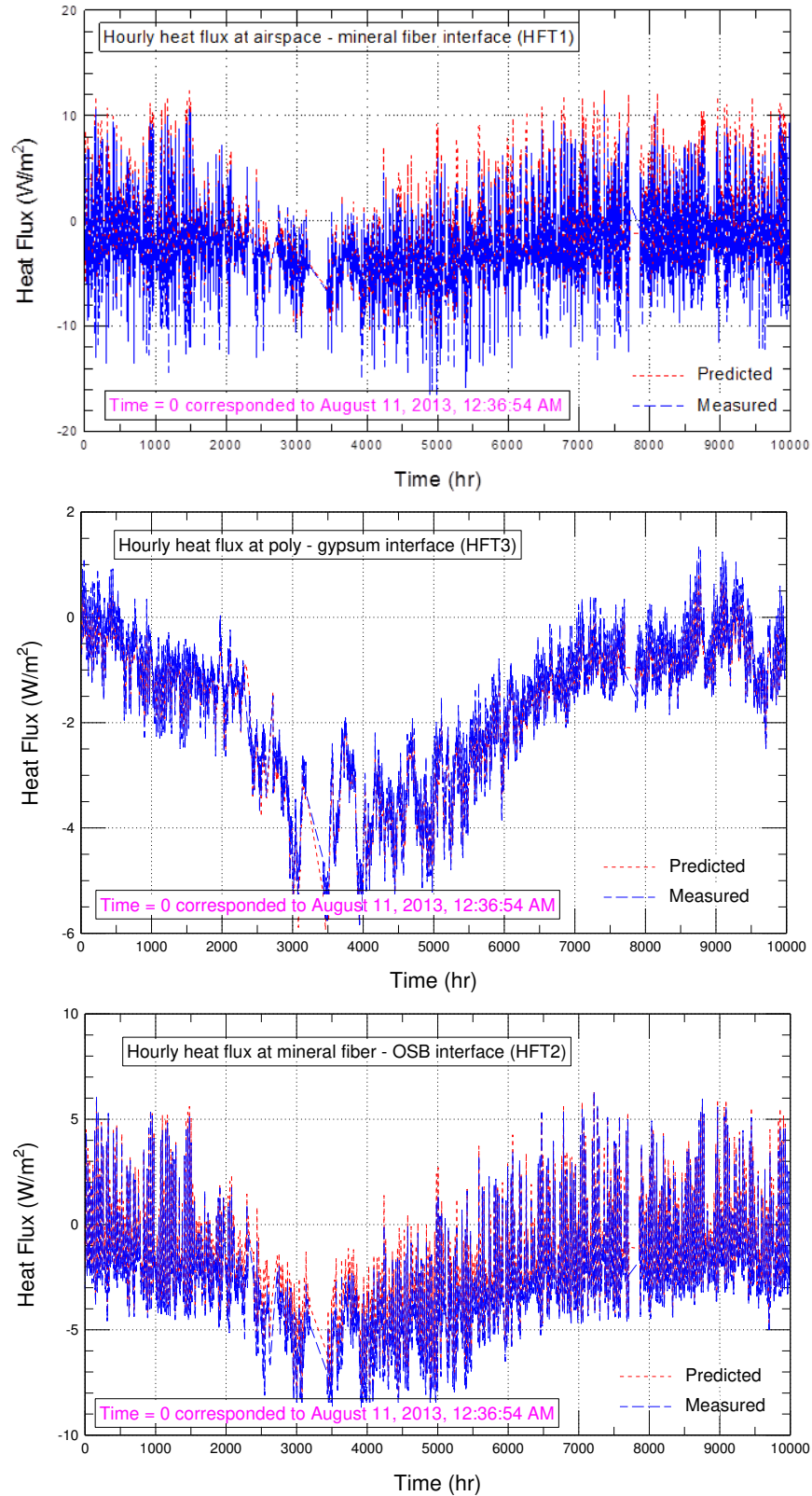
Figure 7. Mineral fibre wall (Wall 3) ─ Comparison between predicted and measured heat fluxes at airspace interface: (i) airspace – mineral fibre; (ii) mineral fibre – OSB; (iii) poly-gypsum

Thus, after benchmarking the present model in this project in respect to heat flux, and having previously benchmarked the model to several tests undertaken in field and controlled laboratory conditions as indicated in the Appendix A1.1, this model was used with confidence in this study to investigate the risk of condensation and mould growth in different wall assemblies with exterior insulations when these walls were subjected different Canadian climatic conditions.

3.6 Wall Assembly Configurations and Simulation Parameters

Hygrothermal simulations of all wall assemblies were conducted using the hygIRC-C model and using the construction details common to all wall assemblies to be modelled as listed in Table 2. For each of the materials or components specified, the rationale for the selection of specific materials is also given in this table.

Table 2. Construction details common to all wall assemblies to be modelled

Material selection	Rationale
An exterior finish consisting of vinyl cladding installed on 19 mm strapping	To minimize the impact of exterior water ingress
A weather-resistive barrier (WRB) with a WVP of 1400 ng/(Pa•s•m²) (25 US perm) such as spun bonded polyolefin membrane	Common construction and highly permeable so as not to limit the application of insulation materials for which the selection of a more vapour tight material might otherwise affect the intent of the project
2 x 6 in wood-frame construction using framing members at 16 in on center	Currently, most common construction framing used in housing
A vapour barrier with a WVP of 60 ng/(Pa•s•m²)	NBCC 2010 minimum requirement 9.25.4.2. (see reference [20])
An interior finish consisting of 12.5 mm gypsum board	Currently the most common construction method for interior finish

Figure 8 shows a schematic of the code-compliant reference wall assembly. Also, Figure 9 shows a schematic of a wall assembly with different types of insulations. The different types of exterior insulation products used in this study are listed in Table 3. As will be explained later, the locations in these wall assemblies at risk of condensation and mould are listed in Table 4.

Whereas the simulated results for moisture content and temperature are produced for every location within the wall system and at every time step (1 hr interval), an analysis of results was performed to establish which locations in the wall showed the greatest susceptibility to risk of condensation for the assemblies studied; this permitted rationalising the presentation of results. Post-processing of simulation results and reporting thus focussed on the locations reported in Table 4.
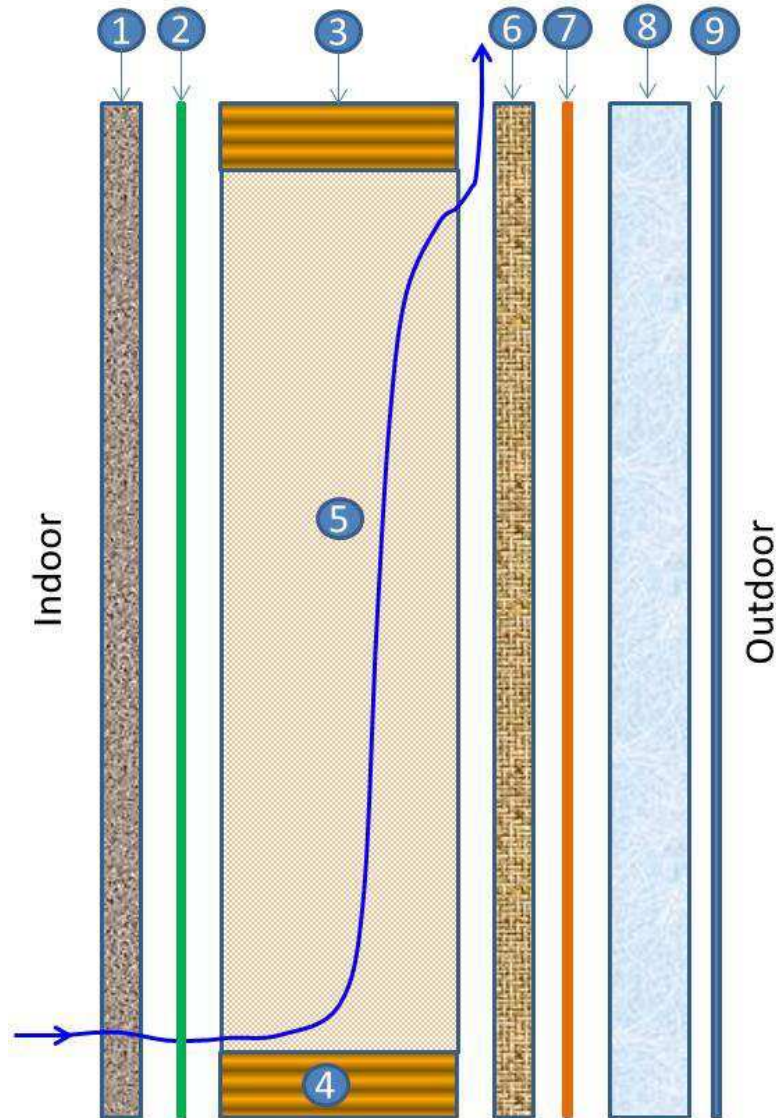
Wall Configuration

Reference wall/code Compliant: no exterior insulation

1. Gypsum board
2. Vapour Barrier (WVP = 60 ng/(Pa.s.m^2))
3. Top plate
4. Bottom plate
5. Fibreglass insulation (R-24)
6. OSB
7. WRB (WVP = 1400 ng/(Pa.s.m^2)
8. Air
9. Vinyl siding installed on 19 mm strapping*

*WVP = 40-70 perms, S.V. Glass, Building Science Corporation (2010)

Figure 8. Schematic of reference wall assembly/code compliant configuration showing different component layers and assumed path of air flow through assembly (no exterior insulation)
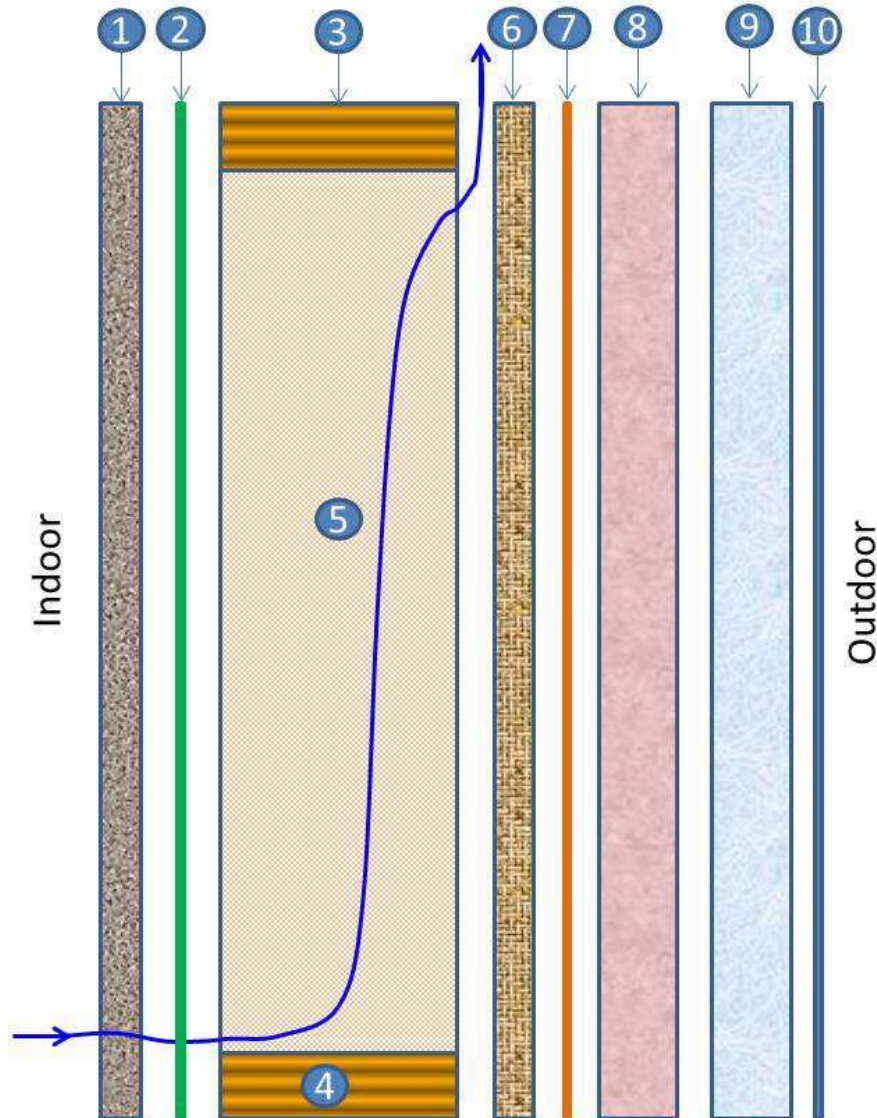
Wall Configurations

Walls with exterior insulation

1. Gypsum board
2. Vapour Barrier (WVP = 60 ng/(Pa.s.m^2))
3. Top plate
4. Bottom plate
5. Fiberglass insulation (R-24)
6. OSB
7. WRB (WVP = 1400 ng/(Pa.s.m^2)
8. **Exterior Insulation:**
   (a) **EPS of 1 in thick (Wall-1)**
   (b) **XPS of 2 in thick (Wall-2)**
   (c) **Roxul of 3 in thick (Wall-3)**
9. Air
10. Vinyl siding installed on 19 mm strapping*

*WVP = 40-70 perms, S.V. Glass, Building Science Corporation (2010)

Figure 9. Schematic of wall assembly configurations with exterior insulations showing different component layers and assumed path of air flow through assembly

Table 3. Wood framed (2 x 6-in.) wall systems with exterior insulations

Parameter	Wall 1	Wall 2	Wall 3
2x6-in. Wood-Framing Cavity Insulation	**Batt Insulation of R-24 (RSI-4.2)**		
Exterior Insulation Details			
Type	EPS	XPS	Mineral fibre
Thickness (in)	**1 (25 mm)**	**2 (51 mm)**	**3 (76 mm)**
Dry Density (kg/m^3)	18	26	122
Dry Thermal Conductivity (W/(m•K))	0.0369	0.0290	0.0347
Vapor Permeability (kg•m/(s•m^2•Pa))	2.91E-12	1.39E-12	1.62E-10
Total Vapor Permeance (ng/(s•m^2•Pa))	114.4	27.4	2129
Vapor Permeance ((ng/(s•m^2•Pa))/25 mm)	**114.4**	**54.9**	**6390**
Total RSI-value (m^2•K/W)	0.69	1.75	2.20
Total R-value (ft^2•hr•^{o}F/BTU)	3.91	9.95	12.47
R-value ((m^2•K/W)/25.4 mm)	0.69	0.88	0.73
R-value ((ft^2•hr•^{o}F/BTU)/in)	**3.9**	**5.0**	**4.2**

Table 4. Locations in wall assembly at risk of condensation and mould growth

Location (see Figure 16)	Depths and heights (mm; inches)
Top plate layer	51 and 63 mm (2 and 2.5 inches)
Insulation at top plate	10 mm by 51 and 63 mm (2 and 2.5 inches)
Interface between top plate and insulation	2.5 inches
Insulation at base of wall assembly	10 mm deep by heights of 152, 305, 457 mm (6, 12 and 18 inches)
Interface between sheathing panel and insulation	152 and 305 mm (6 and 12 inches)

4. Simulation Conditions for Parametric Study

In this section, the different simulation conditions are discussed that were used to conduct the numerical simulations for all wall assemblies shown in and Figure 8 and Figure 9 (see Table 3).

4.1 Vapour Barrier Conditions

As provided in Subsection 9.25.4 of the NBCC [20], the current maximum allowable WVP value for vapour barriers is 60 ng/(Pa•s•m²). This parametric study was conducted using a vapour barrier with a WVP of 60 ng/(Pa•s•m²) as provided in Table 2.

4.2 Air Leakage Conditions

All cases were modeled with some air flow introduced through openings into the assembly, as this is a likely scenario given the imperfections of the air barrier system of wall assemblies. Additionally, completing the investigation without considering the effects of air leakage would not create useful results in terms of assessing the risk to the formation of condensation in wall assemblies given that air leakage of indoor air to the wall assembly (i.e. exfiltration) is the primary cause for the formation of condensation in the assembly itself.

The modelling assumed that the path for air movement is initiated at the interior and is introduced at the bottom of the wall and thereafter moisture is deposited along the interior face of the sheathing panel and exits through the top of the wall. This air leakage path was one of the scenarios used in the study by Ojanen and Kumaran [57] in which it was assumed that air would move through imperfections that existed at the wall top plate and the joint between the interior face of the exterior sheathing and the exterior of the top plate. For the code-compliant reference wall (i.e. no exterior insulation), this air leakage path is shown Figure 8, and that for walls with exterior insulation is shown Figure 9.

The air leakage rate for all cases in all locations was set to 0.1 L/(s•m²) at 75 Pa, which was an assumption used in at least one previous study (see [57, 69, 70]). These air leakage conditions are those assumed for the wall components of a home and would be roughly an order of magnitude smaller than the whole house air leakage of an R-2000 qualified home as provided by NRCan[2].

The impact of this assumption on the hygrothermal performance was investigated in a sensitivity analysis, by modelling a wall assembly with different air leakage rates ranging between 0 and 0.1 L/(s•m²) at 75 Pa. The results from such an analysis permitted deriving the least performing and most vulnerable wall assembly with respect to the formation of condensation and the risk to the formation of mould within the assembly. In this report, rates of air leakage referred to as 0%, 50% and 100% of air leakage relate, respectively, to 0.0, 0.05 and 0.1 L/(s•m²) at 75 Pa. As indicated later, the results of the sensitivity study supported the selection of 0.1 L/(s•m²) at 75 Pa as a means of challenging the wall system with moisture ingress from air leakage.

---

[2] http://www.nrcan.gc.ca/energy/efficiency/housing/new-homes/5089: R-2000 Standard - 2012 Edition; Natural Resources Canada's Office of Energy Efficiency; 16 p; § 4.3 Airtightness Requirements: The building envelope shall be constructed sufficiently airtight such that either the air change rate at 50 Pascals is no greater than 1.5 air changes per hour; 1.5 ACH @ 50 Pa is equivalent to 0.61 L/s-m² @ 50 Pa and would necessarily be higher at 75 Pa.

NRC·CNRC

4.3 Approach to Simulation of Air Leakage

In the present study, the air leakage rate (Q) as a function of the total pressure differential across the wall assemblies (ΔP_{tot}) is given as:

$$Q = a\,\Delta P_{tot}^{n} \tag{1}$$

In a previous NRC project "Wall Energy Rating, WER" [22, 23, 24, 25 and 26], the air leakage rates were measured for a number of 2 x 6 in wood-frame wall systems having different types of thermal insulation in the wall cavities including open cell spray foam, closed cell spray foam, and glass fibre. For the full-scale wall systems with and without penetrations and having glass fibre insulation, the average value of the exponent 'n' in Eq. (1) was 0.7; this value was used in this study and other studies [69, 70]. The value of the coefficient 'a' in Eq. (1) was determined to satisfy the condition at which the air leakage rate is 0.1 L/(s•m²) at ΔP_{tot} = 75 Pa when the exponent n = 0.7. As such, the value of the coefficient 'a' is equal 0.00487 L/(s•m²•Pa$^{0.7}$) where Q in L/(s•m²) and ΔP_{tot} in Pa.

In Eq. (1), the total pressure across the building envelope can be calculated as:

$$\Delta P_{tot} = \Delta P_{wind} + \Delta P_{st} + \Delta P_{ven} \tag{2}$$

Where:

ΔP_{wind} is the pressure differential due to wind;

ΔP_{st} is the pressure differential due to the stack effect; and

ΔP_{ven} is the pressure differential due to mechanical ventilation system (i.e. pressurization or depressurization due to heating and cooling conditions).
In this study, ΔP_{ven} was neglected and thus $\Delta P_{ven} = 0$.

The full details for calculating both the pressure differential due to the stack effect and wind pressure differential given different climatic conditions are available in reference [69]. As indicated in [69] and [70], the greater the exfiltration rate the higher the risk of formation of condensation and mould growth within the wall assembly; the wall is located, as previously noted, at the third storey and facing the direction of the highest exfiltration rate (e.g. see Figure 10 and Figure 11 for Ottawa climate). This would thus represent the worst case scenario for the risk of formation of condensation and mould growth within the wall cavity. As such, all wall assemblies shown in Figure 8 and Figure 9 (see also Table 3) that were investigated in this study represent wall assemblies of the third storey of low-rise buildings.
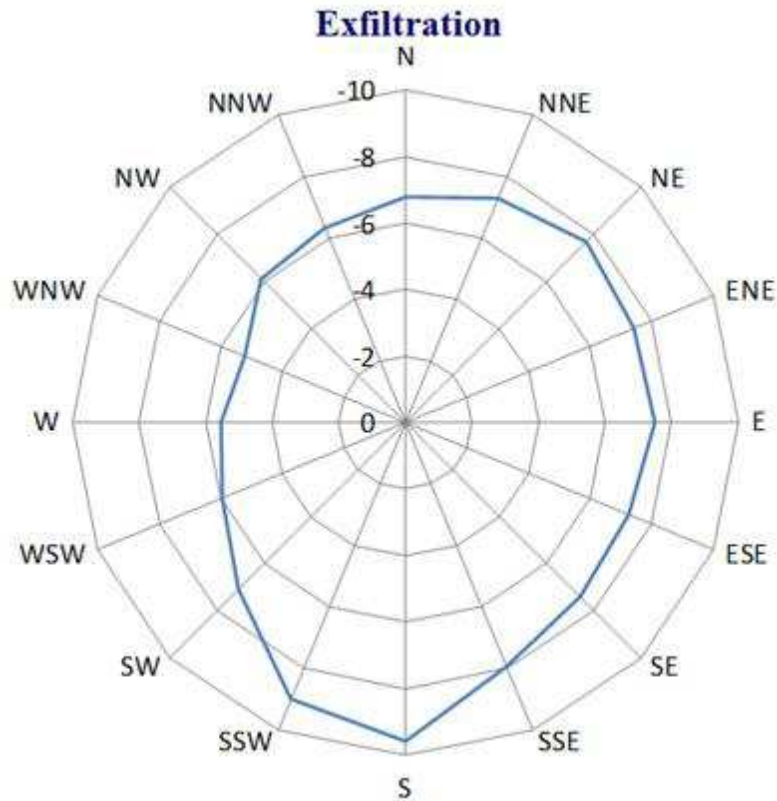
Figure 10. Exfiltration: Average yearly negative wind pressure in Pa (wet year of Ottawa weather)
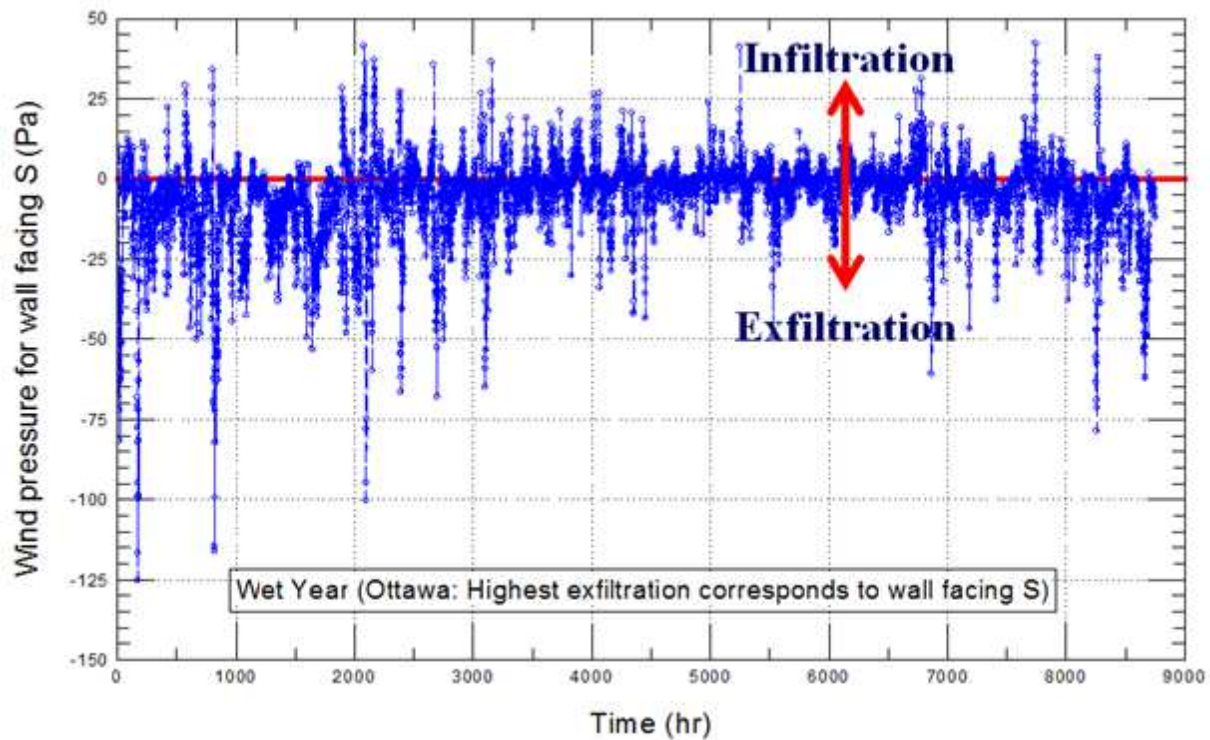
Figure 11. Hourly wind pressure of wall facing south (wet year of Ottawa weather)

4.4 Climatic Conditions

The wall assemblies (see Figure 8, Figure 9 and Table 3) were subjected to different climatic conditions of five different locations within Canada and having differing values of Heating Degree Days (HDD) and Moisture Index (MI), namely:

- **Vancouver, BC** (mild, wet, HDD18 = from 2600 to 3100, MI = 1.44),
- **St John's, NL** (cold, wet, HDD18 = 4800, MI = 1.41),
- **Ottawa, ON** (cold, dry, HDD18 = 4440 - 4500, MI = 0.84),
- **Edmonton, AB** (cold, dry, HDD18 = 5120, MI = 0.48), and
- **Yellowknife, NT** (cold, dry, HDD18 = 8170, MI = 0.58).

The first four cities were recommended by the Task Group (TG) on Properties and Position of Materials in the Building Envelope[‡]. The last city (Yellowknife) was recommended by the client of this project.

As indicated earlier, the wall assemblies of the third storey of low-rise buildings were modeled in the orientation showing the highest average annual air exfiltration rate. The walls were assumed to be shaded to minimize the impact of solar-driven moisture ingress into the assembly and to minimize the solar drying effect on the wall. However, diffuse radiation was taken into consideration.

4.5 Weather Data

Hygrothermal simulations were conducted for a period of two years. The first year corresponded to an average year (conditioning year, where equal drying and wetting potential exists) and the second year corresponded to a wet year. Note that the wet year in each location was the worst-case situation given that the drying potential for a wall assembly is limited during a wet as compared to a drier year. The weather data of the different locations were obtained from the NRC's weather database.

4.7 Indoor Conditions

Regarding to the indoor moisture load, the water vapour pressure differential across the wall assembly (from indoor to outdoor) corresponds to a moisture load of 5.2 g/m³, which is consistent with previous studies, in which a moisture load of 7.1 L/day was chosen for a 1 storey, 80 m² house, with indoor temperature of 21°C, water vapour pressure differential close to 700 Pa, and 0.3 ACH by mechanical ventilation, for which $\Delta P_v = P_{v,indoor} - P_{v,outdoor} = 700$ Pa, which is referred to Option-A. Given the climatic conditions of Ottawa, as an example, the indoor relative humidity (RH_{ind}) of Option-A is shown in Figure 12. As shown in this figure, Option-A resulted in a high value for RH_{ind}, which at times exceeded 100%. As such, four additional different options for the indoor RH profile within a period of one year were compared as shown in Figure 12. Discussions to explore these options took place with the Task Group

---

[‡] TG acting on behalf of the NBCC Standing Committee on Housing and Small Buildings (SCHSB).

NRC·CNRC

(TG) on Properties and Position of Materials in the Building Envelope[§] [69]; to summarise the options considered:

- Option A. ΔP_v = 700 Pa

- Option-B. This option was based on the method given in ASHRAE 160.

- Option-C. This option was similar to Option-A (i.e. ΔP_v = 700 Pa) but the value of RH_{ind} was capped at 70%.

- Option-D. This option was based on a modified ASHRAE 160 by reducing the interior RH with increasingly cold temperatures in the wintertime.

Option-C was the recommended[**] option to evaluate the indoor relative humidity [69] and was used in this study to conduct all numerical simulations of different wall assemblies that are listed in Table 3.

Other indoor conditions (i.e. indoor temperature) were set according to that provided in the ASHRAE Standard 160 [64] with respect to recommendations for conditioned space.
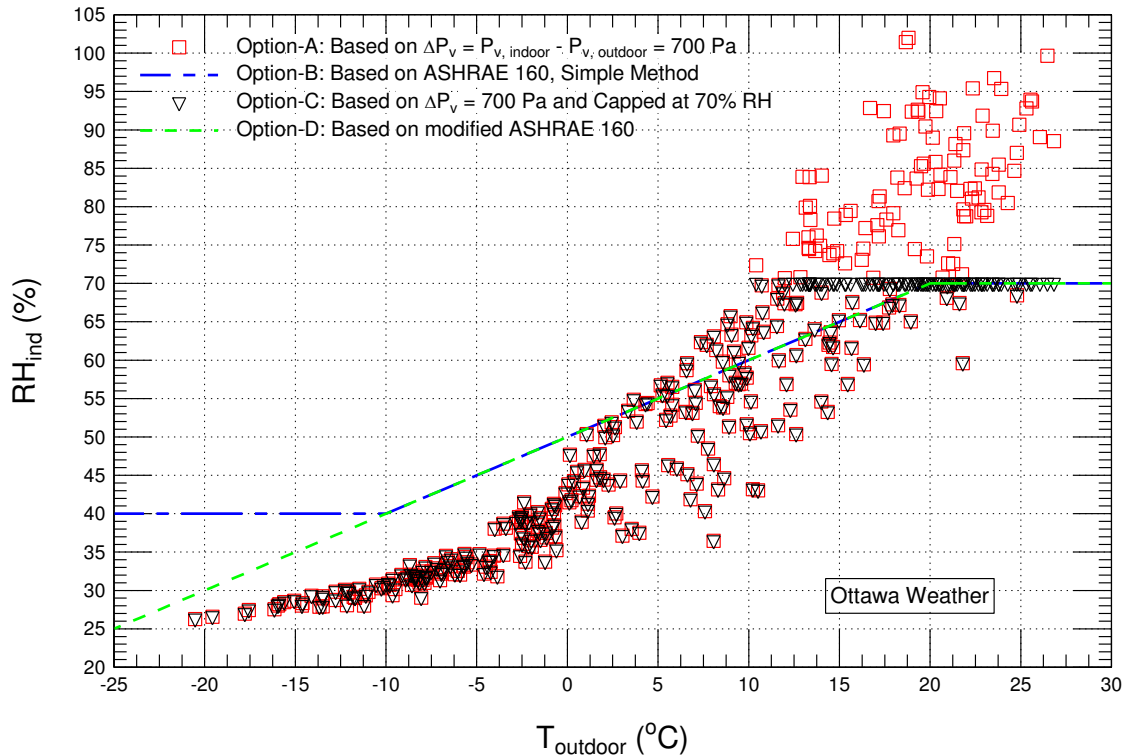
Figure 12. Different options for indoor relative humidity (Ottawa weather)

4.8 Initial Conditions

The initial temperature in all layers of the wall assemblies were taken equal to 21°C and the initial moisture content of all material layers corresponded to a relative humidity of 50%.

[§] TG acting on behalf of the NBCC Standing Committee on Housing and Small Buildings (SCHSB).
[**] NBC TG on Low Permeance Materials [69]

4.9 Material Properties

In this study, the hygrothermal properties for the exterior insulations in Wall 1 (EPS), Wall 2 (XPS) and Wall 3 (Mineral fibre) were measured. A sheathing panel made of 7/16 in (11 mm) thick OSB was considered for all wall assemblies. Glass [65] compiled the available data for the WVP of OSB (11 mm thick), which is shown in Figure 13. The recommended values of WVP of OSB as a function of RH that were used in the numerical simulations are shown by the solid curve in this figure. A curve fit of these data is also provided in Figure 14. The hygrothermal properties of the other material layers shown in Figure 8 and Figure 9 were obtained from the NRC's material database. A summary of the simulated conditions for all wall assemblies are provided in Table 5.

Table 5. Summary of simulated conditions

Criteria	Assumptions/Conditions
Pressure exponent, n	0.7 (see Eq. (1))
Predominant wall orientation	Facing the highest exfiltration rate
ΔP for stack effect	Top storey of a 3-storey building to maximize the effect of exfiltration
ΔP for ventilation	Assume depressurization/pressurization from ventilation source is negligible
Air leakage rate, Q	Corresponds to 0.0, 0.05 & 0.1 L/(s•m^2) at 75 Pa[††]
Interior moisture load	Constant water vapour pressure differential, ΔP_v = 700 Pa and capped at 70% RH
Water vapour permeance of OSB	Function of the relative humidity ranging from 0-100% as recommended by Glass [65]
Modelling period	Two years – Jan to Dec: one average year followed by one wet year
Geographical locations	Ottawa (ON), Edmonton (AB), Vancouver (BC) and St John's (NL)

5. Acceptable Performance

The modelling results for each case were expressed using the mould index (M) criteria developed by Hukka and Viitanen [66], Viitanen and Ojanen [67], and Ojanen et al. [68]. The selected mould index criteria allowed sufficient resolution to assess the risk of moisture condensation in the cases where the modeled assembly currently does not have to comply with the information provided in Table 9.25.5.2 of the NBCC 2010 [20] or where the modeled assembly does not comply, but the requirements apply. The descriptions of the mould index levels are provided in Table 6.

The most recent mould model by Ojanen et al. [68] was used in this study to determine the mould index of different materials of the wall assemblies. In that model [68], the sensitivity of different construction materials for mould growth was classified in four sensitivity classes,

---

[††] These rates of air leakage across the wall components are not unreasonable given that the whole house air leakage for a R-2000 or an ENERGY STAR qualified home is roughly an order of magnitude greater than the wall.

namely, very sensitive, sensitive, medium resistant and resistant (see Table 7). Table 8 provides the assumed correspondence of sensitivity class for materials located within the wall assembly modelled in this study. More specifically, the sensitivity class for the top and bottom plates, OSB and foam was considered "Sensitive", whereas the sensitivity class of the materials for cavity insulation (fiber-based), drywall and membranes was considered "Medium Resistant".
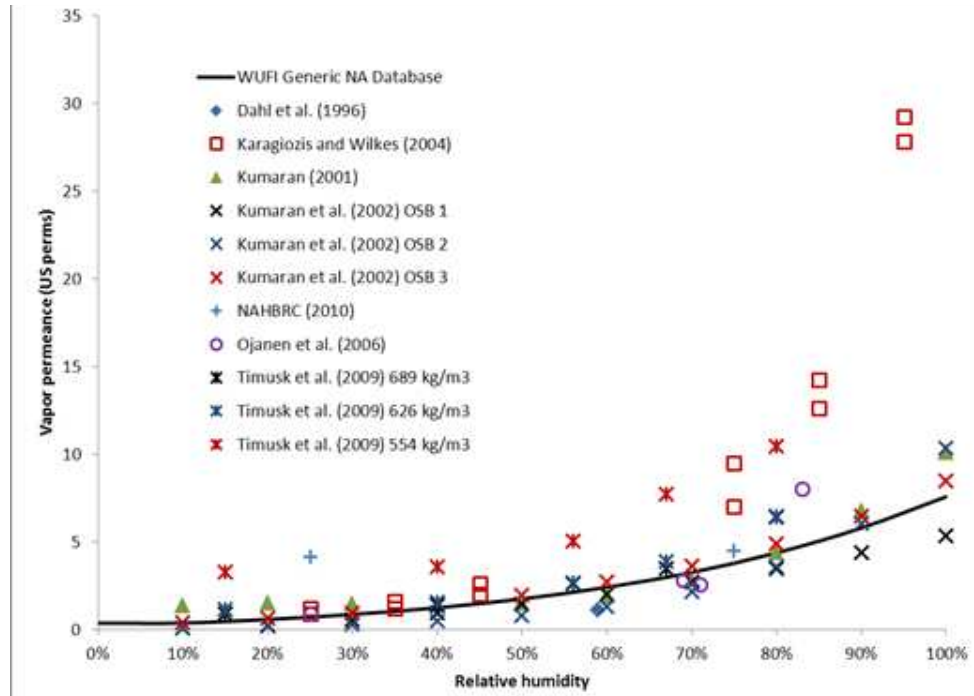
Figure 13. Dependence of water vapor permeance (WVP) of OSB of 11 mm thick on the relative humidity; compilation of data provided by Glass [65]
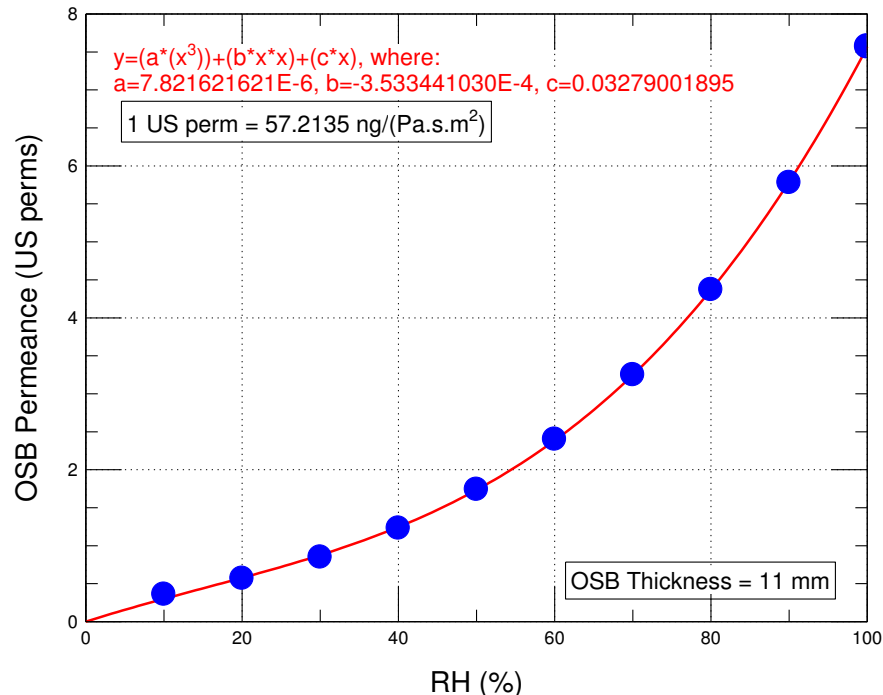
Figure 14. WVP of OSB of 11 mm thick that used in numerical simulations

Table 6. Description of Mould Index (M) levels [66, 67, 68]

M	Mould Index (M) Description of Growth Rate
0	No growth
1	Small amounts of mould on surface (microscope), initial stages of local growth
2	Several local mould growth colonies on surface (microscope)
3	Visual findings of mould on surface, < 10% coverage, or < 50% coverage of mould (microscope)
4	Visual findings of mould on surface, 10%–50% coverage, or > 50% coverage of mould (microscope)
5	Plenty of growth on surface, > 50% coverage (visual)
6	Heavy and tight growth, coverage about 100%

Table 7. Mould growth sensitivity classes and some corresponding materials [68]

Sensitivity Class	Materials	RH_{min} (%)[*]
Very Sensitive	Pine sapwood	80
Sensitive	Glued wooden boards, PUR with paper surface, spruce	80
Medium Resistant	Concrete, aerated and cellular concrete, glass wool, polyester wool	85
Resistant	PUR with polished surface	85

* Minimum relative humidity needed for mould growth

Table 8. Mould growth sensitivity classes for materials of wall assemblies listed in Table 3

Sensitivity Class	Material Layers of Wall Assemblies	RH_{min} (%)[*]
Very Sensitive		80
Sensitive	Top plate, bottom plate, OSB, foam	80
Medium Resistant	Fiberglass insulation, gypsum, membranes	85
Resistant		85

*Minimum relative humidity needed for mould to grow

Defining which level of mould index listed above is critical (i.e. the threshold of mould index) is not available at this time. However, the values of the mould index of client's walls are compared against the value of the mould index of the reference wall/code compliant to determine whether or not the performances of client's walls are as good as the reference wall. Currently, the TC of ASHRAE SSPC 160 is working to implement the mould index in ASHRAE 160. One of the tasks of the TC is consult with the researchers from Finland and Germany who developed the mould index criteria in order to define the threshold of the mould index.

6. Approach for Assessing the Overall Performance

As an example of the variation in values of mould index at different locations within a wall assembly over the simulation period, results for the EPS (Wall 1) wall assembly subjected to the climatic conditions of Ottawa are provided in Figure 15; the results are for the case where the air leakage rate was assumed to be 0.1 L/(s•m²) at 75 Pa (i.e. 100%). The values for the mould index for all the different locations within the wall assembly are shown illustrating the broad variation in values of mould index that arose from the simulation results. The corresponding

results for the reference wall, XPS wall and mineral fibre wall are available in Appendix – A
(Figure A - 6, Figure A - 7 and Figure A - 8). On the basis of this combined information, the
primary locations within the wall assemblies at risk for condensation of moisture and possible
mould growth were identified as those located at either the top or bottom portion of a wall
assembly. All of these "at risk" locations are listed in Table 9 and also identified in Figure 16.

Table 9. List of locations at risk of condensation and at which mould index evaluated

#	Figure 16a	Top Portion of Wall Components at Risk of Mould Growth:
1		Whole top plate layer
2		Whole top plate - cavity insulation interface
3		Top plate layer (51 mm (2 in) long)
4		Top plate layer (64 mm (2.5 in) long)
5		Top plate -cavity insulation Interface (51 mm (2 in) long)
6		Top Plate -cavity insulation Interface (64 mm (2.5 in) long)
7		Top cavity insulation of 10 mm (0.4 in) high (51 mm (2 in) long)
8		Top cavity insulation of 10 mm (0.4 in) high (64 mm (2.5 in) long)
9		Top cavity insulation of 10 mm (0.4 in) high - cavity insulation interface (51 mm (2 in) long)
10		Top cavity insulation of 10 mm (0.4 in) high - cavity insulation interface (64 mm (2.5 in) long)
	Figure 16b	Bottom Portion of Wall Components at Risk of Mould Growth:
11		cavity insulation (10 mm (0.4 in) thick, 457 mm (18 in) high)
12		cavity insulation (10 mm (0.4 in) thick, 305 mm (12 in) high)
13		cavity insulation (10 mm (0.4 in) thick, 152 mm (6 in) high)
14		OSB-cavity insulation Interface (305 mm (12 in) high)
15		OSB-cavity insulation interface (152 mm (6 in) high)

For the purpose of comparing the performance of different wall assemblies, these results are
presented on basis of a simplified form using the following two parameters [69 and 70]:

- M_{AVG}: Overall average value of mould index at different locations in the wall; these
  locations are listed in Table 9 for different wall systems.
- M_{MAX}: Overall maximum value of mould index at different locations in the wall

The two parameters above were determined based on a simulation period of two years, i.e.,
simulation of the average year followed by a wet year for the location of interest (see Table 9).

Both these values are provided for each of the different wall configurations having nominal
insulation in the stud-cavity (referred to as inboard insulation) of R-24, as well as for each of the
exterior insulation conditions (referred to as outboard insulation); exterior insulation conditions
varied from R-0 (i.e. reference wall) to values of R-3.91, R-9.95, and R-12.47. However, for the
climatic conditions of Edmonton, which is the coldest climate amongst the other climates
investigated in this study, stud-cavity insulation of R-19 was also considered in this study to
allow comparison of the risk of condensation and mould growth in these walls to the case of a
wall having stud-cavity insulation of R-24.

Figure 15. Mould index at different locations inside the EPS wall for the case of 100% air leakage rate (Ottawa weather)
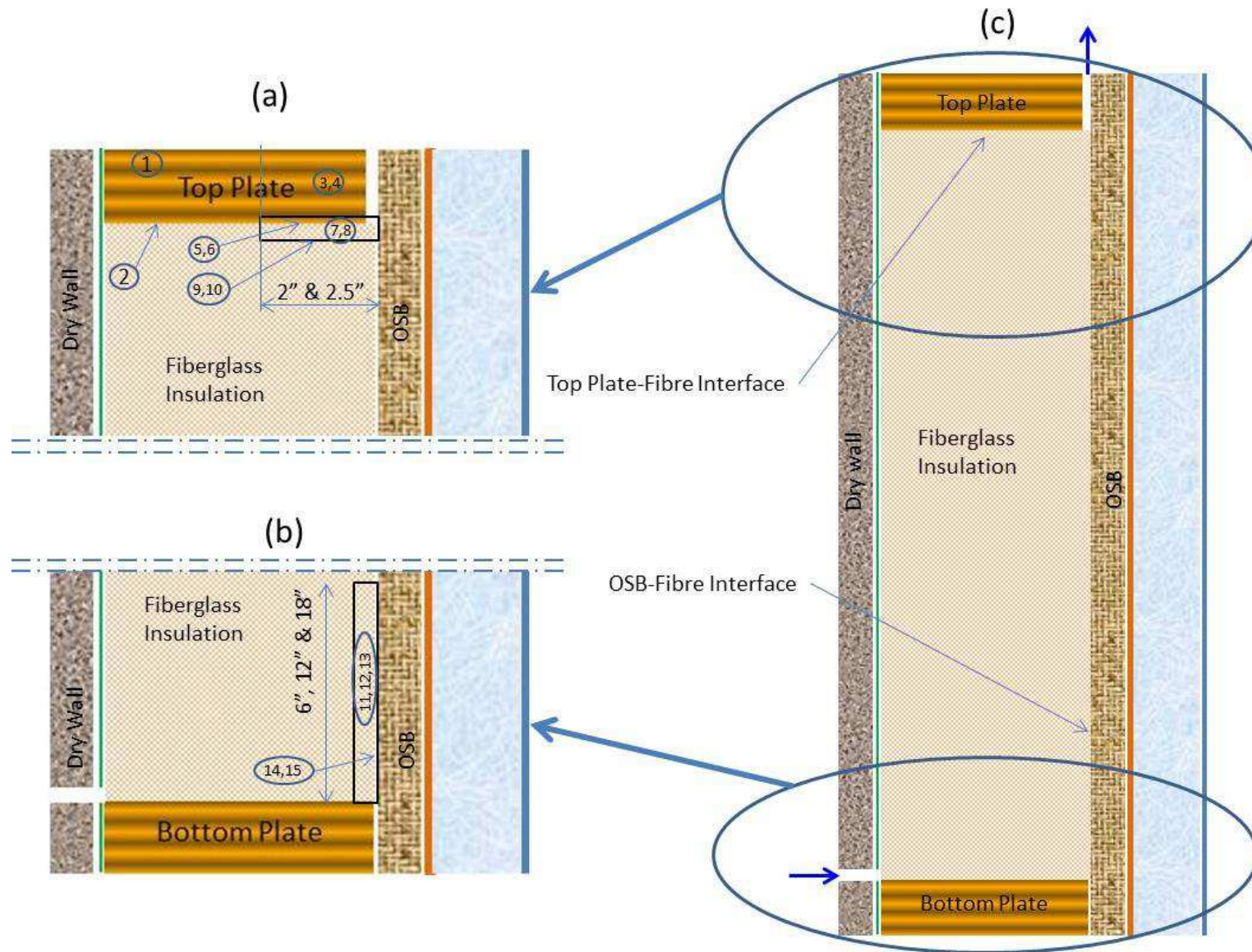
Figure 16. Locations in wall assembly at risk of formation of condensation and mould growth: (a) Location at top plate and in the top plate, the insulation, and along interface between top plate and insulation layers; (b) at base plate of wall assembly in insulation and along interface between sheathing panel and insulation (see Table 9)

7. Results and Discussion

In this section, the effects of different parameters that affect the hygrothermal performance of wall assemblies are discussed. The list of wall assemblies is provided in Table 3. In this report, in instances where the units for Water Vapour Permeance (WVP) and R-value are not reported, the units for each of these parameters are respectively, ng/(Pa•s•m²) and ft²•h•°F/BTU. Note that all results derived for the reference wall having stud-cavity insulation of R-19 and R-24 and that were provided in this report were obtained from a previously published NRC project entitled "Properties and Position of Materials in the Building Envelope for Housing and Small Buildings" (see [69] for more details).

The different parameters affecting the hygrothermal performance of wall assemblies and discussed in this section include the effect of:

- Air leakage rate;
- R-value of stud-cavity insulation; and
- Geographical locations.

7.1 Effect Air Leakage Rate

A parametric study was conducted to investigate the effect of the air leakage rate on the hygrothermal performance of wall assemblies listed in Table 3. This parametric study was conducted to investigate the risk of mould growth in a wall assembly and permit identifying within the assembly the locations of likely mould growth given the different air leakage rates to which it was subjected. In these analyses, the full amount of the air leakage rate given by Eq. (1) (i.e. ξ = 100%) and different percentages of that value (ξ = 0% and 50%) were considered.

The Mould Index (M) was calculated for different wall assemblies on the basis of the mould sensitivity classes of the different material layers within the wall assembly as provided in Table 8. It is important to point out that the locations within the wall assemblies at risk of condensation and mould growth are based on the respective air leakage paths that were considered in this study and shown in Figure 8 and Figure 9. It is noted that a different air leakage path, however, would result in different locations within the wall assemblies at risk of condensation and mould growth.

Figure 17a and Figure 17b, respectively, show the overall average mould index (M_{AVG}) and overall maximum mould index (M_{MAX}) for different percentages of the air leakage rate of ξ = 0% (no air leakage), 50%, and 100% for the wall system with exterior insulation of EPS (RSI-0.69 and WVP = 114 (R-3.9 and WVP = 2.0 US perm)), subjected to different climatic conditions. As shown in these figures, decreasing the air leakage rate resulted in decreasing the risk of condensation and mould growth, whereas no risk of condensation occurred at ξ = 0%. For example, the values of M_{AVG} for the case of ξ = 50% are 29%, 44%, 75% and 56% of the values of M_{AVG} for ξ = 100%, respectively, for Ottawa, Edmonton St John's, and Vancouver (Figure 17a). Note that at a pressure difference (ΔP) of 75 Pa, ξ = 50% corresponds to an air leakage of 0.05 L/(s•m²) whereas ξ = 100% corresponds an air leakage rate of 0.1 L/(s•m²). Furthermore, the values of M_{MAX} for the case of ξ = 50% are 42% and 56%, 83% and 70% of the values of M_{MAX} for the case of ξ = 100% for Ottawa, Edmonton St John's, and Vancouver, respectively (Figure 17b).

For the wall system with XPS exterior insulation of R-10 and WVP = 27, Figure 18a and Figure 18b show the effect of air leakage rate on the overall maximum and average mould index. Similar to the results obtained for the EPS wall, decreasing the air leakage rate resulted in decreasing the risk of condensation and mould growth.   As shown in Figure 18a, the values of M_{AVG} for the case of ξ = 50% are 18% and 32%, 58% and 40% of the values of M_{AVG} for ξ = 100%, respectively for Ottawa, Edmonton St John's, and Vancouver. The corresponding values of M_{MAX} for the case of ξ = 50% are 56% and 52%, 90% and 79%, respectively, of the values of M_{MAX} for ξ = 100% for Ottawa, Edmonton St John's, and Vancouver (Figure 18b).

Figure 19a and Figure 19b show M_{AVG} and M_{MAX} for different air leakage rates for the wall system with mineral fibre exterior insulation of R-12.5 and WVP = 2130, when this wall was subjected to different climatic conditions. As shown in these figures, the values of M_{AVG} for ξ = 50% are 31% and 40%, 79% and 66% of the values of M_{AVG} for ξ = 100%, respectively, for Ottawa, Edmonton St John's, and Vancouver (Figure 19a). Also, the values of M_{MAX} for ξ = 50% are 56% and 52%, 90% and 79% of the values of M_{MAX} for ξ = 100% for Ottawa, Edmonton St John's, and Vancouver, respectively (Figure 19b).

The air leakage in buildings has consistently improved since the 1990s when the NBCC began to mandate a 'designated' air barrier system. The air barrier system is to provide a 'designated' element to be the 'principal plane of airtightness' and accessories and components to maintain continuity of the airtightness across joints and penetrations. The value of the air leakage rate for an air barrier system was recommended to be 0.1 L/(s•m²), at a pressure difference of 75 Pa, for typical indoor winter conditions of 27% to 55% RH at 21°C. This recommended air leakage rate was introduced in the 1995 NBCC [14] and continues to be referenced in the 2010 NBCC (A-5.4.1.2. (1) and (2)) [16]. In the previous study [69], the Task Group (TG) on Properties and Position of Materials in the Building Envelope[‡‡] recommended using an air leakage rate of 0.1 L/(s•m²) to investigate the risk of condensation in different wall systems. This value for the air leakage rate was also used in the present study.

7.2 Effect of Inboard and Outboard Insulations

In a previous NRC project [69] and for the case of a 100% air leakage rate, numerical simulations were conducted to investigate the effect of the inboard (stud-cavity) insulation on the risk of condensation and mould growth for different wall assemblies. In a previous project [69], two types of stud-cavity fibre insulation products having nominal R-values of RSI-3.35 (R-19) and RSI-4.23 (R-24) were investigated for wall systems with and without outboard insulation, and having of wide range of R-values (R-4, R-5 and R-6) and values of WVP (2 to 1800 ng/(Pa•s•m²)), when these walls were subjected to the climates of Ottawa, Edmonton, St John's and Vancouver. The results of that study [69] showed that the wall systems having stud-cavity insulation of R-24 have a higher risk of condensation and mould growth than that for wall systems with stud-cavity insulation of R-24. This project focuses on wall systems with stud-cavity insulation of R-24. However, as an example, simulations were conducted when the EPS wall, XPS wall and mineral fibre wall have stud-cavity insulation of R-19 and R-24 when these walls were subjected to the climate of Edmonton.

[‡‡] TG acting on behalf of the NBCC Standing Committee on Housing and Small Buildings (SCHSB).
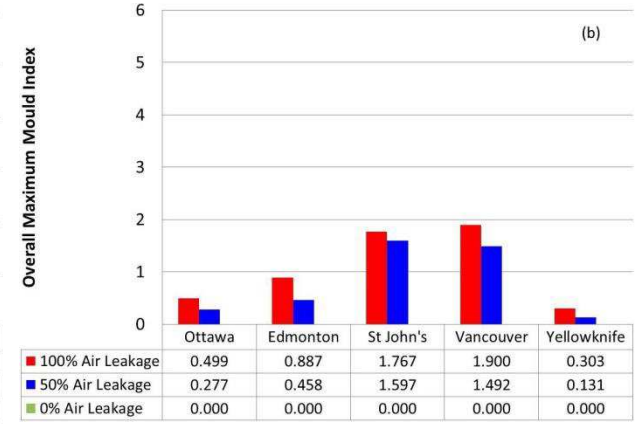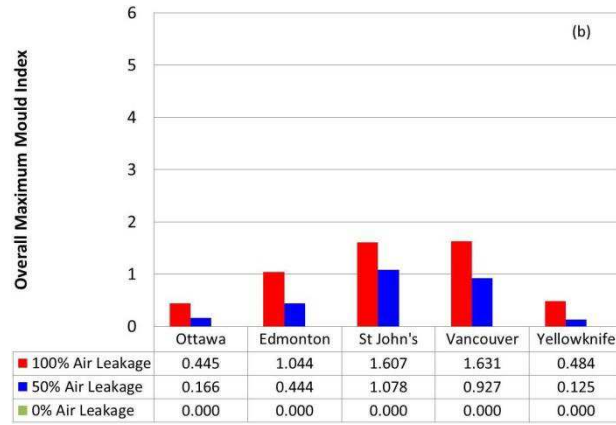
Figure 17. EPS wall - Effect of air leakage rate on overall maximum and average mould index
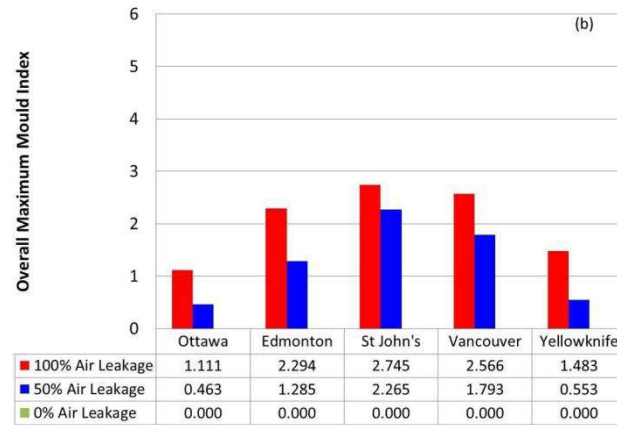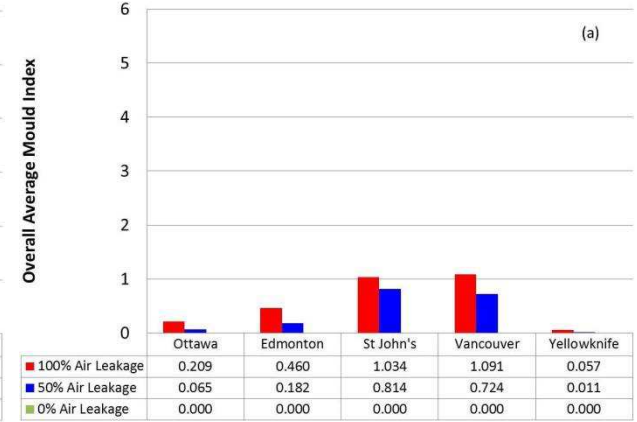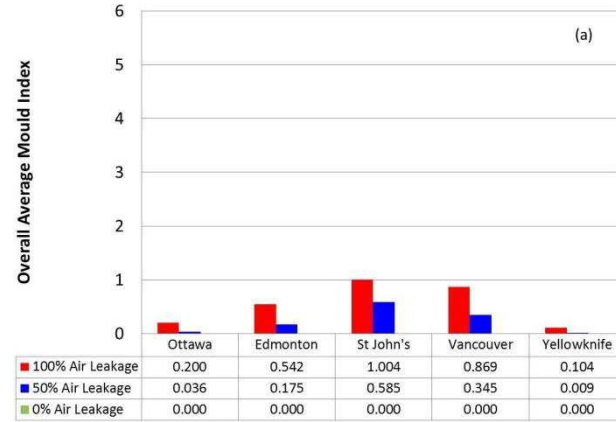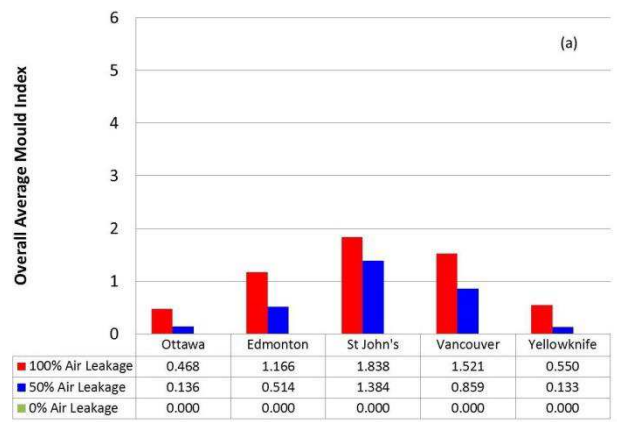
Figure 18. XPS wall - Effect of air leakage rate on overall maximum and average mould index

Figure 19. Mineral fibre wall - Effect of air leakage rate on overall maximum and average mould index

Figure 20a and Figure 20b, respectively, show the overall average mould index (M_{AVG}) and overall maximum mould index (M_{MAX}) in different wall assemblies. For the purposes of comparison, the performance of the code-compliant reference wall that was obtained in a previous NRC project [69] is included in these figures. As shown in these figures, increasing the R-value of the stud-cavity insulation resulted in a slightly higher risk of condensation and mould growth. For example, the values of M_{AVG} for walls having a R-24 stud-cavity insulation were 5% (reference wall), 4% (EPS wall), 14% (XPS wall) and 15% (mineral fibre wall) higher than that for a wall having R-19 stud-cavity insulation (Figure 20a). The corresponding values of M_{MAX} for walls having R-24 stud-cavity insulation were 5%, 4%, 14% and 15% higher than that for walls having R-19 stud-cavity insulation (Figure 20b).

The higher the R-value of the outboard, exterior insulation (R-0, R-3.9, R-10.0 and R-12.5 for Reference wall, EPS wall, XPS wall and mineral fibre wall, respectively), the warmer the average wall cavity temperature, and consequently, the less likely the formation of interstitial condensation occurring during the cold periods, and hence the lower the mould index. As shown in Figure 20a, the values of M_{AVG} for the EPS wall, XPS wall and mineral fibre wall, respectively, were 59%, 27% and 23% of the value of M_{AVG} for the reference wall. Also, the corresponding M_{MAX} values for these walls were 68%, 31% and 26% of that for the reference wall (Figure 20b).

Comparisons for the yearly heat losses in winter season and yearly heat gains in the summer season for the reference wall and walls with exterior insulations with stud-cavity insulations of R-19 and R-24 are provided in Figure 21 and Figure 22, respectively, for both the average year and wet year. It is important to point-out that the yearly heat losses and yearly heat gains shown in these figures are the heat losses in the wall systems and are not necessarily the heat losses one can expect in a house. Note that the summer season in this report was defined as when the outdoor temperature was greater than the indoor temperature, and vice versa for the winter season.

As shown in Figure 21 and Figure 22, increasing the stud-cavity thermal resistance resulted in a decrease in both yearly heat loss and yearly heat gain. For example, the yearly heat losses of walls with R-24 stud-cavity were 22% (reference wall), 19% (EPS wall), 15% (XPS wall) and 14% (Mineral fibre wall) lower than that for walls with R-19 stud-cavity. Conversely, as indicated above, the risk of condensation and mould growth for walls with R-24 stud-cavity was 4% – 15% higher than the walls with R-19 stud-cavity. Note that the percentage decrease in the heat loss for wall with R-24 as compared to wall with R-19 was for the case of 100% air leakage rate. Considering a lower air leakage rate, however, would result in greater percentage decrease in the heat loss for wall with R-24 as compared to wall with R-19.

Adding outboard, exterior insulation not only decreases the yearly heat losses and yearly heat gains (see Figure 21 and Figure 22), but also decreases the risk of condensation and mould growth as explained earlier (see Figure 20). For example, the yearly heat losses of walls with R-19 stud-cavity were 19% (EPS wall with R-3.9), 47% (XPS wall with R-10.0) and 58% (mineral fibre wall with R-12.5) lower than that for the reference wall (no exterior insulation). The corresponding yearly heat losses of walls with R-24 stud-cavity were 16%, 39% and 48%, respectively, lower than that for the reference wall.
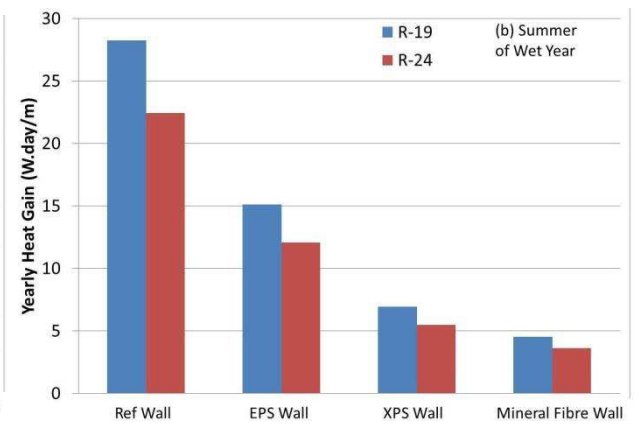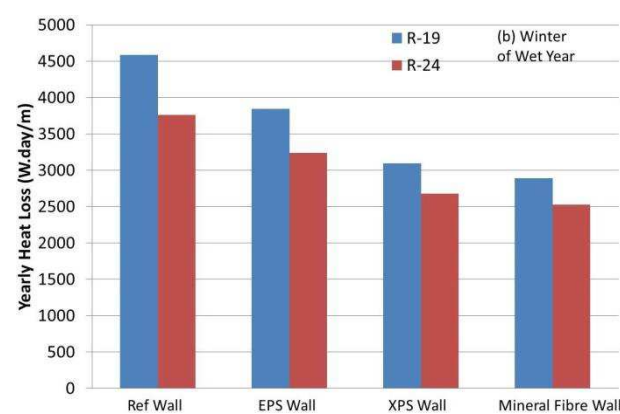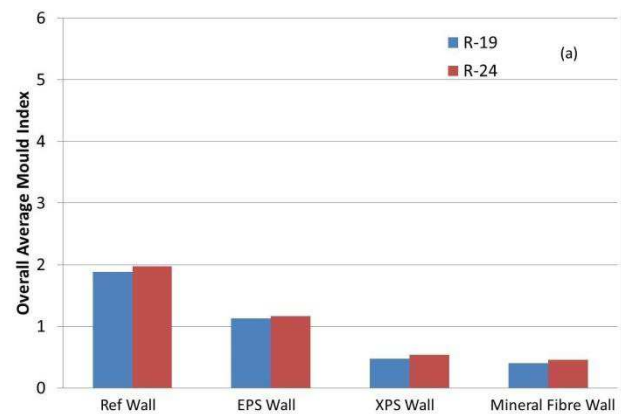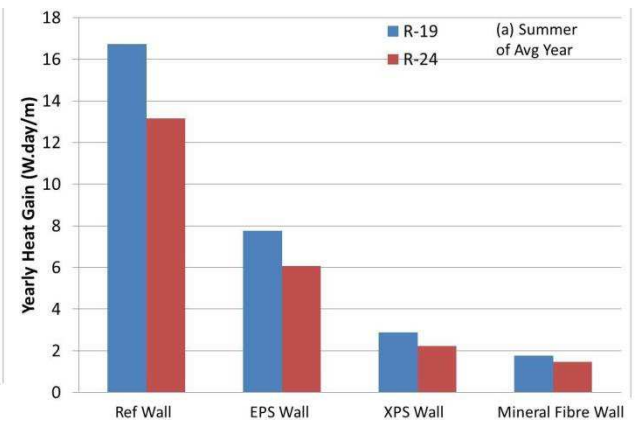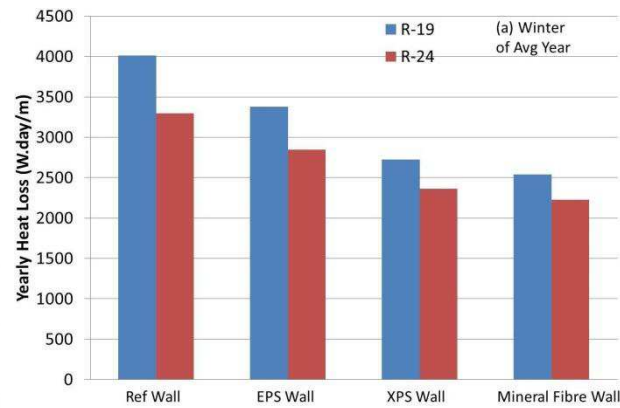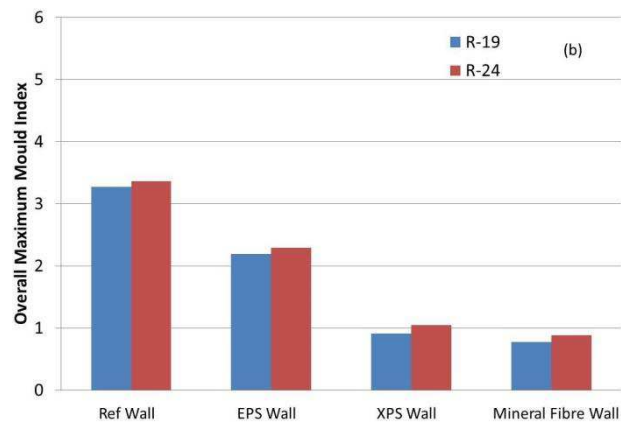
Figure 20. Effect of stud-cavity insulation on the overall maximum and average mould index at 100% air leakage rate (Edmonton weather)

Figure 21. Effect of stud-cavity insulation on the yearly heat loss at 100% air leakage rate (Edmonton weather)

Figure 22. Effect of stud-cavity insulation on the yearly heat gain at 100% air leakage rate (Edmonton weather)

For the case of stud-cavity insulation of R-24, similar comparisons for the yearly heat loss and yearly heat gain for the reference wall and wall systems with exterior insulations are provided in the Appendix – 3 for the case of 100% air leakage rate when these wall were subjected to the weather of Ottawa (Figure A - 10), Edmonton (Figure A - 9), St John's (Figure A - 12) and Vancouver (Figure A - 11).

In summary, the yearly heat loss and heat gain are lower for walls with R-24 stud-cavity insulation than that for walls with R-19 stud-cavity insulation, but the risk of condensation in the former is higher than that in latter. For a given stud-cavity insulation, wall systems having additional exterior insulation resulted not only in higher energy performance but also lower risk of condensation and mould growth than walls without exterior insulation.

7.3 Effect of Geographical Locations

The hygrothermal performance for different wall assemblies (see Table 3) were obtained when these walls were subjected to the climates of five Canadian cities each differing in geographical location and that included: Ottawa (ON), Edmonton (AB), Vancouver (BC), St John's (NL) and Yellowknife (NT). The primary environmental parameters that greatly affected the hygrothermal performance related to the risk of condensation and mould growth were:

- The outdoor temperature which can be represented by the Heating Degree Days (HDD). The greater the number of HDD the higher the risk for mould growth in a wall assembly. Amongst the geographical locations considered in this study, Yellowknife had the highest HDD (HDD = 8170), followed by Edmonton (HDD = 5120).

- The outdoor relative humidity which can be represented by the Moisture Index (MI). The higher the MI value, the smaller the drying potential of a wall assembly and hence, the higher the risk of mould growth. Amongst the geographical locations considered in this study, Vancouver had the highest value of MI (MI = 1.44), followed by St John's (MI = 1.41).

- The wind speed; the higher the wind speed, the greater the air leakage rate across the wall assembly, and hence, the higher the risk for mould growth within the wall assembly as indicated earlier.

Details for determining the air leakage rates of the different geographical locations are provided in reference [69][§§]. Also, the air leakage rate of the different locations are provided in Appendix – 1 (see Figure A - 1 for Ottawa, Figure A - 2 for Edmonton, Figure A - 3 for Vancouver, Figure A - 4 for St John's, and Figure A - 5 for Yellowknife). As shown in these figures, amongst the geographical locations considered in this study, St John's provided the highest air leakage rate across wall assemblies.

Figure 23a and Figure 23b show a comparison of the overall average value for mould index (M_{AVG}) and overall maximum value of mould index (M_{MAX}) for different wall assemblies having R-24 as stud-cavity insulation at a 100% air leakage rate when subjected to different climatic conditions. As shown in these figures, the combined effects of the three environmental parameters, listed above, have brought about, in the case of walls subjected to the climatic conditions of Ottawa and Yellowknife, the lowest value of mould index.

[§§] see also the subsection 4.3 Approach to Simulation of Air Leakage"

For example, the overall average values for mould index for the reference wall were 1.18, 1.98, 2.41, 3.05 and 1.06, respectively, for the climatic conditions of Ottawa, Edmonton, Vancouver, St John's and Yellowknife (Figure 23a). Whereas the highest value of overall average mould index can be found for the reference wall, EPS wall and XPS wall subjected to the climatic conditions of St John's. For the mineral fibre wall subjected to the climatic conditions of St John's and Vancouver, the values of overall average mould (1.03 and 1.09, respectively) were approximately the same. Details about the risk of condensation and mould growth in wall assemblies with exterior insulation over a broad range of values for thermal resistance (e.g. R-values of 4, 5 and 6 $ft^2 \cdot h \cdot {}^\circ F/BTU$) and WVP (2 to 1800 ng/(Pa•s•m²)) and subjected to different climatic conditions are available in reference [69].
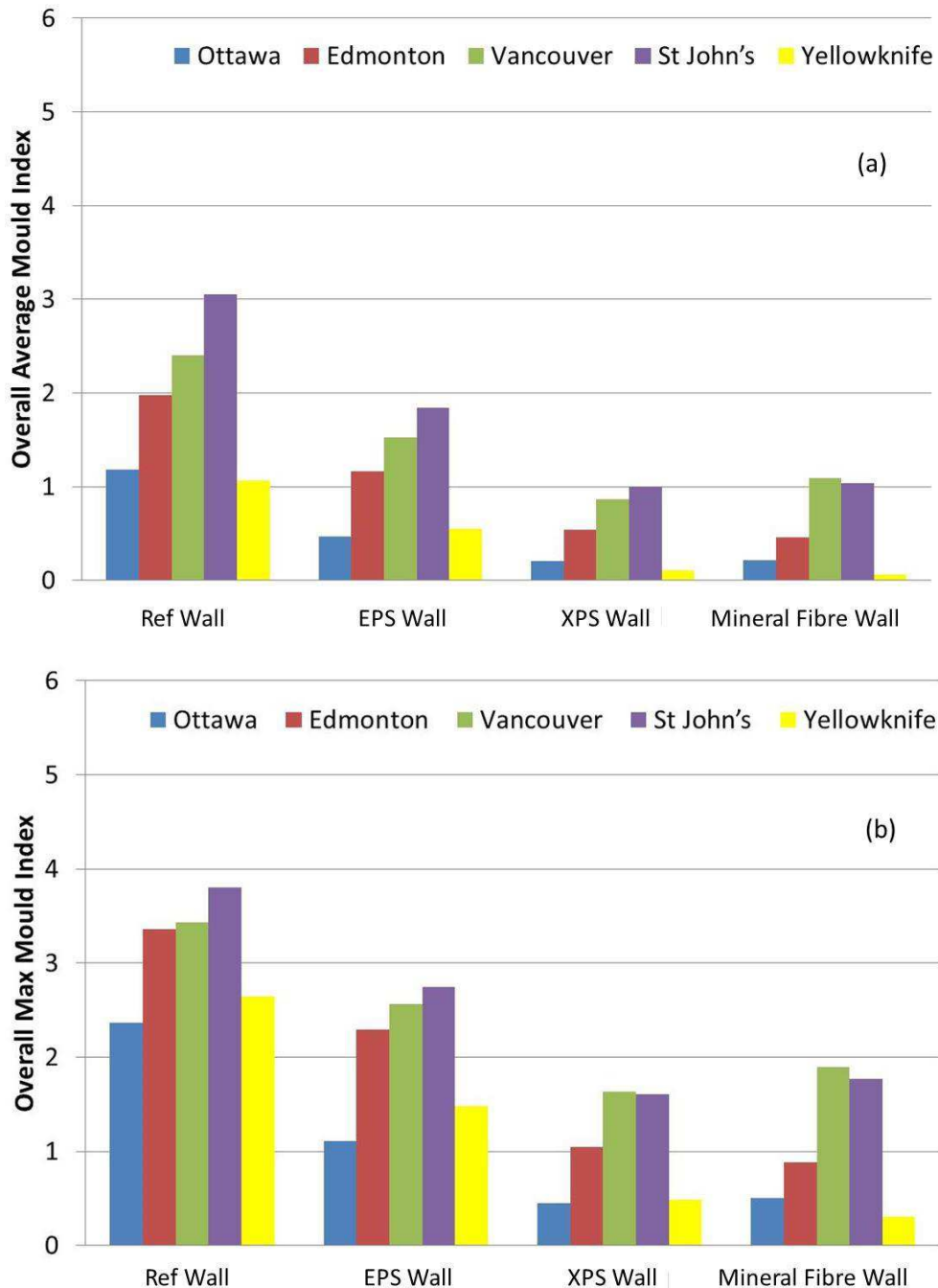

Figure 23. Effect of geographical locations on the overall maximum and average mould index at 100% air leakage rate

8. Summary of Simulation Results for different Walls

For all wall assemblies having R-24 stud-cavity insulation and with 100% air leakage rate, the results of the risk of condensation and mould growth are presented in through in the following order: Edmonton, Ottawa, Vancouver, Yellowknife and St John's, and where:

- Figure 24 for Edmonton, AB (cold, dry climate with HDD18 = 5120, MI = 0.48),
- Figure 25 for Ottawa, ON (cold, dry climate with HDD18 = 4440 to 4500, MI = 0.84),
- Figure 26 for Vancouver, BC (mild, wet climate with HDD18=2600 to 3100, MI = 1.44);
- Figure 27 for Yellowknife, NT (cold, dry climate with HDD18 = 8170, MI = 0.58); and
- Figure 28 for St John's, NL (mild, wet climate with HDD18 = 4800, MI = 1.41).

The results of thermal performance, expressed in terms of the yearly heat losses and yearly heat gains, of these wall systems are available in Appendix – 3: Figure A - 9 for Edmonton, Figure A - 10 for Ottawa, Figure A - 11 for Vancouver, Figure A - 12 for St John's, Figure A - 13 and for Yellowknife.

8.1 Edmonton, AB

As might be expected, increasing the R-value of the outboard, exterior insulation (see Table 3) decreases the overall average value of M_{AVG} and overall maximum value, M_{MAX}. In Figure 24a and Figure 24b is shown that in all instances, the values derived for both M_{AVG} and M_{MAX} for wall assemblies with exterior insulation are less than those for the code-compliant reference wall (Figure 24a). The values for M_{AVG} for these walls range from 1.98 to 0.46; corresponding values for M_{MAX} of these walls range from 0.89 to 3.36 (Figure 24b).

8.2 Ottawa, ON

As was the case for Edmonton, in all instances, the values derived for the overall average mould index and overall maximum mould index for walls with exterior insulations are less than those for the reference wall. The values derived for both M_{AVG} and M_{MAX} for all wall assemblies range from 1.18 to 0.20 (Figure 25a). The corresponding values for M_{MAX} for these walls range from 2.37 to 0.44 (Figure 25b). As compared to the results obtained for Edmonton, however, the values for M_{AVG} and M_{MAX} for these sets of walls are lower. For example, the values of M_{AVG} of reference wall and EPS wall are 1.18 and 0.47, respectively, for Ottawa (Figure 25a), whereas for Edmonton these values are 1.98 and 1.17 (Figure 24a). The corresponding values of M_{MAX} are 2.37 and 1.11 for Ottawa (Figure 25b), whereas for Edmonton these values are 3.36 and 2.29 (Figure 24b).

8.3 Vancouver, BC

Values of M_{AVG} and M_{MAX} for walls subjected to a Vancouver climate are comparatively greater than that of Ottawa, and slightly greater than those of Edmonton. As shown in Figure 26a, the values for M_{AVG} for these walls range from 2.41 to 0.87. The corresponding values for M_{MAX} for these walls range from 3.43 to 1.63 (Figure 26b).

8.4 Yellowknife, NT

Values of M_{AVG} and M_{MAX} for walls subjected to a Yellowknife climate are approximately the same as that of Ottawa. As shown in Figure 27a for Yellowknife, the values for M_{AVG} for different wall systems range from 1.06 to 0.06 compared to the range of 1.18 to 0.21 for Ottawa (Figure 25a). The corresponding values for M_{MAX} for these walls range from 2.65 to 0.30 for Yellowknife (Figure 27b) and from 2.37 to 0.44 for Ottawa (Figure 25b).

8.5 St John's, NL

The greatest values for the overall M_{AVG} of the reference, EPS and XPS wall configurations occur in St John's as compared to the other cities investigated. Note that the St John's climate has the highest air leakage rate compared to the other geographical locations investigated (Figure A - 1 through Figure A - 5). Also St John's climate is a wet climate with moisture index (MI = 1.41) slightly lower than that of Vancouver climate (MI = 1.44). Figure 28a shows that the values for M_{AVG} for all walls range from 3.05 to 1.0, whereas the corresponding values for M_{MAX} for these walls range from 3.8 to 1.61 (Figure 28b).

9. Concluding Remarks

NRC's hygrothermal numerical model, hygIRC-C, was first benchmarked against experimental work carried out in the FEWF; the benchmarking exercise consisted of completing transient numerical simulations, as was done in a number of other studies, to benchmark the model against experimental work. This model simultaneously solves the 2D and 3D Heat, Air and Moisture (HAM) transport equations.

The numerical results derived for values of heat flux attained at different locations within the respective wall assemblies were compared with the measured values for assemblies incorporating different exterior insulation products that included: (i) EPS of 1" thick (R-3.9 and WVP = 114), (ii) XPS of 2" thick (R-10 and WVP = 27), and (iii) Mineral fibre insulation products of 3" thick (R-12.5 and WVP = 2130). The results showed that the comparison between the present model predictions and experimental data were in good agreement.

Following the benchmarking of the present model, it was then used to conduct a parametric study to investigate the risk of condensation and mould growth in different wall assemblies when these assemblies were subjected to different climatic conditions in Canada, specifically, the climates of Vancouver (BC), Edmonton (AB), Ottawa (ON), St John's (NL), and Yellowknife (NT).

The Modelling results for the different wall assemblies were expressed using the mould index criteria. The most recent mould growth model developed by Ojanen et al. [68] was used to determine the expected value of mould index of different materials within the respective wall assemblies.

Based on the air leakage path that was considered in this study, the simulation results showed that the critical locations inside the wall assembly at risk of mould growth are the top and bottom portions of the wall assembly. However, had a different air leakage path been consider, in this study, it would have resulted in different locations within the wall assemblies being at risk of condensation and mould growth.

Similar to a previous study [69], the simulation results were presented on the basis of a simple form using the following two parameters:

- The overall average value of mould index which is the average value of mould index at all locations within the assembly.
- The overall maximum value of mould index which is the average value of the maximum mould index values at all locations within the assembly.
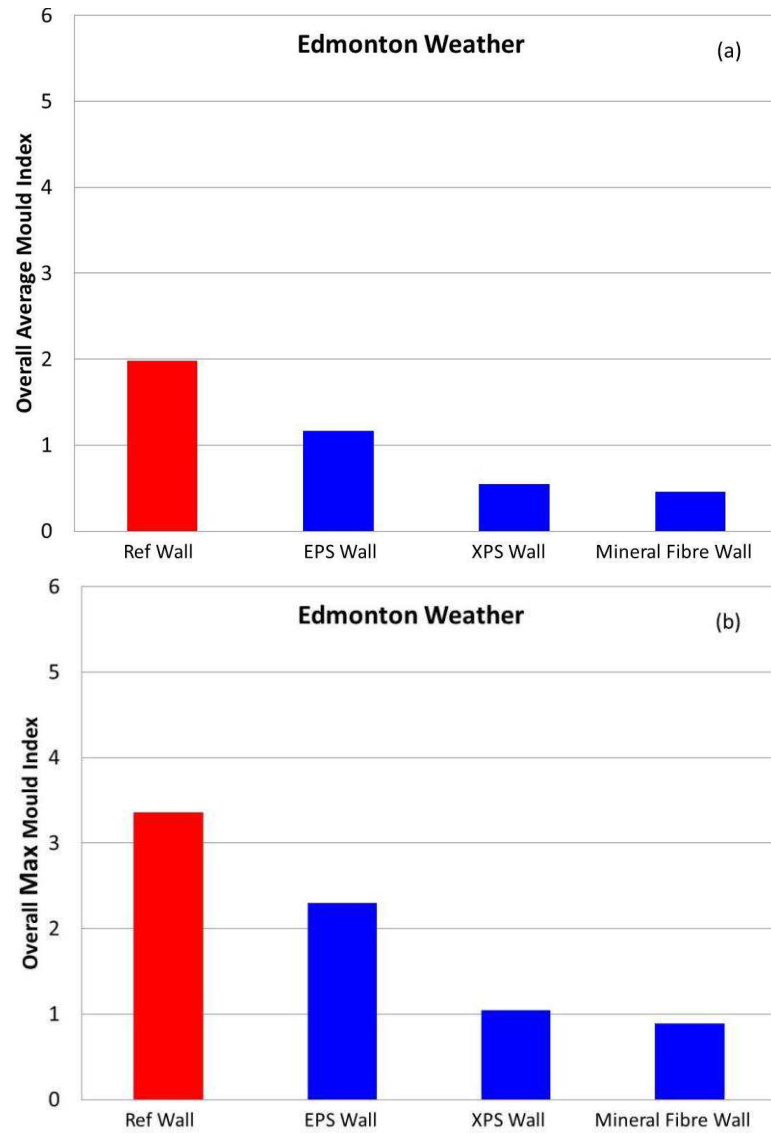
Figure 24. Effect of R-value and WVP on the overall maximum and average mould index at 100% air leakage rate (Edmonton weather)
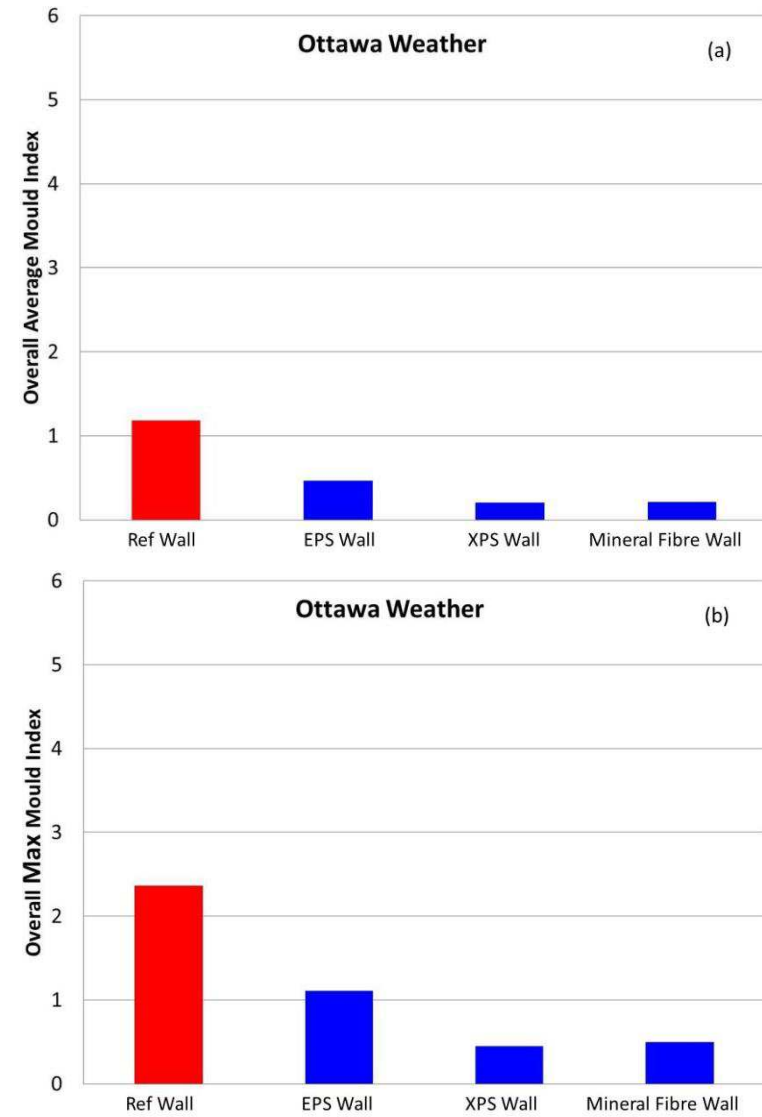
Figure 25. Effect of R-value and WVP on the overall maximum and average mould index at 100% air leakage rate (Ottawa weather)
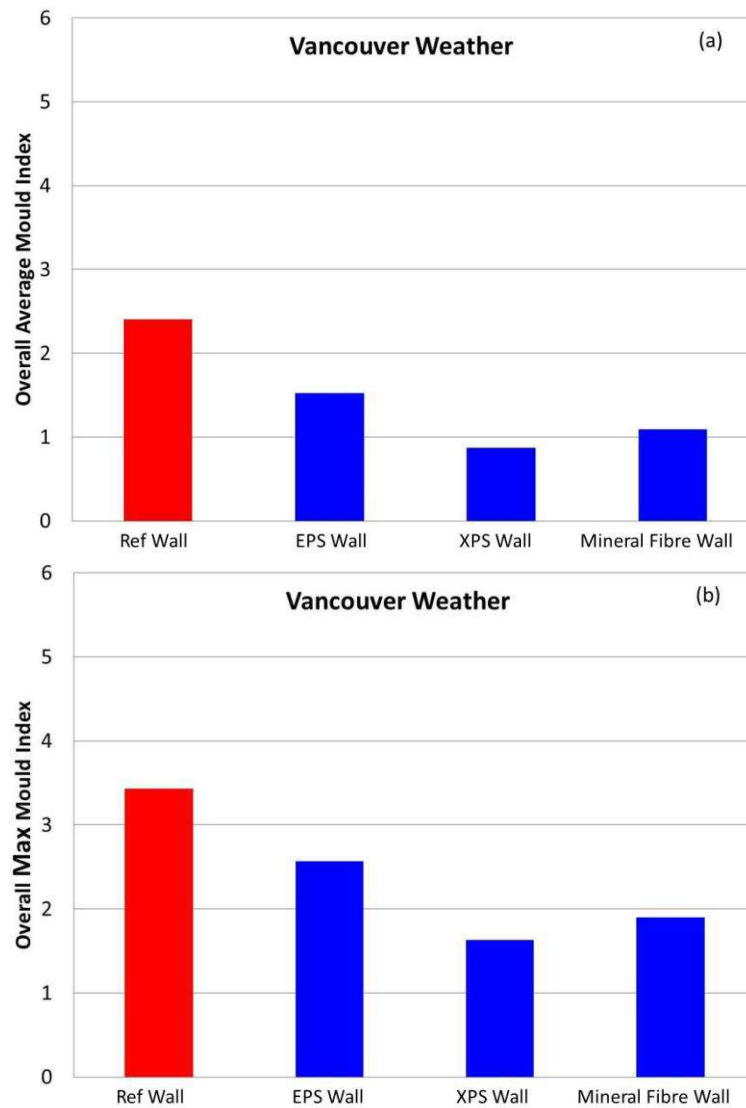
Figure 26. Effect of R-value and WVP on the overall maximum and average mould index at 100% air leakage rate (Vancouver weather)
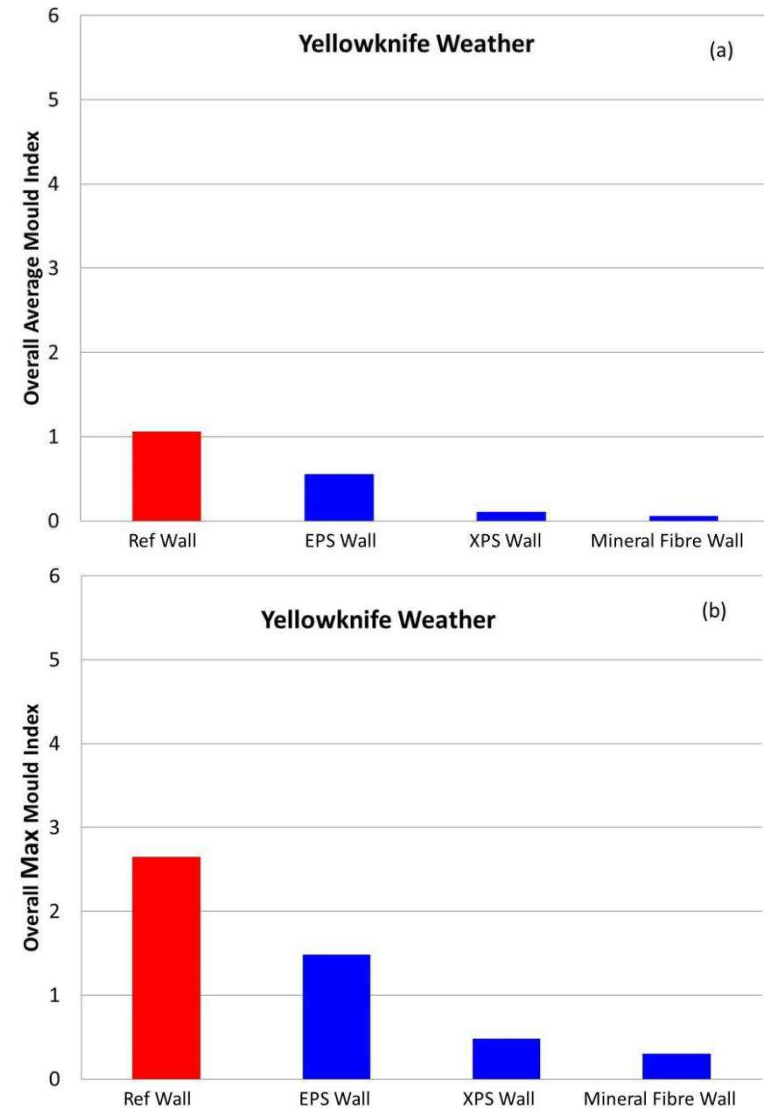
Figure 27. Effect of R-value and WVP on the overall maximum and average mould index at 100% air leakage rate (Yellowknife weather)
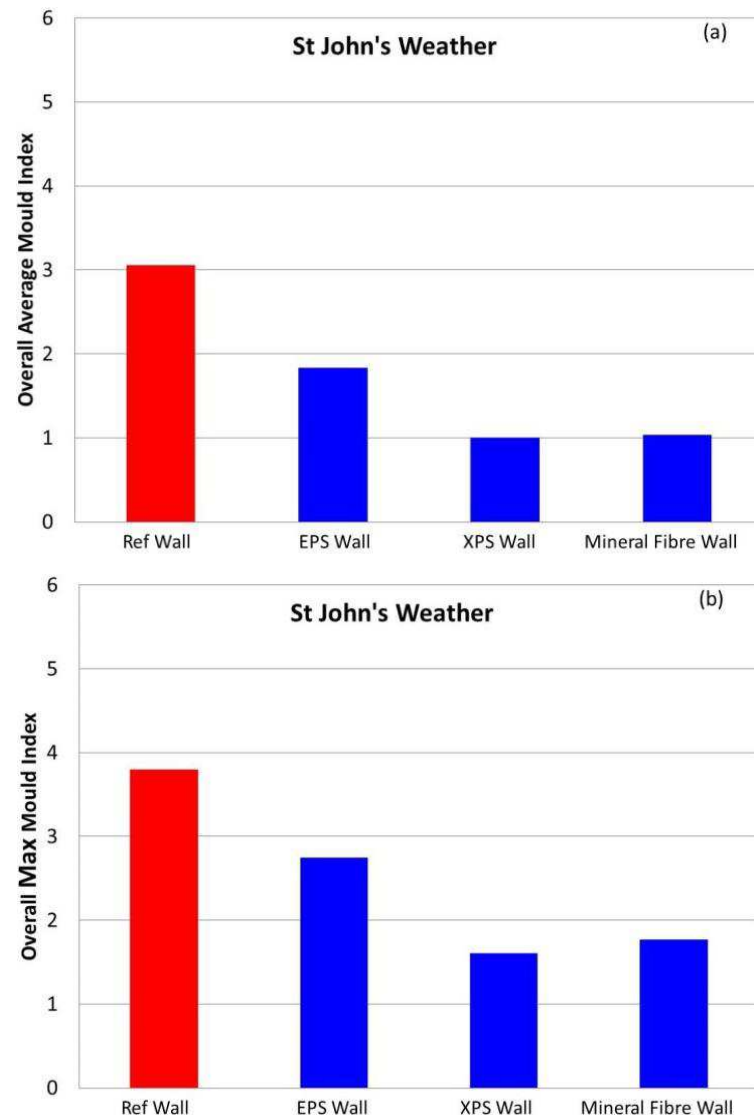
Figure 28. Effect of R-value and WVP on the overall maximum and average mould index at 100% air leakage rate (St John's weather

A sensitivity analysis was conducted to investigate the effect of different air leakage rates of 0% (no air leakage), 50%, and 100% on the hygrothermal performance of wall assemblies. No risk of condensation occurred in the wall assemblies for the case of no air leakage. The case of 100% air leakage rate (i.e. 0.1 L/(s•m²) at 75 Pa)) resulted in higher risk of condensation and mould growth than that for the case of 50% air leakage rate (i.e. 0.05 L/(s•m²) at 75 Pa).

The values for the overall average mould index and overall maximum mould index in different wall assemblies with the inboard stud-cavity insulation of R-24 were higher than that of walls having stud-cavity insulation of R-19.

The values for the overall average mould index and overall maximum mould index in walls with different types of outboard, exterior insulations were lower than that of the code-compliant reference wall.

For the code-compliant reference wall, the EPS wall and XPS wall, St John's (NL) appeared to have the most severe climate in comparison to the other four locations investigated (Vancouver (BC), Ottawa (ON), Edmonton (AB) and Yellowknife (NT)); the greatest values of the overall average mould index in the wall configurations amongst the five locations occurred in this location. For the wall having mineral fibre as exterior insulation, the values of the overall average mould index were approximately the same for St John's and Vancouver.

10. References

1. Ojanen, T., and Kumaran, M.K., "Air Exfiltration and Moisture Accumulation in Residential Wall Cavities", Thermal Performance of Exterior Envelopes of Buildings V, Clearwater, FL, 1992.

2. Karagiozis, A.N., and Kumaran, M. K., "Computer Model Calculations on the Performance of Vapor Barriers in Canadian Residential Buildings", ASHRAE Transactions, 99(2), pp. 991-1003, 1993.

3. Ojanen, T., and Kumaran, M.K., "Effect of Exfiltration on the Hygrothermal Behaviour of a Residential Wall Assembly", J. of Thermal Insulation and Building Envelopes, vol. 19, 1996.

4. Kumaran, M. K., and Haysom, J. C., "Low Permeance Materials in Building Envelopes", Institute for Research in Construction, National Research Council of Canada; Construction Technology Update #41, 2000.

5. Kumaran, M.K., and Haysom, J.C., "Avoiding Condensation with Low-Permeance Materials", Solplan Review (96), pp.18-19, 2001.

6. Chown, G. A., and Mukhopadhyaya, P., "NBC 9.25. 1.2.: The On-going Development of Building Code Requirements to Address Low Air and Vapour Permeance Materials", 10th Canadian Conference on Building Science and Technology: Building Science and integrated Design Process, Ottawa ON, May 12-13, 2005, v. 1, pp. 48-58.

7. Straube, J., "The influence of Low-Permeance Vapor Barriers on Roofs and Wall Performance", Buildings VIII Conference proceedings, paper # 184, 2001.

8. Brown, W.C., Roppel, P., and Lawton, M., "Developing a Design Protocol for Low Air and Vapour Permeance Insulating Sheathing in Cold Climates", Buildings X Proceedings, paper # 242, 2007.

9. Roppel, P., Brown, W.C., and Lawton, M., "Modeling of uncontrolled Indoor Humidity for HAM Simulations of Residential Buildings", Buildings X Proceedings, paper #212, 2007.

10. Maref, W., Rousseau, M.Z., Armstrong, M.M., Lee, W., Leroux, M., and Nicholls, M., Evaluating the Effects of Two Energy Retrofit Strategies for Housing on the Wetting and Drying Potential of Wall Assemblies: Summary Report for Year 2007-08 Phase of the Study, Report RR-315, pp. 1-118, NRC Institute for Research in Construction, 2011.

11. Maref, W., Armstrong, M.M., Rousseau, M.Z., Nicholls, M., and Lei, W., "Effect of Wall Energy Retrofit on Drying Capability", Solplan Review, (150), pp. 1-2, 2010.

12. Maref, W., Armstrong, M. M., Rousseau, M.Z., Thivierge, C., Nicholls, M., Ganapathy, G. and Lei, W., "Field Hygrothermal Performance of retrofitted Wood-Frame Wall Assemblies in Cold Climate", 13th Canadian Conference on Building Science and Technology - Winnipeg, Canada, 2011.

13. National Building Code of Canada (1990), Canadian Commission on Building and Fire Codes, National Research Council of Canada, Ottawa, Canada.

14. National Building Code of Canada (1995), Canadian Commission on Building and Fire Codes, National Research Council of Canada, Ottawa, Canada.

15. National Building Code of Canada (2005), Canadian Commission on Building and Fire Codes, National Research Council of Canada, Ottawa, Canada.

16. National Building Code of Canada (2010), .Section 9.25, Canadian Commission on Building and Fire Codes National Research Council of Canada, Ottawa, Canada.

17. Shaw, C. Y. (1987), "Methods for estimating air change rates and sizing mechanical ventilation systems for houses." ASHRAE Transactions 93(2): pp. 2284-2302.

18. Scanada Consultants Ltd. (1992), Consolidated Report on the 1989 Survey of Airtightness of Merchant Built Houses, Prepared for Energy, Mines and Resources Canada, Ottawa.

19. Airtightness and Energy Efficiency in New Conventional and R2000 Houses in Canada, 1997; CANMET Energy Technology Centre, Natural Resources Canada, Ottawa, 1997.

20. National Building Code of Canada (Section 9.25), Canadian Commission on Building and Fire Codes National Research Council of Canada, 2010.

21. Maref, W., Saber, H.H., Glazer, R., Armstrong, M.M., Nicholls, M., Elmahdy, A.H., Swinton, M.C., "Energy Performance of Highly Insulated Wood-Frame Wall Systems Using a VIP", 10th Int. Vacuum Insulation Symposium, Ottawa, Canada, 2011, pp. 68-76.

22. Maref, W., Saber, H.H., Armstrong, M.M., Glazer, R., Ganapathy, G., Nicholls, M., Elmahdy, A.H., Swinton, M.C., Integration of Vacuum Insulation Panels into Canadian Wood Frame Walls, Report 1- Performance Assessment in the Laboratory, Client Report – B1253, Building Envelope Engineering Materials Program, Construction Portfolio, National Research Council of Canada, Ottawa, Canada, 2012.

23. Elmahdy, A.H., Maref, M., Saber, H.H., Swinton, M.C, and Glazer, R., "Assessment of the Energy Rating of Insulated Wall Assemblies a Step Towards Building Energy Labelling", 10th Int. Conference for Enhanced Building Operations (ICEBO2010), Kuwait, Oct. 2010.

24. Elmahdy, A.H., Maref, W., Swinton, M.C., Saber, H.H., and Glazer, R., "Development of energy ratings for insulated wall assemblies", Building Envelope Symposium, San Diego, California, October 26, pp. 21-30, 2009.

25. Saber, H.H., Maref, W., Elmahdy, A.H., Swinton, M.C., and Glazer, R., "3D Heat and Air Transport Model for Predicting the Thermal Resistances of Insulated Wall Assemblies", International Journal of Building Performance Simulation, vol. 5, No. 2, p. 75–91, 2012.

26. Saber, H.H., Maref, W., Elmahdy, A.H., Swinton, M.C., and Glazer, R., "3D Thermal Model for Predicting the Thermal Resistances of Spray Polyurethane Foam Wall Assemblies", Building XI conference, Clearwater, Florida, 2010.

27. Maref, W., Saber, H.H., Ganapathy, G., and Nicholls, M., Field Energy Performance and Hygrothermal Evaluation of Different Strategies of Energy Retrofit for Residential Wood-Frame Wall Systems Field using VIP, Client report B-1266.3, National Research Council of Canada, Ottawa, August 2012.

28. Saber, H.H., Maref, W., Lacasse, M.A., Swinton, M.C., and Kumaran, K., "Benchmarking of Hygrothermal Model against Measurements of Drying of Full-Scale Wall Assemblies" International Conference on Building Envelope Systems and Technologies, ICBEST 2010, Vancouver, Canada, June 27-30, 2010.

29. Saber, H.H., Maref, W., and Swinton, M.C., "Thermal Response of Basement Wall Systems with Low Emissivity Material and Furred Airspace" *Journal of Building Physics,* vol. 35, no. 2, pp. 353-371, 2012, (NRCC-53962).

30. Saber, H.H., Maref, W., Armstrong, M.M., Swinton, M.C., Rousseau, M.Z., and Ganapathy, G., "Benchmarking 3D Thermal Model against Field Measurement on the Thermal Response of an Insulating Concrete Form (ICF) Wall in Cold Climate", Eleventh International Conference on Thermal Performance of the Exterior Envelopes of Whole Buildings XI (Clearwater, FL, USA, December 4-9, 2010).

31. Armstrong, M., Saber, H.H., Maref, W., Rousseau, M.Z., Ganapathy, G., and Swinton, M.C., "Field Energy Performance of an Insulating Concrete Form (ICF) Wall", 13th CCBST conference - Winnipeg 2011, The 13th Canadian Conference on Building Science and Technology, Winnipeg, Manitoba May 10 – 13, 2011.

32. Saber, H.H., Swinton, M.C., "Determining through Numerical Modeling the Effective Thermal Resistance of a Foundation Wall System with Low Emissivity Material and Furred – Airspace" International Conference on Building Envelope Systems and Technologies, ICBEST 2010, Vancouver, Canada, June 27-30, 2010.

33. Saber, H.H., Maref, W., Swinton, M.C., and St-Onge, C., "Thermal analysis of above-grade wall assembly with low emissivity materials and furred-airspace," Journal of Building and Environment, vol. 46, issue 7, pp. 1403-1414, 2011.

34. Saber, H.H, and Laouadi, A., "Convective Heat Transfer in Hemispherical Cavities with Planar Inner Surfaces (1415-RP)" Journal of ASHRAE Trans., vol. 117, Part 2, 2011.

35. Saber, H.H., and Maref, W., "Effect of Furring Orientation on Thermal Response of Wall Systems with Low Emissivity Material and Furred-Airspace", The Building Enclosure Science & Technology (BEST3) Conf., held in April 2-4, 2012 in Atlanta, Georgia, USA.

36. Saber, H.H., "Thermal Performance of Wall Assemblies with Low Emissivity" Journal of Building Physics, vol. 36, no. 3, pp. 308-329, 2013.

37. Saber, H.H., "Investigation of Thermal Performance of Reflective Insulations for Different Applications" Journal of Building and Environment, 52, p. 32-44, 2012.

38. Saber, H.H., Maref, W., Sherrer, G., Swinton, M.C., "Numerical Modelling and Experimental Investigations of Thermal Performance of Reflective Insulations", Journal of Building Physics, vol. 36, no. 2, pp. 163-177, 2012 (NRCC-54538).

39. Saber, H.H., Swinton, M.C., Kalinger, P., and Paroli, R.M., "Hygrothermal Simulations of Cool Reflective and Conventional Roofs", 2011 NRCA International Roofing Symposium, Emerging Technologies and Roof System Performance, held in Sept. 7-9, 2011, Washington D.C., USA.

40. Saber, H.H., Swinton, M.C., Kalinger, P., and Paroli, R.M., "Long-Term Hygrothermal Performance Of White And Black Roofs In North American Climates", Journal of Building and Environment, 50, p. 141-154, 2012.

41. Armstrong, M., Maref, W., Saber, H.H., Rousseau, M.Z., Ganapathy, G., Swinton, M.C., "The impact of the thermal mass on field energy performance of insulating concrete form (ICF) wall" International Workshop on Whole Building Testing, Evaluation and Modelling for Energy Assessment (Copenhagen, Denmark 2011-05-18), pp. 1-12.

42. Saber, H.H., Maref, W., Armstrong, M.M., Swinton, M.C., Rousseau, M.Z., Ganapathy, G., Numerical Simulations to Predict the Thermal Response of Insulating Concrete Form (ICF) Wall in Cold Climate, Research Report-310, NRC Research Council of Canada, Ottawa, Canada, 2011.

43. Maref, W., Kumaran, M.K., Lacasse, M.A., Swinton, M.C., and van Reenen, D., "Laboratory measurements and benchmarking of an advanced hygrothermal model", Proc. 12th International Heat Transfer Conference, Grenoble, France, Aug. 18, 2002, pp. 117-122 (NRCC-43054).

44. Saber, H.H., "Practical Correlation for Thermal Resistance of Low-Sloped Enclosed Airspaces with Downward Heat Flow for Building Applications", HVAC&R Research Journal, vol. 20 (1), pp. 92-112, 2014.

45. Saber, H.H., "Practical Correlation for Thermal Resistance of Horizontal Enclosed Airspaces with Downward Heat Flow for Building Applications", Journal of Building Physics, vol. 37 (4), pp. 403-435, 2014.

46. Saber, H.H., "Practical Correlation for Thermal Resistance of 45° Sloped Enclosed Airspaces with Downward Heat Flow for Building Applications", Journal of Building and Environment, vol. 65, pp. 154-169, 2013.

47. Saber, H.H., "Practical Correlations for Thermal Resistance of Horizontal Enclosed Airspaces with Upward Heat Flow for Building Applications", Journal of Building and Environment, vol. 61, pp. 169-187, 2013.

48. Saber, H.H., "Practical Correlations for the Thermal Resistance of Vertical Enclosed Airspaces for Building Applications", Journal of Building and Environment, vol. 59, pp. 379-396, 2013.

49. Saber, H.H., Maref, W., Gnanamurugan, G., and Nicholls, M., "Energy Retrofit Using VIPs: - an Alternative Solution for Enhancing the Thermal Performance of Wood-Frame Walls", Journal of Building Physics, vol. 39(1), pp. 35-68, 2015.

50. Saber, H.H., Maref, W., Gnanamurugan, G. and Nicholls, M., "Model Benchmarking for Field Energy Retrofit towards Highly Insulated Residential Wood-Frame Construction Using VIPs" 11th International Vacuum Insulation Symposium (IVIS2013), September 19-20, 2013, Empa, Switzerland.

51. Maref, W., Saber, H.H., Gnanamurugan, G. and Nicholls, M., "In-Situ Performance of Residential Wood-Frame Construction Retrofitted Using VIPs" 11th International Vacuum Insulation Symposium (IVIS2013), September 19-20, 2013, Empa, Switzerland.

52. ASTM C 1363, Standard Test Method for the Thermal Performance of Building Assemblies by Means of a Hot Box Apparatus, 2006 Annual Book of ASTM Standards 04.06:717–59, www.astm.org.

53. ASTM C 518-04, Steady-State Thermal Transmission Properties by Means of the Heat Flow Meter Apparatus, Section 4, vol. 04.06, Thermal Insulation, 2007 Book of ASTM Standards.

54. ASHRAE. 2009. 2009 ASHRAE Handbook –Fundamentals (SI), Chapter 26, Atlanta: American Society of Heating, Refrigerating, and Air-Conditioning Engineers Inc.

55. Mukhopadhyaya, P., and Van Reenen, D., Heat Flow Characterization of Three GDDC (Geometrically Defined Drainage Cavity) Specimens, Client Report: A1-003165.1, National Research Council of Canada, Construction Portfolio, Ottawa, Canada, July 2013.

56. ASTM C 177-04, Standard Test Method for Steady-State Heat Flux Measurements and Thermal Transmission Properties by Means of the Guarded-Hot-Plate Apparatus, Section 4, vol. 04.06, Thermal Insulation, 2012 Book of ASTM Standards.

57. Ojanen, T. and Kumaran, M.K., "Effect of exfiltration on the hygrothermal behaviour of a residential wall assembly: results from calculations and computer simulations", International Symposium On Moisture Problems In Building Walls, Porto - Portugal, 11 - 13 September, pp. 157, 1995.

58. ASHARE Handbook – Fundamentals, SI Edition, Chapter 16: Airflow around Buildings. Atlanta: American Society of Heating, Refrigerating and Air-Conditioning Engineers, Inc., 2005.

59. Dalgliesh, W.A.; Boyd, D.W. Wind on buildings, *Canadian Building Digest,* 28, pp. 4, (CBD-28), 1962.

60. Swami M.V, Chandra S., "Correlations for pressure distribution on buildings and calculation of natural-ventilation airflow", ASHRAE Transactions, 94 (1), p. 243–266, 1988.

61. Walker, I.S. and D.J. Wilson. 1994. Practical Methods for Improving Estimates of Natural Ventilation Rates. Proc. 15th AIVC Conference, Buxton, U.K., 1994: 517-525.

62. Akins, R.E., Peterka, J.A., and Cermak, J.E., (1979), "Averaged Pressure Coefficients for Rectangular Buildings", Wind Engineering, Vol. 1, Proc. 5th Int. Conf. on Wind Engineering, pp.369,380.

63. ASHARE Handbook – Fundamentals, In-Pound Edition, Chapter 16, p. 16.7. Atlanta: American Society of Heating, Refrigerating and Air-Conditioning Engineers, Inc., 2009.

64. ASHRAE 160-2009 Standard - Criteria for Moisture-Control Design Analysis in Buildings (ANSI/ASHRAE Approved), ASHRAE 2009, Atlanta, GA, 16 p.).

65. Glass, S.V., Hygrothermal Analysis of Wood-Frame Wall Assemblies in a Mixed-Humid Climate, United States Department of Agriculture, Forest Service, Forest Products Laboratory, Research Paper FPL–RP–675, pp. 1-25, April 2013.

66. Hukka, A., and Viitanen, H.A., "A mathematical model of mould growth on wooden material, Wood Science and Technology", vol. 33 (6), pp 475-485, 1999.

67. Viitanen, H.A., and Ojanen, T., "Improved model to predict mould growth in building materials" Proceedings of Thermal Performance of the Exterior Envelopes of Whole Buildings X, 8 p., 2007.

68. Ojanen, T., Viitanen, H.A., Peuhkuri, R, Lähdesmäki, K., Vinha, J., and Salminen, K., "Mold Growth Modeling of Building Structures Using Sensitivity Classes of Materials", 11th International Conference on Thermal Performance of the Exterior Envelopes of Whole Buildings XI (Clearwater, (FL), USA, December-05-10), 10 p., 2010.

69. Saber, H.H., Maref, W. and Abdulghani, K., Properties and Position of Materials in the Building Envelope for Housing and Small Buildings, Report No. A1-004615.1, NRC-Construction, National Research Council of Canada, Ottawa, Canada, Dec., 31, 2014.

70. ASTM Designation: C 1130-07, "Standard Practice for Calibrating Thin Heat Flux Transducers", Annual Book of ASTM Standards, sec 4, Construction, vol. 04.06, Thermal Insulation; Building & Environment Acoustic, pp. 577-584, 2009.

71. Saber, H.H., and Maref, W., "Risk of Condensation and Mould Growth in Wood-Frame Wall Systems with Different Exterior Insulations", BEST Building Enclosure Science & Technology Conference (BEST4), held in April 12-15, 2015, Kansas City, Missouri, USA, 19 p.

72. Lacasse, M. A., Saber, H.H., G. Ganapathy and M. Nicholls, "Evaluation of Thermal and Moisture Response of Highly Insulated Wood-Frame Wall Assemblies — Phase 1; Part I: Experimental trials in Field Exposure of Walls test Facility"; Report No. A1-000444.5; NRC-Construction, National Research Council of Canada, Ottawa, Canada; 12 January, 2016.

Appendix

A1 Description of Numerical Simulation model – hygIRC-C

The NRC's hygrothermal model, hygIRC-C was used in this project to predict the risk of condensation and mould growth in wall assemblies with and without exterior insulations when these walls were subjected to different air leakage rates and different climatic conditions in Canada. It is important to emphasize that the predictions by such a model for the airflow, temperature, and moisture (or relative humidity) distributions within a wall assembly, when subjected to a pressure differential (and resulting air leakage rate) across the assembly, are necessary to accurately determine the mould index in different layers of the wall assembly.

The hygIRC-C model simultaneously solves the highly nonlinear two-dimensional and three-dimensional Heat, Air and Moisture (HAM) equations that define values of heat, air and moisture transfer across building components. The HAM equations were discretized using the Finite Element Method (FEM). The model has been extensively benchmarked in a number of other projects and has been used in several related studies to assess the thermal and hygrothermal performance of wall and roofing systems [21-51].

A1.1 Record of Benchmarking hygIRC-C Model

In a previous project called "Wall Energy Rating (WER)", the three-dimensional version of this model was used to conduct numerical simulations for different full-scale 2 x 6 wall assemblies incorporating, or not, penetrations representative of a window installation, such that the effective thermal resistance (R-value) of the assemblies could be predicted, taking into consideration air leakage across the assembly. The stud-cavity of these walls incorporated open cell polyurethane foam, closed cell spray polyurethane foam or glass fibre insulation. The predicted R-values for these walls were in good agreement (within ± 5% which is the same as the uncertainty of test data, see [23-26]) with the measured R-values that were obtained from testing in the NRC's Guarded Hot Box (GHB) according to the ASTM C-1363 standard test method [52].

The model was also benchmarked against GHB test results according to the ASTM C-1363 standard test method [52] and heat flow meter according to the ASTM C-518 standard test method [53], and then used to conduct numerical simulations to investigate the effect of foil emissivity on the effective thermal resistance of different wall systems with foil bonded to different types of thermal insulations placed in furred assemblies, in which the foil was adjacent to the airspace [29, 32, 33, and 35-38]. The accurate calculations of the airflow and temperature distributions within the test specimens resulted in that the predictions of the present model for the R-values were in good agreements with the measured R-values (within the uncertainties of the experimental data, see [33, 36, 37, 38] for more details). Furthermore, the model was used to determine the reductions in the R-values of the specimens as a result of increasing the foil emissivity due to water vapour condensation and/or dust accumulation on the surface of the foil.

In a number of previous studies by Saber [44-48], the model was used to conduct numerical simulations to predict the airflow and temperature distributions as well as the R-values of vertical,

horizontal and inclined enclosed airspaces, subjected to different directions of heat flow. The predicted R-values were compared with the R-values for enclosed airspaces of different thicknesses and operating conditions as provided in the ASHRAE handbook of fundamentals [54]. In these same studies, the dependence of the R-value on a wide range of the airspace aspect ratio (i.e. ratio of the length or height of the airspace to its thickness) of the enclosed airspace was also investigated. Additionally, practical correlations were developed for determining the R-values of enclosed airspaces of different thicknesses, and for a wide range of values for various parameters, namely, aspect ratio, temperature differential, average temperature, and emissivity of the different surfaces of the airspaces [44-48]. These correlations are ready to be implemented in energy simulations models such as Energy Plus, ESP-r and DOE.

For Insulated Concrete Form (ICF) wall systems when placed in NRC-Construction's Field Exposure of Walls Facility (FEWF) and subjected to yearly periods of local Canadian climate, the present model was used to interpret the readings of the instrumentations and to improve the experiment design by repositioning these instrumentations at critical locations. Subsequently, the present model was benchmarked against the measured data. Results showed that the predictions of the present model for the heat flux distributions within the ICF wall systems were in good agreements with the test data [30-31, 41-42]. Recently, the present model was benchmarked against field data obtained in the NRC's FEWF of highly insulated residential wood-frame construction in which Vacuum Insulation Panels (VIPs) were used as the primary insulation components; the results from this work showed that the model predictions were in good agreement with the test data [49-51].

More recently, the hygIRC-C model was benchmarked against test results of a number of samples of Exterior Insulation and Finishing Systems (EIFS) [55]. The test results were obtained using the NRC's Guarded-Hot-Plate (GHP) apparatus in accordance of the ASTM C-177 standard test method [56]. The accurate calculations of the airflow and temperature distribution within the test specimens had resulted that the model predictions for the R-values of different samples were in good agreements with the test results (within ±5%). Thereafter, the present model was used to investigate the effect of air leakage due to infiltration and exfiltration on the effective R-values of different EIFS assemblies, subjected to different climatic conditions. The results of this study will be published at a later date. These studies focused on predicting the thermal performance of different types of walls [21-25, 29-30, 31-33, 35-42, 44-51]; however, no account was made for moisture transport across the wall assemblies.

In instances where the model has been used to account for moisture transport across wall assemblies, the present model predicted the drying rate of a number of wall assemblies subjected to different outdoor and indoor boundary conditions [28] in which there was a significant vapor drive across the wall assemblies. The results showed that there was overall agreement between the results derived from the present model and the hygIRC-2D model, a model that had previously been developed and benchmarked at NRC-Construction [43]. As well, model predictions were in good agreement with the experimental measurements of the drying and drying rate of the assembly with respect to the shape of the drying curve and the length of time predicted for drying. Additionally, the predicted average moisture content of the different wall assemblies over the test periods were in good agreement, all being within ±5% of those measured experimentally [28].

Additionally, with respect to the prediction of the hygrothermal performance of roofing systems, the present model was used to investigate the moisture accumulation and energy performance of reflective (white coloured) and non-reflective (black coloured) roofing systems that were subjected to different climatic conditions of North America [39, 40]. The results of these studies showed that the climatic conditions of St John's and Saskatoon resulted in a high risk of long-term moisture accumulation in the white roofing systems. In case of climatic conditions in which white roofing systems have no risk of moisture accumulation, however, the results of these studies provided the amount of energy saving due to using white roofing systems compared to using black roofing systems (see [39, 40] for more details).

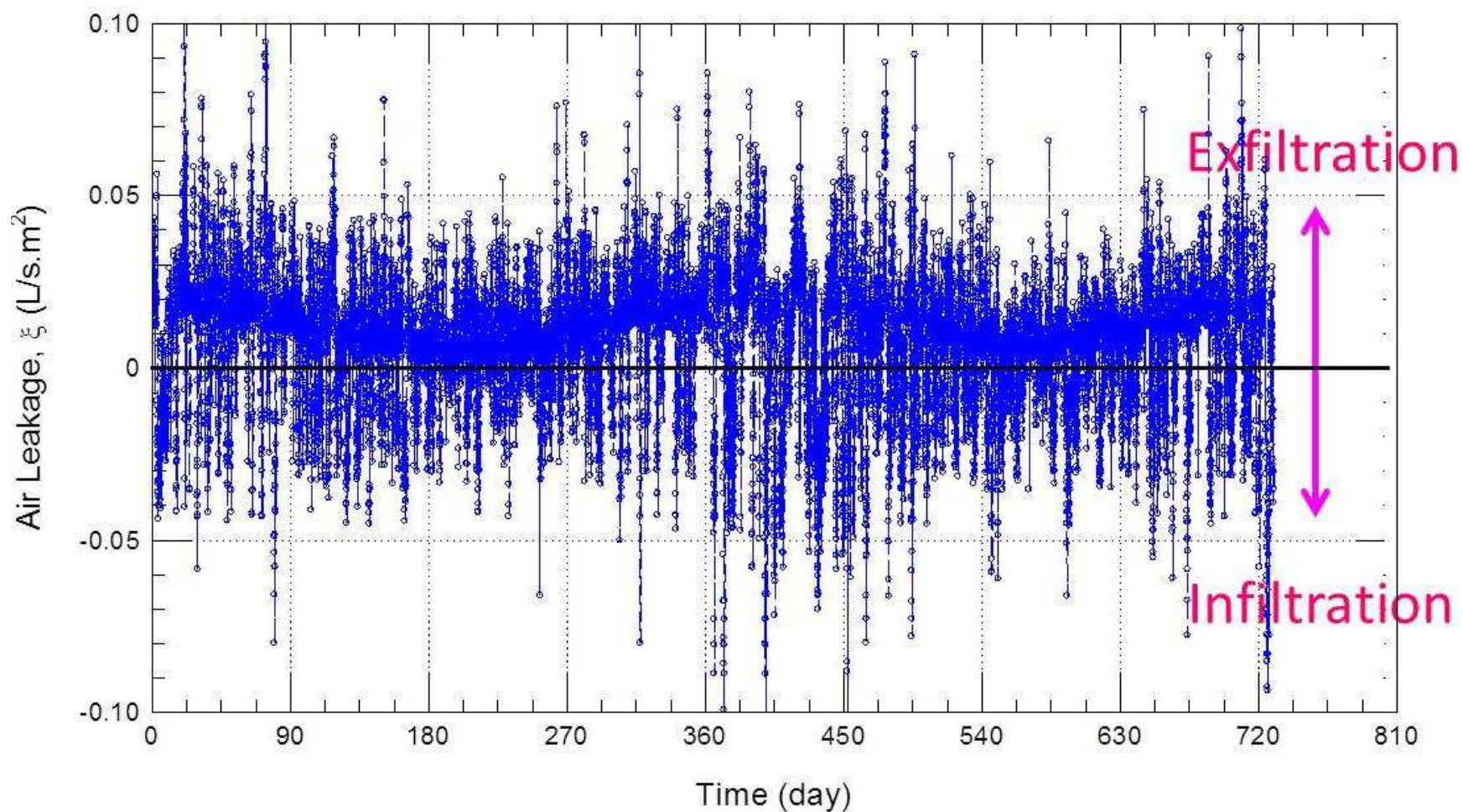## Appendix – A2: Air leakage rates of different geographical locations

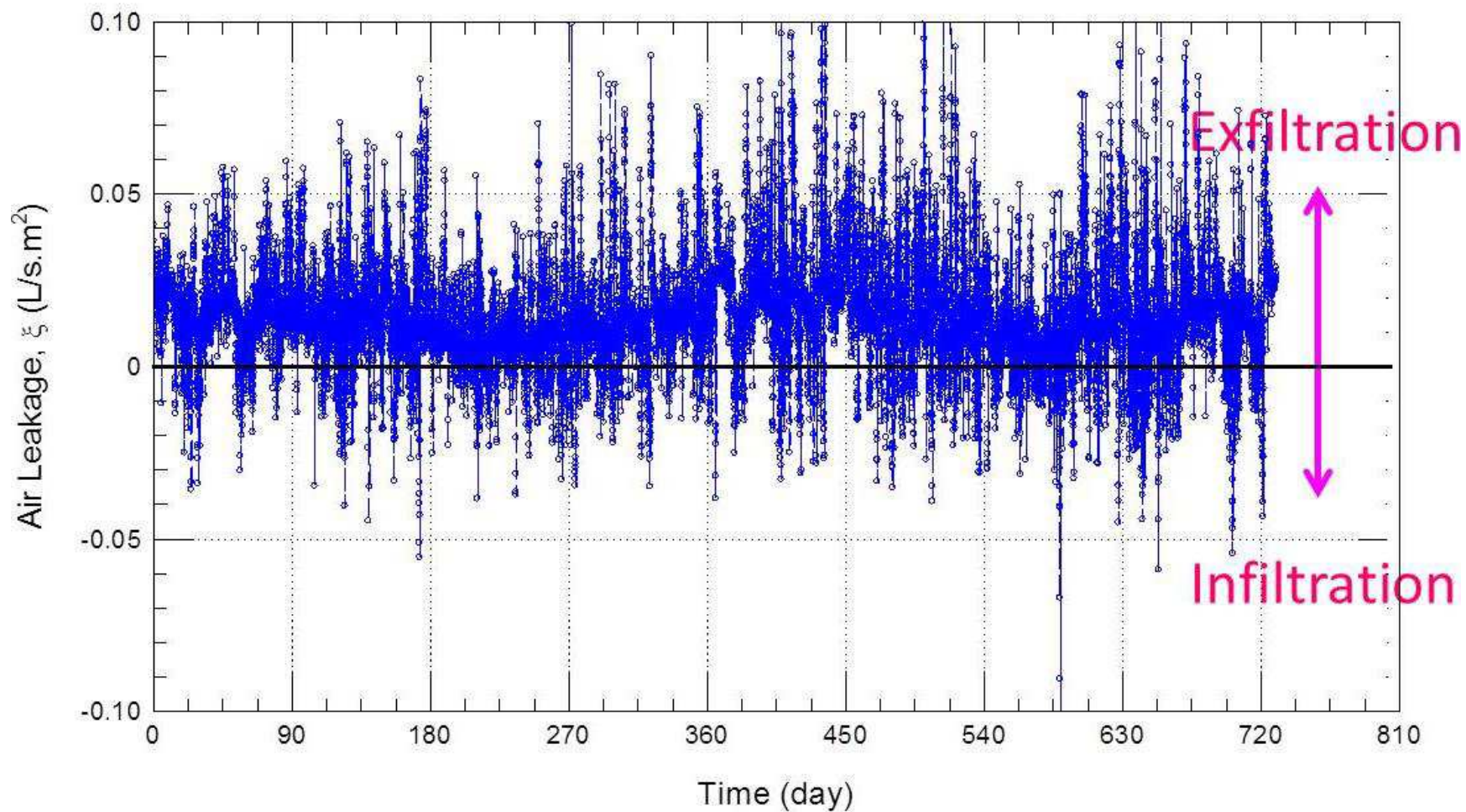**Figure A - 1 Air leakage rate due to exfiltration and infiltration of Ottawa weather**

Figure A - 2. Air leakage rate due to exfiltration and infiltration of Edmonton weather
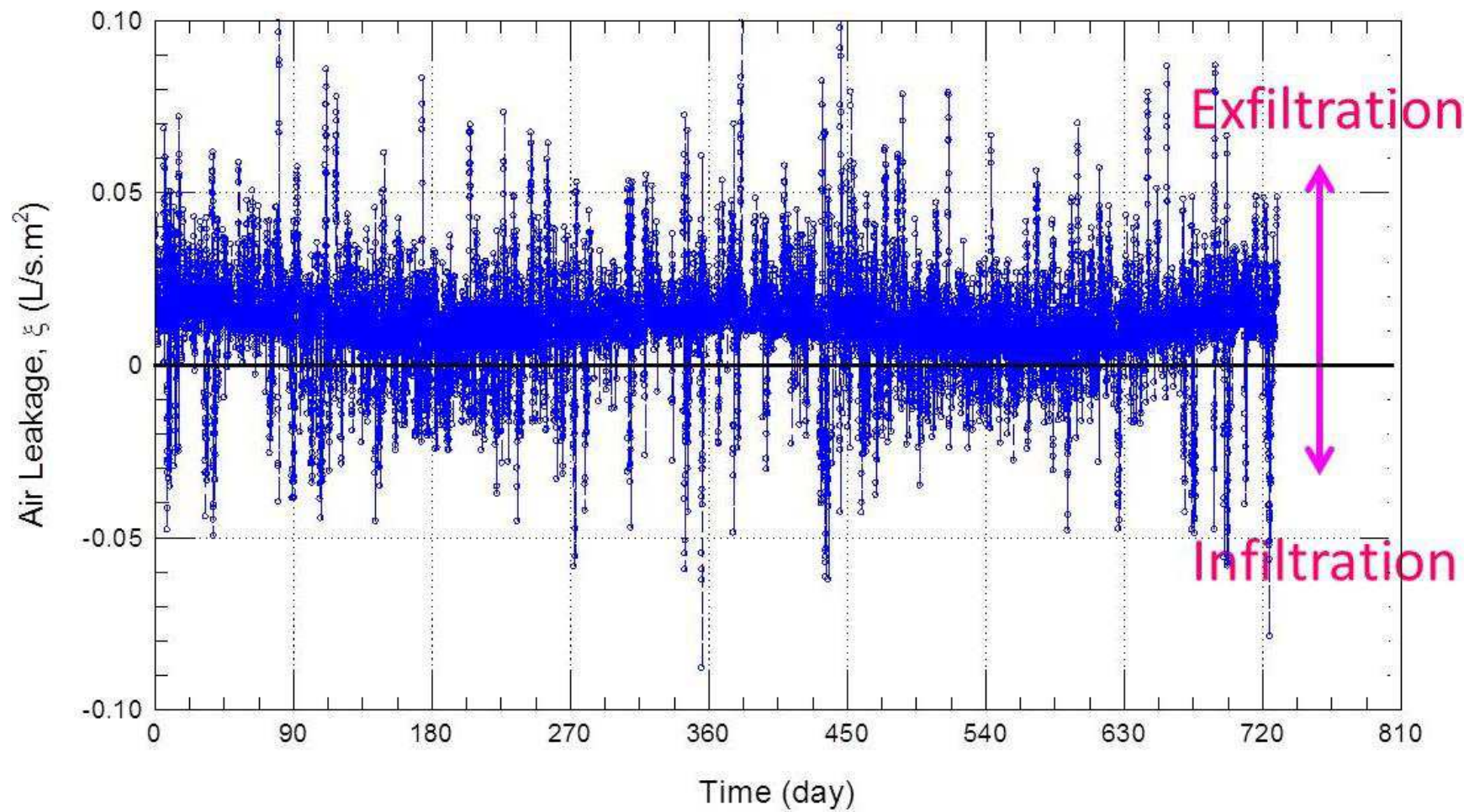
Figure A - 3. Air leakage rate due to exfiltration and infiltration of Vancouver weather
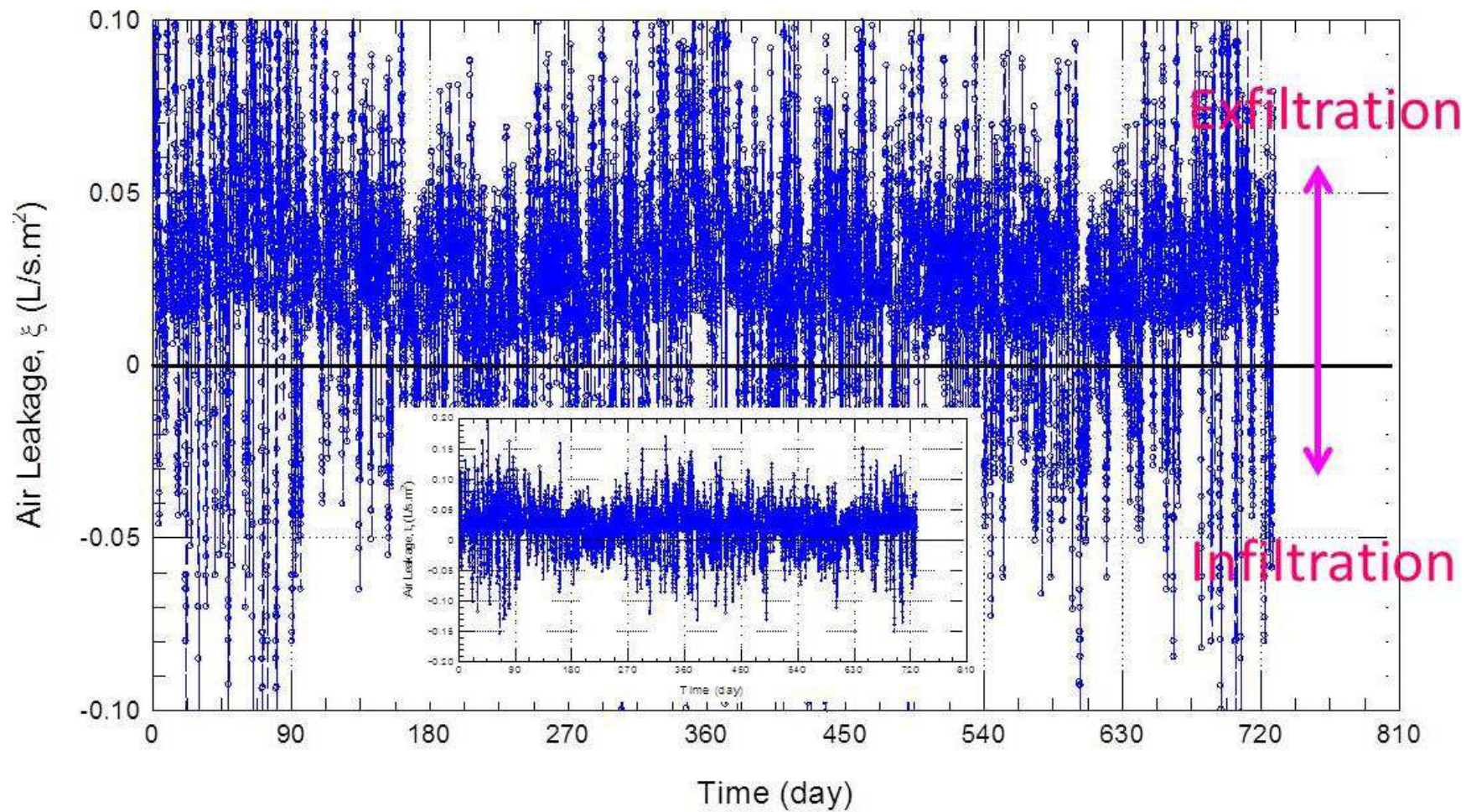
Figure A - 4. Air leakage rate due to exfiltration and infiltration of St John's weather
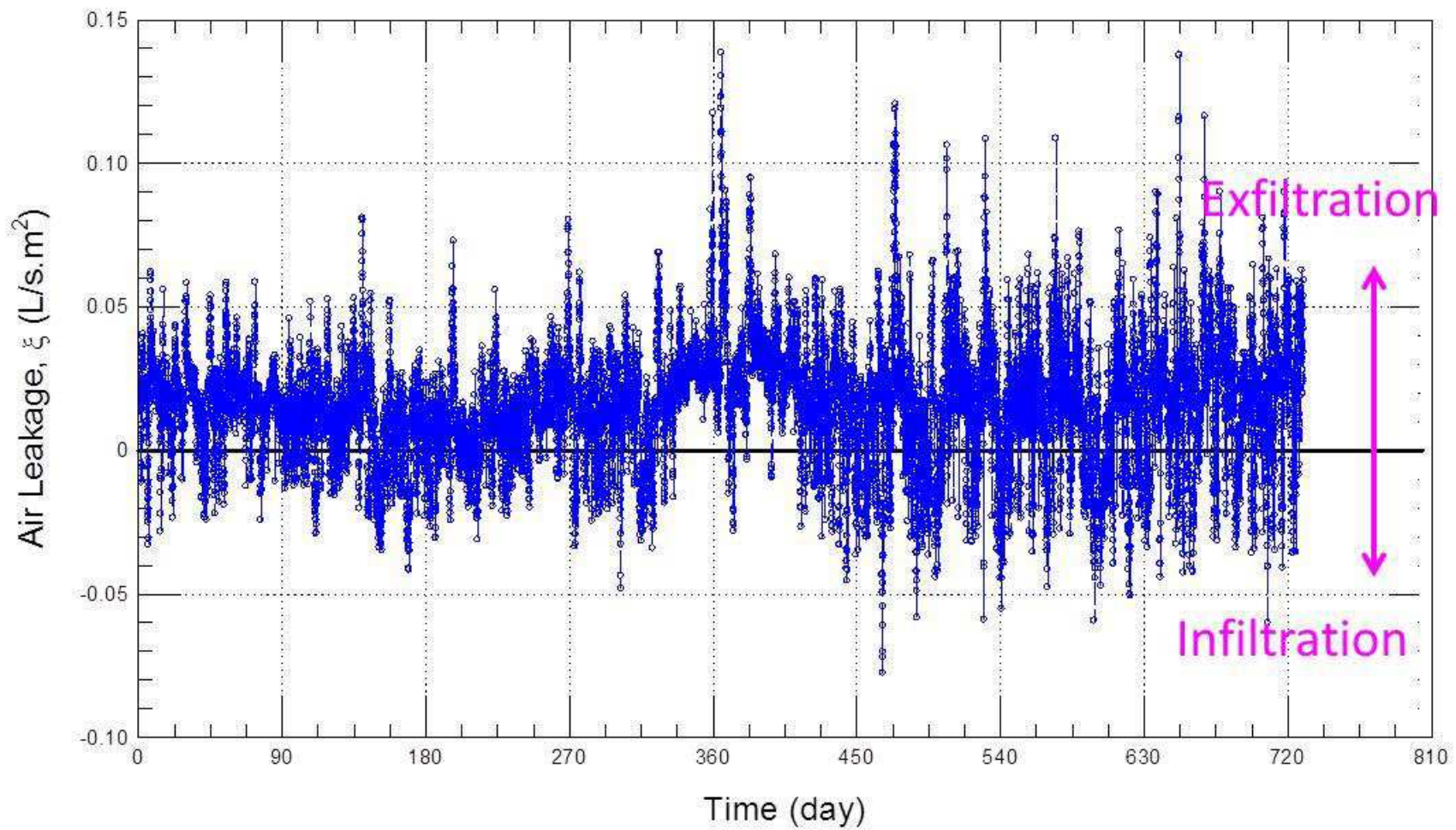
Figure A - 5. Air leakage rate due to exfiltration and infiltration of Yellowknife weather

Appendix – A3: Mould index of different wall systems
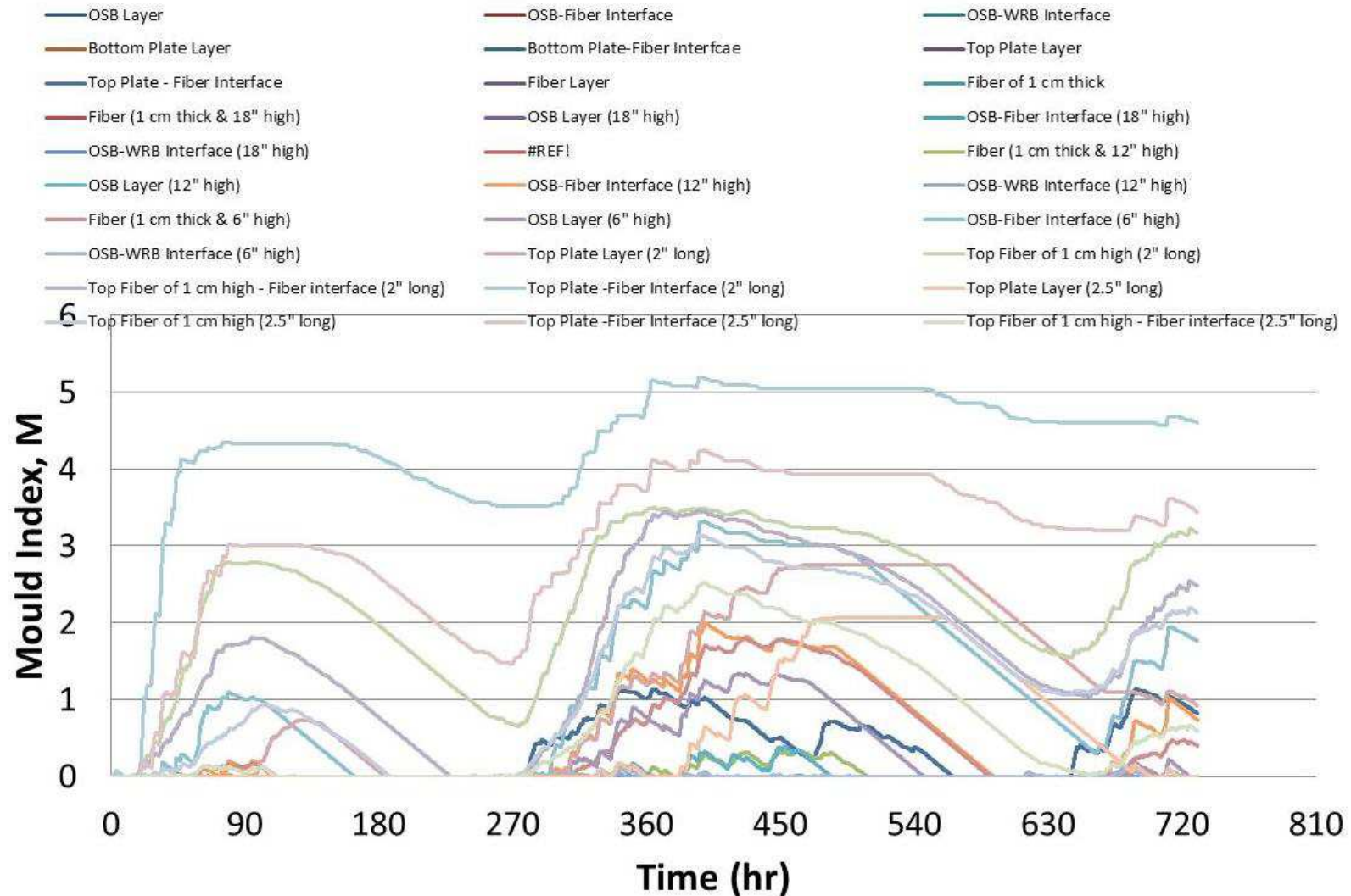
Reference Wall - All Locations

Figure A - 6. Mould index at different locations inside the reference wall for the case of 100% air leakage rate (Ottawa weather)
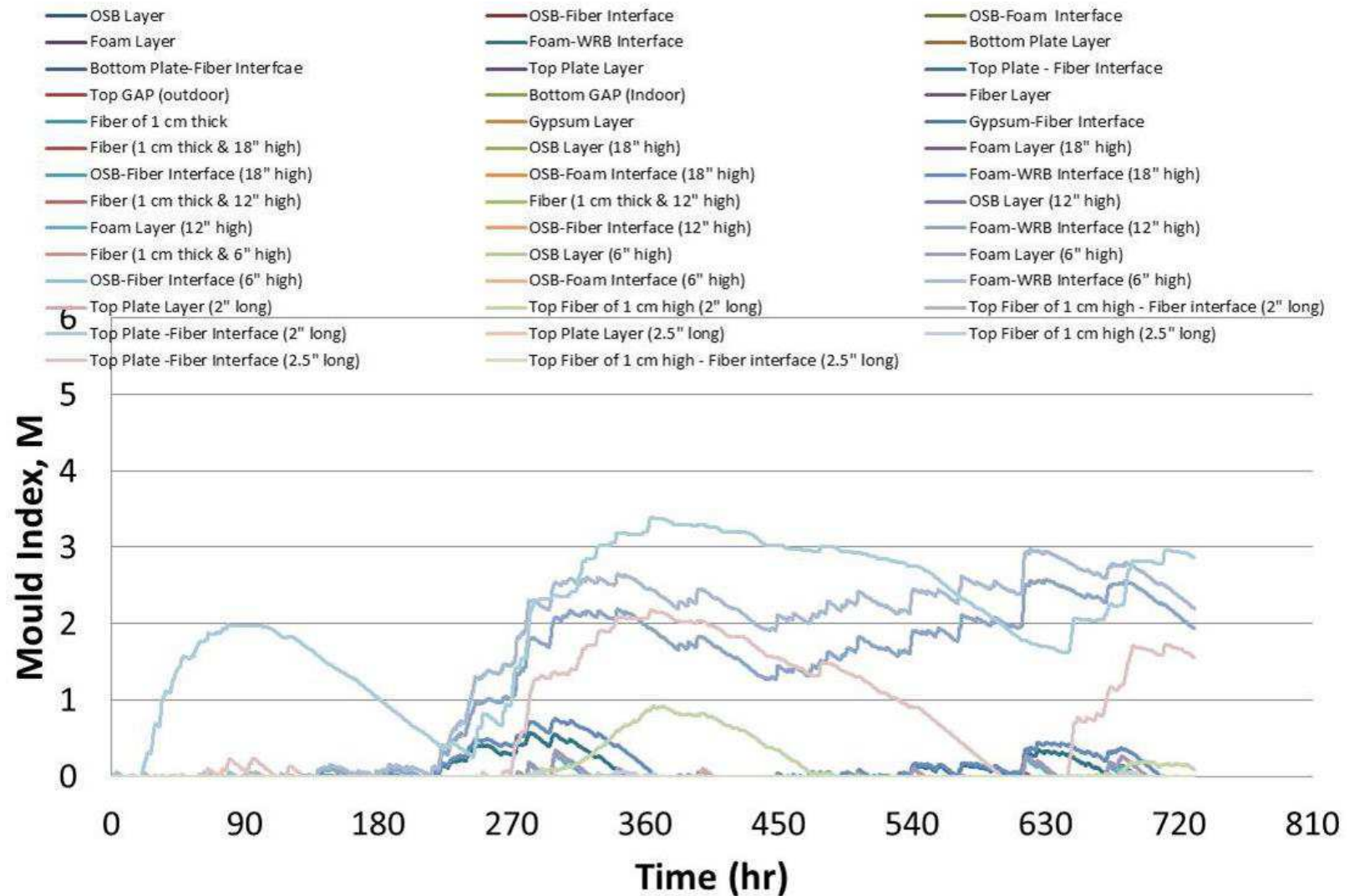
XPS Wall - All Locations

Legend:
- OSB Layer
- OSB-Fiber Interface
- OSB-Foam Interface
- Foam Layer
- Foam-WRB Interface
- Bottom Plate Layer
- Bottom Plate-Fiber Interfcae
- Top Plate Layer
- Top Plate - Fiber Interface
- Top GAP (outdoor)
- Bottom GAP (Indoor)
- Fiber Layer
- Fiber of 1 cm thick
- Gypsum Layer
- Gypsum-Fiber Interface
- Fiber (1 cm thick & 18" high)
- OSB Layer (18" high)
- Foam Layer (18" high)
- OSB-Fiber Interface (18" high)
- OSB-Foam Interface (18" high)
- Foam-WRB Interface (18" high)
- Fiber (1 cm thick & 12" high)
- Fiber (1 cm thick & 12" high)
- OSB Layer (12" high)
- Foam Layer (12" high)
- OSB-Fiber Interface (12" high)
- Foam-WRB Interface (12" high)
- Fiber (1 cm thick & 6" high)
- OSB Layer (6" high)
- Foam Layer (6" high)
- OSB-Fiber Interface (6" high)
- OSB-Foam Interface (6" high)
- Foam-WRB Interface (6" high)
- Top Plate Layer (2" long)
- Top Fiber of 1 cm high (2" long)
- Top Fiber of 1 cm high - Fiber interface (2" long)
- Top Plate -Fiber Interface (2" long)
- Top Plate Layer (2.5" long)
- Top Fiber of 1 cm high (2.5" long)
- Top Plate -Fiber Interface (2.5" long)
- Top Fiber of 1 cm high - Fiber interface (2.5" long)

Figure A - 7. Mould index at different locations inside the XPS wall for the case of 100% air leakage rate (Ottawa weather)
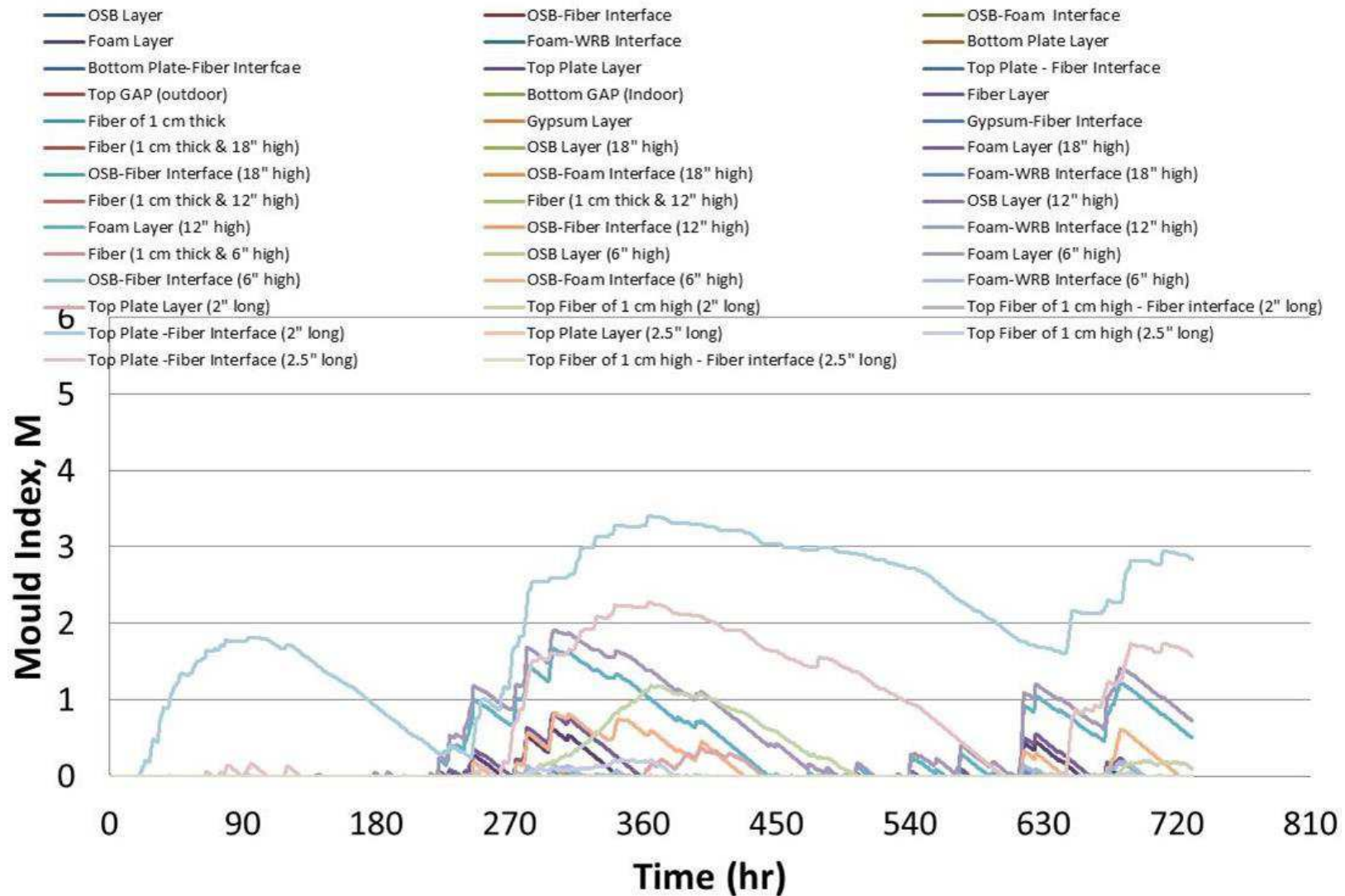
Figure A - 8. Mould index at different locations inside the mineral fibre wall for the case of 100% air leakage rate (Ottawa weather)

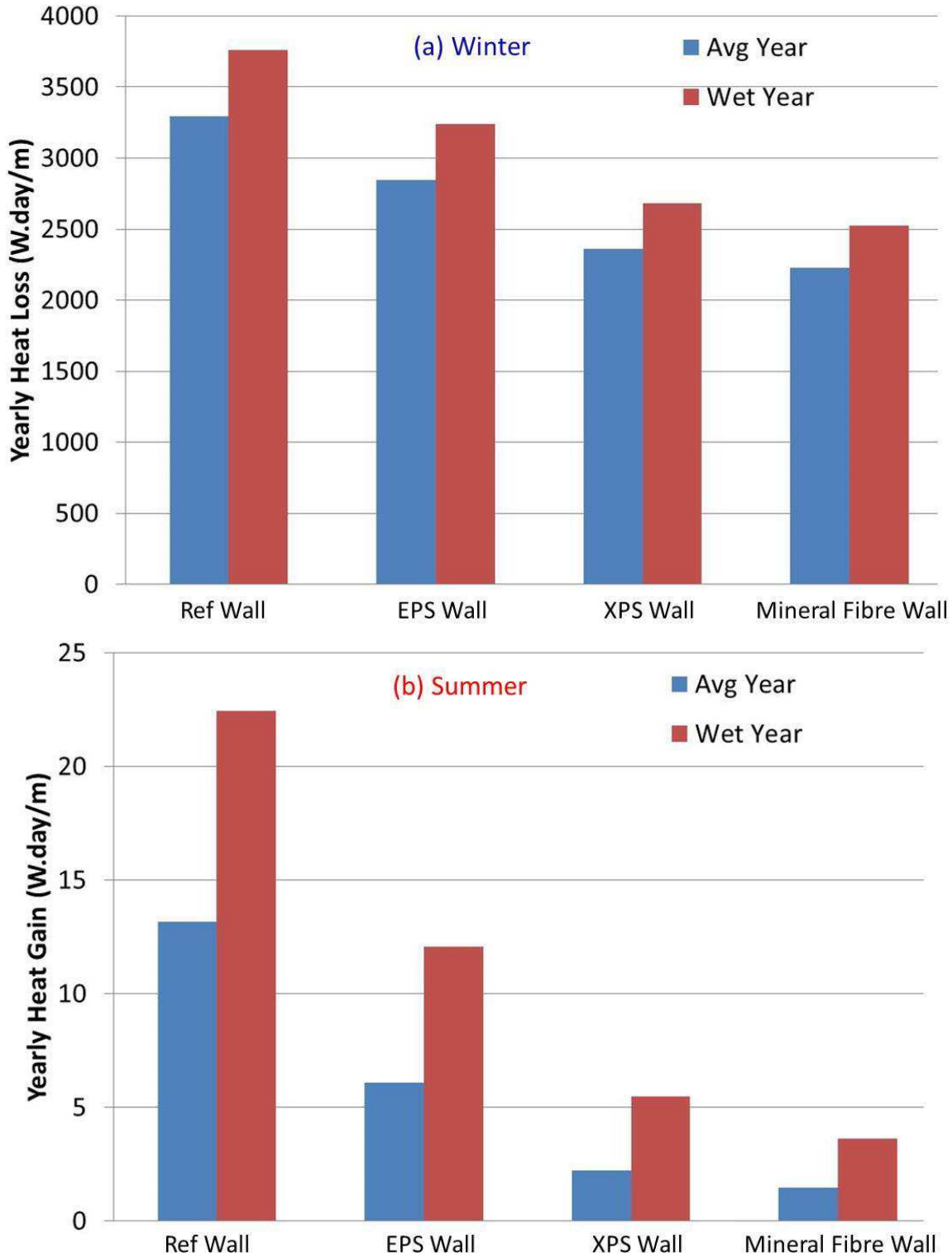# Appendix – A4: Yearly heat loss and heat gain

Figure A - 9. Effect of exterior insulation on the yearly heat loss and heat gain of wall systems with R-24 stud-cavity at 100% air leakage rate (Edmonton weather)
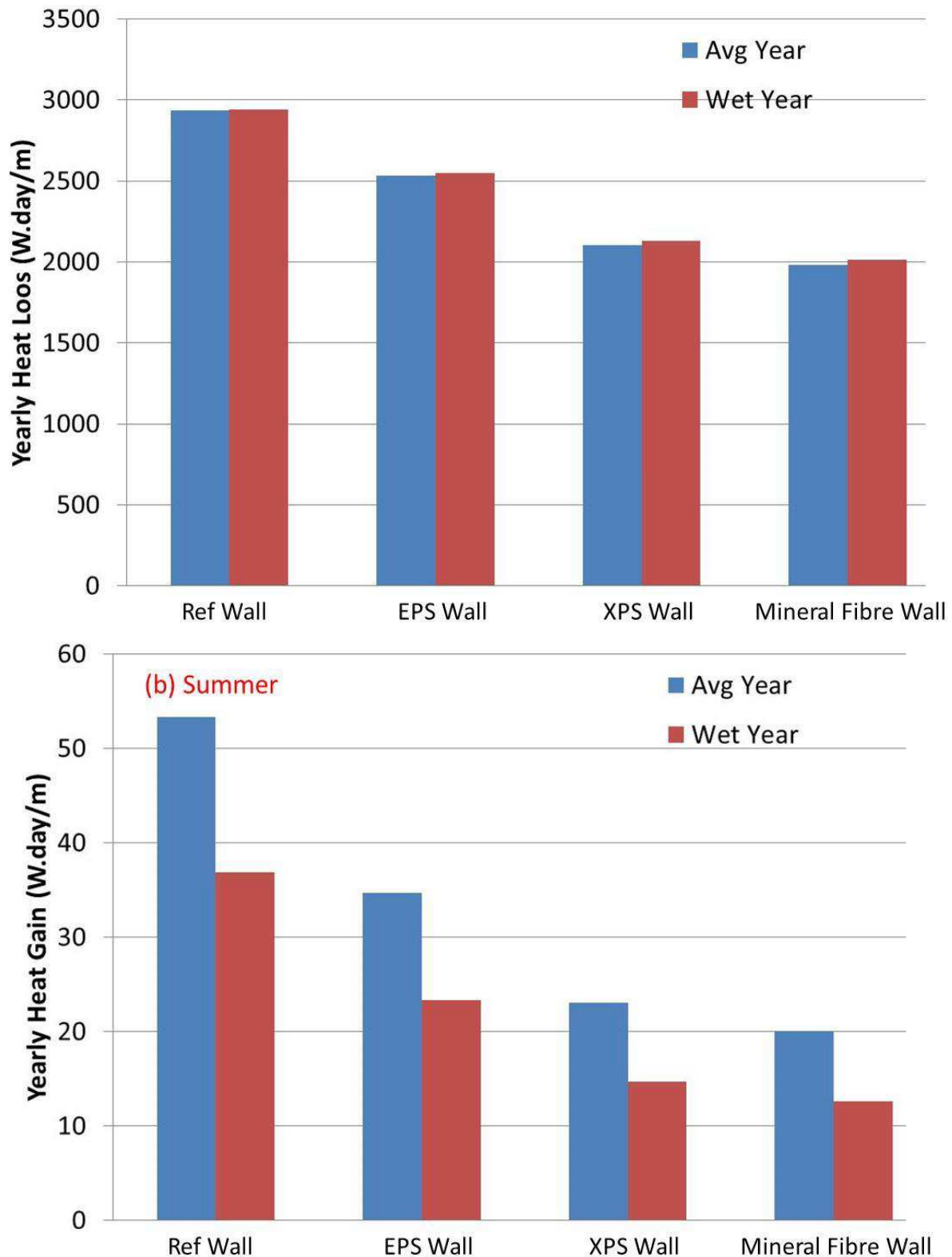
NRC·CNRC

Figure A - 10. Effect of exterior insulation on the yearly heat loss and heat gain of wall systems with R-24 stud-cavity at 100% air leakage rate (Ottawa weather)
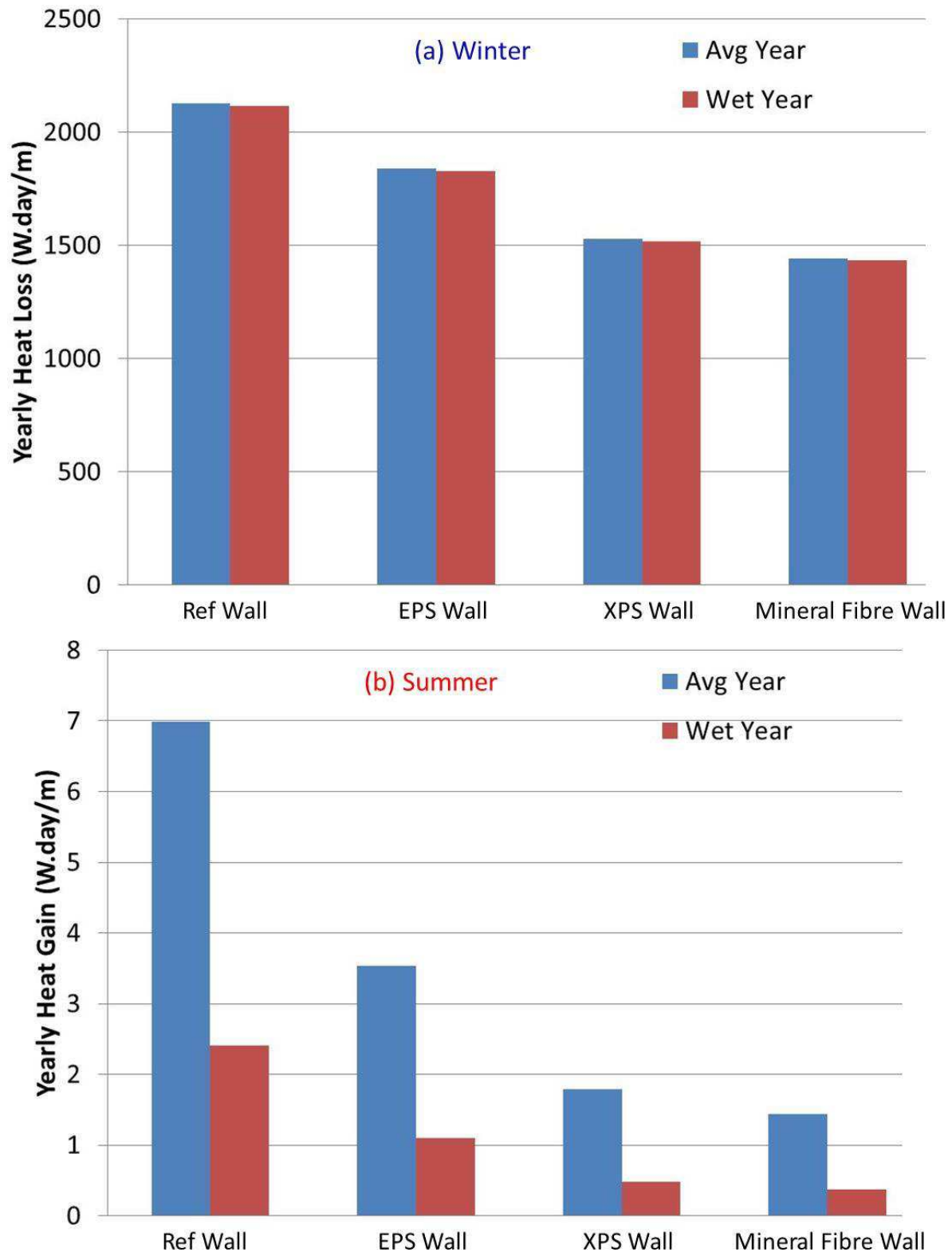
Figure A - 11. Effect of exterior insulation on the yearly heat loss and heat gain of wall systems with R-24 stud-cavity at 100% air leakage rate (Vancouver weather)
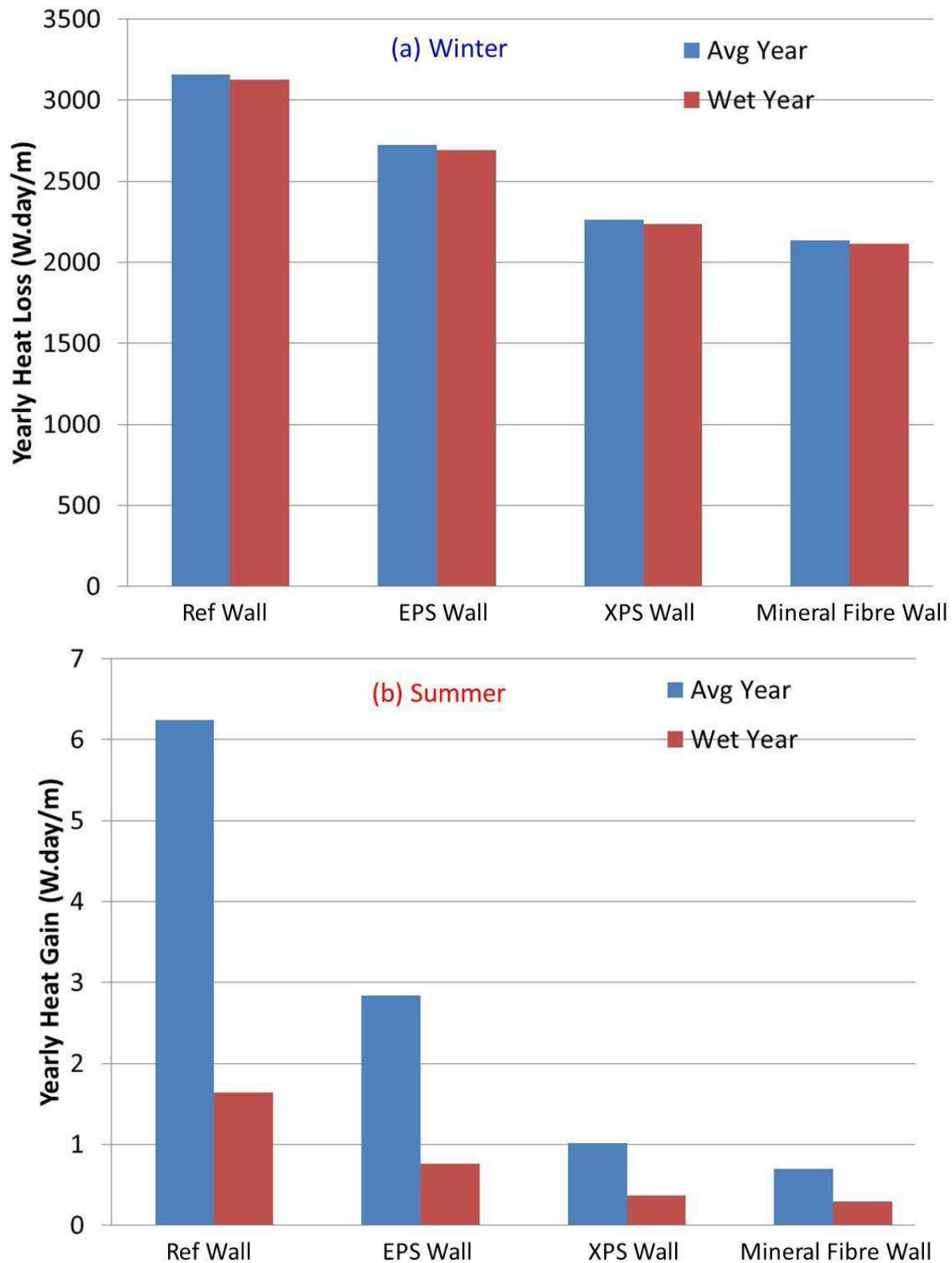
NRC · CNRC

Figure A - 12. Effect of exterior insulation on the yearly heat loss and heat gain of wall systems with R-24 stud-cavity at 100% air leakage rate (St John's weather)
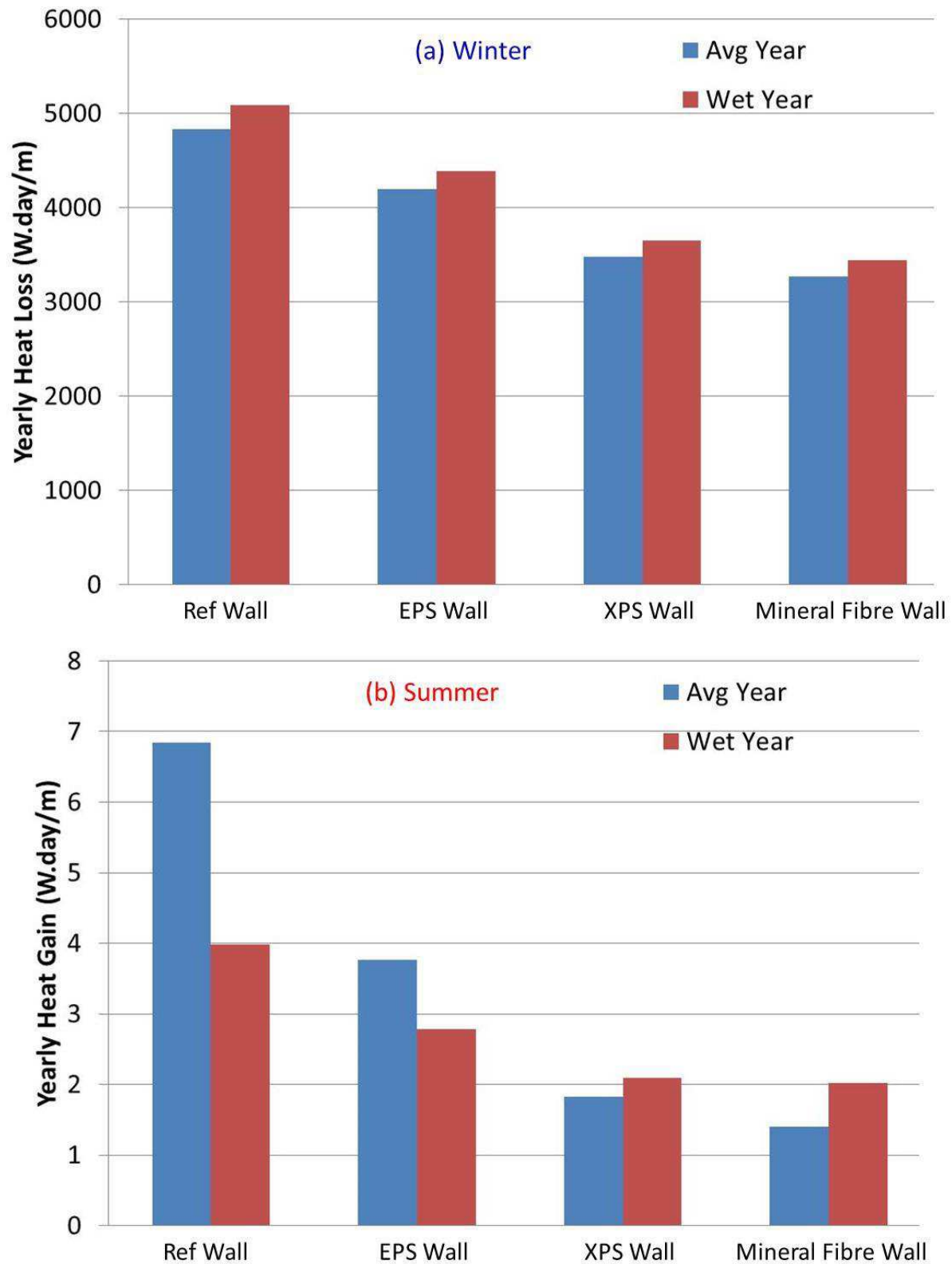
NRC·CNRC

Figure A - 13. Effect of exterior insulation on the yearly heat loss and heat gain of wall systems with R-24 stud-cavity at 100% air leakage rate (Yellowknife weather)